



INSTITUTO  
UNIVERSITÁRIO  
DE LISBOA

---

## **Towards a New Cloud-based Planning & Optimisation Methodology for Mobile Communication Networks**

Daniel Filipe Sobral Fernandes

*PhD* in Information Science and Technology

Supervisors:

Doctor Francisco António Bucho Cercas, Full Professor,  
Iscte - Instituto Universitário de Lisboa

Doctor Rui Miguel Henriques Dias Morgado Dinis, Associate Professor,  
Faculdade de Ciências e Tecnologia - Universidade Nova de Lisboa

September 2020





TECNOLOGIAS  
E ARQUITETURA

---

Department of Information Science and Technology

**Towards a New Cloud-based Planning & Optimisation Methodology for Mobile Communication Networks**

Daniel Filipe Sobral Fernandes

*PhD* in Information Science and Technology

Supervisors:

Doctor Francisco António Bucho Cercas, Full Professor,  
Iscte - Instituto Universitário de Lisboa

Doctor Rui Miguel Henriques Dias Morgado Dinis, Associate Professor,  
Faculdade de Ciências e Tecnologia - Universidade Nova de Lisboa

September, 2020





TECNOLOGIAS  
E ARQUITETURA

---

Department of Information Science and Technology

**Towards a New Cloud-based Planning & Optimisation Methodology for Mobile Communication Networks**

Daniel Filipe Sobral Fernandes

*PhD* in Information Science and Technology

Jury:

Doctor Américo Manuel Carapeto Correia, Full Professor, Iscte - Instituto  
Universitário de Lisboa (President)

Doctor Adão Paulo Soares da Silva, Assistant Professor, Universidade de Aveiro

Doctor Marco Alexandre Cravo Gomes, Assistant Professor, Universidade de  
Coimbra

Doctor João Francisco Martinho Ledo Guerreiro, Assistant Professor, Faculdade de  
Ciências e Tecnologia - Universidade Nova de Lisboa

Doctor Nuno Manuel Branco Souto, Assistant Professor, Iscte - Instituto  
Universitário de Lisboa

Doctor Francisco António Bucho Cercas, Full Professor, Iscte - Instituto  
Universitário de Lisboa

September, 2020



*"What we know is a drop, what we don't know is an ocean."*

Isaac Newton



# *Acknowledgements*

As in every thesis, I begin by thanking the supervisors for their constant support, guidance, motivation, and encouragement. However, the reasons for which I'm thankful are due to much more than mere support. To the Professors Francisco Cercas and Rui Dinis I must give a special thanks for the freedom that over the last years has always allowed me to choose the areas of research that I found most interesting.

Another special thanks are addressed to Professors Pedro Sebastião and Lúcio Ferreira, who supported me in a new research line with new challenges and approaches. Professor Lúcio's concern in aggregating all ideas, the motivation and encouragement he gave me and the brilliant contact with MULTIVISION must be mentioned.

To all MULTIVISION's collaborators, I owe a thank you. Emphasising engineer Andreia Carregueira and all METRIC's development team: the engineers Nuno Valente, Ricardo Costa, and Sameer Ibraimo. A special thank to Gabriela Soares for her precious words on the meaning of having a PhD.

Family is always one of the main pillars of support, and my case was no exception. I have to thank my parents, grandparents, sister, niece, and all my family. Their constant support made this adventure easier.

Another pillar of constant support are friends, those who existed before this adventure began, as well as the ones I made during this chapter. So I have to thank all those who have crossed my path and helped me to improve. In particular, I must highlight some names, who advised me and who I believe I also helped in a certain way: Inês, Pedro, Rodrigo, Miriam, André, António, Diogo, among others. It is clear that these are the people I rely on, and with whom I seek answers to certain situations.

When we embark on an adventure like this, we usually think that our personal life is on hold, but in fact, it didn't happen to me. So I have to thank my colleagues and friends from Portuguese Red Cross - Delegation of Setúbal who supported me during this period.

This work is part of the OptiNET-5G project, co-funded by CENTRO2020/Portugal2020/ European Union (project 023304). I wish to thank Instituto de Telecomunicações and Iscte - Instituto Universitário de Lisboa for all the support and installations that allowed me to successfully finish this PhD thesis.



# Resumo

A grande preocupação dos operadores de telecomunicações em oferecerem serviços de alta qualidade aos seus clientes leva a um constante cuidado com o estado das redes. Estas redes podem apresentar alguns problemas que implicam que a experiência oferecida aos clientes seja desagradável. De forma a monitorizar estas situações, os operadores recolhem, com bastante regularidade, dados, como *drive tests*, que lhes permitem avaliar e corrigir pequenos problemas. Esta tese aproveita os dados recolhidos e utiliza-os no planeamento da rede de forma a obter fielmente a estimativa de cobertura de uma rede. De forma a automatizar mecanismos de correção de falhas, é apresentado um modelo de propagação completamente automático, que descreve de forma precisa o estado da rede permitindo que seja aplicado em algoritmos de planeamento e otimização da rede. Após a sua implementação, este modelo foi comparado com um segundo modelo, gerado através de Inteligência Artificial, que é completamente agnóstico a todo o conhecimento de telecomunicações. Estes modelos, para os cenários estudados, atingiram erros absolutos médios entre os valores estimados e os valores reais de 6.1 dB com um desvio padrão de 4 dB.

A existência de diversos dados reais das redes de telecomunicações e a evolução para os sistemas *Multiple Input, Multiple Output* (MIMO) motivou não só a investigação no impacto da cobertura com a mudança de um sistema *Single Input, Single Output* (SISO) para um sistema MIMO, mas também a investigação na redução de complexidade dos recetores utilizados em sistemas MIMO. Quanto mais próxima a *Bit Error Rate performance* do recetor estiver do *Matched Filter Bound*, menor será a redução na área de cobertura com a transição de um sistema SISO para um sistema MIMO.

**Palavras-chave:** Coverage Estimation, Network Planning, Drive Tests, Propagation Model, BER Performance.



# *Abstract*

The great concern of telecommunication operators to offer high-quality services to their customers requires a constant care with the state of the networks. These networks can present some problems that imply that the experience offered to customers is unsatisfactory. In order to monitor these situations, operators collect, on a fairly regular basis, data, like drive tests, that allow them to monitor and correct minor issues. This thesis takes advantage of the data collected and uses it in network planning in order to precisely obtain the coverage estimation of a network. In order to automate failure correction mechanisms, a totally automatic propagation model is presented, which precisely describes the state of the network, allowing it to be used for network planning and optimisation. After its implementation, the model was compared to a second model, generated through Artificial Intelligence, which is completely agnostic to all telecommunications knowledge. These models, for the considered scenarios, reached average absolute errors between estimated and actual values of 6.1 dB with a standard deviation of 4 dB.

The existence of several real telecommunication network measures and their evolution to Multiple Input, Multiple Output (MIMO) systems motivated not only the investigation on the coverage impact with the change from a Single Input, Single Output (SISO) to a MIMO system, but also the investigation on the reduction of complexity of the receivers used in MIMO systems. The closer the Bit Error Rate performance of the receiver is to the Matched Filter Bound, the smaller will be the reduction in the coverage area with the transition from a SISO system to a MIMO system.

**Keywords:** Coverage Estimation, Network Planning, Drive Tests, Propagation Model, BER Performance.



# Contents

<b>Acknowledgements</b>	<b>ix</b>
<b>Resumo</b>	<b>xi</b>
<b>Abstract</b>	<b>xiii</b>
<b>List of Figures</b>	<b>xvii</b>
<b>List of Tables</b>	<b>xix</b>
<b>List of Acronyms</b>	<b>xxi</b>
<b>List of Symbols</b>	<b>xxv</b>
<b>1 Introduction</b>	<b>1</b>
1.1 Motivation and Scope . . . . .	1
1.2 Objectives . . . . .	5
1.3 Contributions of Research . . . . .	6
1.4 Thesis Overview . . . . .	12
<b>2 Novel Semi-Empirical Propagation Model</b>	<b>19</b>
<b>3 Comparison between Semi-Empirical and Artificial Intelligence Propagation Models</b>	<b>39</b>
<b>4 Extension of SISO propagation models to MIMO systems</b>	<b>51</b>
<b>5 Analysis of BER performance achieved in MIMO systems</b>	<b>67</b>
<b>6 Conclusions</b>	<b>81</b>
6.1 Future Work . . . . .	83
<b>Bibliography</b>	<b>85</b>



# List of Figures

1.1	Synthesis of research identifying all contributions. . . . .	13
1.2	Evolution of the results achieved in coverage estimation. . . . .	14
2.1	A new cell coverage estimation architectural framework composed by four layers for the cloud-based management of radio resources. . . . .	26
2.2	Illustration of the combination of various aspects for the construction of the ACSPM. . . . .	28
2.3	Steps for the computation of a propagation grid. . . . .	28
2.4	Drive Test to a given cell, obtained through the METRIC platform. . . . .	30
2.5	Mobile network monitoring and optimisation architecture, with work pattern using AWS services that implements the ACSPM. . . . .	31
2.6	Cell coverage estimation module integrated in the Metric platform. . . . .	32
2.7	Horizontal and vertical radiation pattern of the reference antenna. . . . .	33
2.8	Propagation of a cell represented in the METRIC platform. . . . .	33
2.9	Terrain elevation of the reference scenario, with indication of the antenna's azimuth. . . . .	33
2.10	Estimated received signal level using the proposed propagation model. . . . .	34
2.11	Estimated received signal level using the SPM model. . . . .	34
2.12	Polynomial regression for MAE values. . . . .	35
2.13	Signal received in a certain area. . . . .	36
2.14	Carrier to Interference ratio in a certain area. . . . .	36
3.1	Scenario A depicted in METRIC platform. . . . .	43
3.2	Scenario B depicted in METRIC platform. . . . .	44
3.3	Cell coverage estimation model framework. . . . .	45
3.4	Configuration example of an ANN with three neurons in the input layer, one hidden layer and two output neurons. . . . .	45
3.5	Custom architecture design of the implemented ANN algorithm. . . . .	46
3.6	DT occurrences distributed by their $P_{rx}$ value. . . . .	46
3.7	Loss values of Training and Validation sets. . . . .	47
3.8	Estimated received power level using the AIPM model for the entire service area and considering all the antennas for scenario A. . . . .	47
3.9	Estimated received power level using the ACSPM model for the entire service area and considering all the antennas for scenario A. . . . .	47
3.10	Estimated received power level using the ACSPM model for scenario B.1. . . . .	47

3.11	Estimated received power level using the AIPM model for scenario B.1. . . . .	48
3.12	Estimated received power level using the ACSPM model for scenario B.2. . . . .	48
4.1	Motivation for this study. . . . .	54
4.2	IB-DFE receiver structure. . . . .	55
4.3	Theoretical BER performance for the 1 <sup>st</sup> iteration when using IB-DFE for different $R/P$ values. . . . .	58
4.4	Theoretical BER performance for the 3 <sup>rd</sup> iteration when using IB-DFE for different $R/P$ values. . . . .	59
4.5	Difference between theoretical BER performance for SISO and MIMO systems for the 1 <sup>st</sup> iteration when using IB-DFE. . . . .	59
4.6	Difference between theoretical BER performance for SISO and MIMO systems for the 3 <sup>rd</sup> iteration when using IB-DFE. . . . .	60
4.7	Considered scenario to validate our model. . . . .	61
4.8	Coverage area of the considered scenario. . . . .	62
4.9	Coverage area extrapolated for a MIMO system with a BER of $10^{-2}$ and for the first iteration of IB-DFE. . . . .	62
4.10	Estimated coverage area of the considered scenario for a MIMO system with a BER of $10^{-4}$ when using the 3 <sup>rd</sup> iteration of IB-DFE receivers, based on coverage estimation with DTs for a SISO system. . . . .	63
5.1	System scenario. . . . .	70
5.2	Iterative Block Decision Feedback Equalization (IB-DFE) receiver combined with the Maximum Ratio Combining (MRC) structure. . . . .	73
5.3	Theoretical/simulated BER performance and correlation factor for IB-DFE and MRC receivers in a Multiple Input Multiple Output (MIMO) system with 3 iterations. <b>(a)</b> BER performance. <b>(b)</b> Correlation factor ( $\rho$ ). . . . .	75
5.4	Theoretical/simulated BER performance and correlation factor for a receiver that combines IB-DFE and MRC in a MIMO system with 3 iterations. <b>(a)</b> BER performance. <b>(b)</b> Correlation factor ( $\rho$ ). . . . .	76
5.5	Theoretical/simulated BER performance and correlation factor for IB-DFE and MRC receivers in an mMIMO system with 3 iterations. <b>(a)</b> BER performance. <b>(b)</b> Correlation factor ( $\rho$ ). . . . .	77
5.6	Theoretical/simulated BER performance and correlation factor for a receiver that combines IB-DFE and MRC in an mMIMO system with 3 iterations. <b>(a)</b> BER performance. <b>(b)</b> Correlation factor ( $\rho$ ). . . . .	77

# List of Tables

1.1	Timeline of contributions. . . . .	6
2.1	Conditions under which the models are applicable. . . . .	24
2.2	Typical values for the SPM coefficient parameters. . . . .	24
2.3	Parameters used in the propagation model. . . . .	27
2.4	Absolute error between estimated values and DT values for the 247 DT pixels. . . . .	34
2.5	Computing time of the ACSPM, for 3304 cells, on the AWS and not on the AWS. The format of the values is hh:mm:ss. . . . .	35
3.1	Synthesis of antennas parameters. . . . .	43
3.2	Specification of the number of DTs for each scenario, for the calibration ( $t$ ) and evaluation ( $t + 1$ ) time periods. . . . .	44
3.3	Correlation classification. . . . .	44
3.4	Synthesis of results for each of the scenarios understudy. . . . .	48
5.1	$E_b/N_0$ [dB] for the Bit Error Rate (BER) performance of the scenarios. . . . .	70



# List of Acronyms

1G	1 <sup>st</sup> generation network of mobile communication
2G	2 <sup>nd</sup> generation network of mobile communication
3G	3 <sup>rd</sup> generation network of mobile communication
4G	4 <sup>th</sup> generation network of mobile communication
5G	5 <sup>th</sup> generation network of mobile communication
ACSPM	Automatically Calibrated Standard Propagation Model
AI	Artificial Intelligence
AIPM	Artificial Intelligence Propagation Model
Amazon EC2	Amazon Elastic Compute Cloud
Amazon RDS	Amazon Relational Database Service
Amazon S3	Amazon Simple Storage Service
ANACOM	Autoridade Nacional de Comunicações
ANNs	Artificial Neural Networks
API	Application Programming Interface
AWS	Amazon Web Services
BCCH	Broadcast Control Channel
BER	Bit Error Rate
BEREC	Body of European Regulators for Electronic Communications
BS	Base Station
CM	Configuration Management
CRAN	Cloud Radio Access Network

DOI	Digital Object Identifier
DR	Deliverable Reports
DTs	Drive Tests
EARFCN	E-UTRA Absolute Radio Frequency Channel Number
EGC	Equal Gain Combining
ETL	Extracts, Transforms and Loads
FDE	Frequency-Domain Equalization
GSM	Global System for Mobile Communications
IB-DFE	Iterative Block Decision Feedback Equalization
IC	International Conferences
IJ	International Journals
IoT	Internet of Things
ISI	Inter-Symbol Interference
KPIs	Key Performance Indicators
LiDAR	Light Detection and Ranging
LoS	Line of Sight
LTE	Long Term Evolution
MAE	Mean Absolute Error
MDT	Minimisation of Drive Tests
MFB	Matched Filter Bound
MIMO	Multiple Input, Multiple Output
mMIMO	Massive MIMO
MRC	Maximum Ratio Combining
MT	Mobile Terminal
NC	National Conference
NFV	Network Functions Virtualisation
ODbL	Open Database License
OFDM	Orthogonal Frequency Division Multiplexing

OSS	Operations Support System
PCI	Physical Cell ID
PR	Prototype
QoS	Quality of Service
QPSK	Quaternary Phase Shift Keying
R&D	Research and Development
RAN	Radio Access Network
RANaaS	Radio Access Network-as-a-Service
SaaS	Software-as-a-Service
SC	Scrambling Codes
SC-FDE	Single-Carrier with Frequency-Domain Equalization
SISO	Single Input, Single Output
SNR	Signal-to-Noise Ratio
SON	Self-Organising Network
SPM	Standard Propagation Model
UMTS	Universal Mobile Telecommunication System
ZF	Zero Forcing



# List of Symbols

$A$	service area of an antenna
$B_k$	feedback equalizer coefficient for the $k^{th}$ frequency
$B_{k,p}$	feedback equalizer coefficient for the $k^{th}$ frequency of the $p^{th}$ user
$C_a$	coverage area for an antenna located at vector location $\mathbf{a}$
$E_b$	average bit energy
$F_k$	feedforward equalizer coefficient for the $k^{th}$ frequency
$F_{k,p}$	feedforward equalizer coefficient for the $k^{th}$ frequency of the $p^{th}$ user
$G(p)$	antenna gain for pixel $p$
$G_{tx}$	transmitted antenna gain
$Geo_{hash}$	geohash length
$H_k$	overall channel frequency response for the $k^{th}$ frequency
$H_{k,p}$	overall channel frequency response for the $k^{th}$ frequency of the $p^{th}$ user
$K_1$	constant offset of SPM model
$K_2$	coefficient for $\log(d_{BS})$ in SPM model
$K_3$	coefficient for $\log(h_{BS})$ in SPM model
$K_4$	coefficient for diffraction calculation in SPM model
$K_5$	coefficient for $\log(d_{BS})\log(h_{BS})$ in SPM model
$K_6$	coefficient for $h_{MT}$ in SPM model
$K_7$	coefficient for $\log(h_{MT})$ in SPM model
$K_{clutter}$	coefficient for $f(clutter)$ in SPM model

$L$	path loss attenuation
$L(d_{ho})$	loss at handover distance
$L(d_{wal})$	loss at $d_{wal}$
$N$	number of samples/sub-carriers
$N_k$	channel noise for the $k^{th}$ frequency
$N_o$	noise power spectral density (unilateral)
$P$	number of users
$P_{rxDT}$	received signal power in a DT point
$P_{rxmin}$	minimum received signal level required to establish a connection
$P_{rx}$	received signal power
$P_{tx}$	transmitted power
$P_{rxho}$	handover power
$R$	number of receiving antennas
$Y_k$	received sample for the $k^{th}$ frequency
$\mathbf{I}_N$	$N \times N$ identity matrix
$\mathbf{P}$	correlation coefficients matrix
$\mathbf{a}$	vector with antenna's latitude, longitude and height
$\mathbf{p}$	vector identifying a position with its latitude, longitude and height
$d_{BS}$	distance between BS and the MT
$d_{ho}$	handover distance
$d_{max}$	maximum communication range
$d_{wal}$	minimum distance for application of the Walfish-Ikegami propagation model
$f$	frequency variable
$f(\text{clutter})$	average of weighted losses due to clutter
$h$	height from the obstacle top to the Tx-Rx axis
$h_{BS}$	height of BS
$h_{MT}$	height of MT
$i$	iteration index

$k$	frequency-domain sample index
$n$	time-domain sample index
$p$	user index
$r$	pearson correlation coefficient (chapter 3) / receiving antenna index (chapter 4 and 5)
$x_n$	$n^{th}$ time-domain data symbol
$x_{n,p}$	$n^{th}$ time-domain data symbol of the $p^{th}$ user
$y_n$	$n^{th}$ time-domain received sample
$L_{n,p}^{Im}$	quadrature log-likelihood ratio for the $n^{th}$ time-domain data symbol of the $p^{th}$ user
$L_{n,p}^{Re}$	in-phase log-likelihood ratio for the $n^{th}$ time-domain data symbol of the $p^{th}$ user
$\Delta_{k,p}$	error term for the $k^{th}$ frequency-domain "hard decision" estimate of the $p^{th}$ user
$\Theta_{k,p}$	overall error for the $k^{th}$ frequency-domain symbol of the $p^{th}$ user
$\bar{X}_{k,p}$	"soft decision" for the $k^{th}$ frequency-domain data symbol of the $p^{th}$ user
$\bar{X}_k$	"soft decision" for the $k^{th}$ frequency-domain data symbol
$\bar{x}_{n,p}$	"soft decision" for the $n^{th}$ time-domain data symbol of the $p^{th}$ user
$\bar{x}_n$	"soft decision" for the $n^{th}$ time-domain data symbol
$\hat{P}_{rx}$	estimated values of $P_{rx}$
$\hat{x}_{n,p}$	"hard decision" for the the $n^{th}$ time-domain data symbol of the $p^{th}$ user
$\kappa$	normalisation constant for the FDE
$\lambda$	wavelength
$\Lambda_{k,p}$	diagonal matrix whose elements are the eigenvalues for the $k^{th}$ frequency-domain data symbol of the $p^{th}$ user
$\nu$	Knife-Edge parameter

$\overline{P_{rx}}$	average value of $P_{rx}$
$\overline{\hat{P}_{rx}}$	average value of $\hat{P}_{rx}$
$\rho_p$	correlation coefficient of the $p^{th}$ user
$\sigma_N^2$	variance of the channel noise
$\sigma_S^2$	variance of the transmitted frequency-domain data symbols
$\sigma_{n,p}^2$	variance of the channel noise for the $p^{th}$ user
$\sigma$	standard deviation
$\theta_p$	overall error for the $p^{th}$ user
$\theta_{eleBS}$	antenna electrical tilt
$\theta_{mecBS}$	antenna mechanical tilt
$\theta$	vertical direction between two vector points
$\tilde{X}_k$	estimate for the $k^{th}$ frequency-domain data symbol
$\tilde{X}_{k,p}$	estimate for the $k^{th}$ frequency-domain of the $p^{th}$ user
$\tilde{x}_n$	sample estimate for the $n^{th}$ time-domain data symbol
$\tilde{x}_{n,p}$	sample estimate for the $n^{th}$ time-domain data symbol of the $p^{th}$ user
$\varphi_{BS}$	antenna azimuth
$\varphi$	horizontal direction between two vector points

# Chapter 1

## Introduction

This chapter introduces all the work developed in this research, namely the motivation, the objectives, and how the results were disseminated.

### 1.1 Motivation and Scope

Throughout the years, telecommunications reinforced their importance to society, in particular, due to the ease with which users can establish video and voice communication channels to one another, even at great distances, which represents one of the major factors in the proliferation of telecommunications. This aspect has been crucial in recent times, where people have been forced to work from home, due to COVID-19, and to use home networks that were prepared for the occasional needs of their users. According to the report provided by *Autoridade Nacional de Comunicações Portuguesa* (ANACOM) by April 2020, electronic communications in Portugal had grown 47% in voice traffic and 52% in data traffic compared to previous months [1], in line with other European Union countries. This growth required the European Commission and the Body of European Regulators for Electronic Communications (BEREC) to take preventive measures in order to avoid network congestion allowing for a good Quality of Service (QoS) [2].

From a very early stage, the QoS of each user, which concerns resources and services provided by telecommunications operators, is one of providers' main concerns. In order to offer better quality to users, networks have evolved from a simple analog (1G) network to more complex (4G) networks that support applications with multimedia content, with speed and bandwidth that offer users a good experience. The need for new and improved features lead to the development of the 5<sup>th</sup> generation (5G) mobile networks, which allows connected devices, such as Internet of Things (IoT) devices, and a data rate 1000 times higher when compared to 4G [3]. According to the report presented in [4], it is expected that by 2025 90% of the world population will be covered by 4G technology and 65% by 5G technology, which indicates that there will be an overlap of technologies in the same network, as already happens with 2G, 3G, and 4G technologies. This overlap makes networks heterogeneous and complex.

Heterogeneous networks are a challenge as each of the technologies presents different characteristics meaning that different algorithms for monitoring, planning and optimisation have to be used. This challenge was a fundamental pillar to a Research and Development (R&D) project of MULTIVISION [5], funded by the European Commission, called OptiNet-5G [6]. The main goal of OptiNet-5G project was: *"R&D of functional prototype of Heterogeneous 5G Networks Planning and Optimisation platform, independent of hardware and software, accessible worldwide, with optimised management in a context of Big Data in a Cloud environment that contributes to innovative 5G SON solutions of high industrial value."* [5].

In fact, MULTIVISION owns a Software-as-a-Service (SaaS) tool, called METRIC [7], which enables the monitoring, planning, and optimisation of networks, acting as a facilitator tool in the work of telecommunications engineers. The OptiNet-5G project's main mission was to enable the METRIC platform with new, more robust, and more efficient functionalities for heterogeneous networks, being the ultimate goal to turn these networks into a Self-Organising Network (SON).

The SON paradigm attributes to the networks the characteristic "plug & play" since it is based on four principles: Self-Planning, Self-Deployment, Self-Optimisation, and Self-Healing. These four principles allow the automation of network planning, implementation, and optimisation actions, as well as the automation of preventive actions in the network, reducing human interventions. This network automation reduces operating and investment costs and leads to better QoS for the users [8, 9]. In order to see a network as SON, it is necessary to have good algorithm implementations that are triggered under certain conditions [10].

The METRIC platform is currently used by several operators all over the globe and aggregates Configuration Management (CM), Key Performance Indicators (KPIs), and Drive Tests (DTs) for each of the network cells. The information generated per cell in each time period is large and implies the storage of a huge amount of data in different formats. This stored information can later be used through the Big Data concept [11]. Like other platforms on the market, such as ATOLL [12], the METRIC platform is vendor and technology-agnostic, however its greatest advantage compared to the others is the fact that it is not an application installed locally on a machine, but a remote application that uses cloud services, namely Amazon Web Services (AWS) [13], in specific microservices such as AWS Lambda, Amazon Elastic Compute Cloud (Amazon EC2), or Amazon Simple Storage Service (Amazon S3). This use of cloud resources allows easier distribution of the solution, easier access, faster processes, more dynamic use, improved storage capacity, and scalability of networks.

Being technology-agnostic, the METRIC platform aggregates data from different equipment and manufacturers whose formats are quite distinct. Initially, after being inserted in the METRIC platform and before being correctly stored for future use, the data undergoes a process called Extracts, Transforms and Loads (ETL) that normalises it in a pre-defined format, being then available for any type of use.

In order to match the SON concept, the METRIC platform must be able to use all the data collected from the Operations Support System (OSS) and the Radio Access Network (RAN) and apply it to correct small faults, in coverage, or to

help operators when they have to make certain decisions, such as configuring new antennas to offer better services for a given area.

Coverage is the core for all network planning and has always been one of the main problems operators deal with, as poor coverage implies a bad experience for the end customer [14]. An accurate coverage estimation allows not only better planning, but also savings through the optimisation of resources, such as cell planning, estimation of neighboring cells, or even the energy efficiency of the antennas. The use of real and updated data in estimating coverage takes networks to a much higher level of excellence since it allows the validation of network coverage conditions in real time.

Coverage estimation is a complex, time-consuming, and resource-intensive process. Nevertheless, it must be done, whenever a network optimisation algorithm is to be applied. In order to simplify these tasks, simplistic models are sometimes used that speed up the whole process. However, these models do not present the best results, which results in a lower capacity for network optimisation. In the METRIC platform, the coverage estimation is done using only theoretical expressions of propagation models. This method does not take into consideration network measures, so it is important to enable the platform with a robust coverage estimation using the real measurements, recomputed whenever there are changes in the data, being quickly accessible when its use is necessary. This work intends to extend the platform with these features.

Although networks are providing more and more services to users, a new technology that will be based on new prerequisites and new functionalities is being developed. This new technology will replace the systems with one transmitting and receiving antenna, named Single Input, Single Output (SISO) systems, by systems with multiple transmitting and receiving antennas, named Multiple Input, Multiple Output (MIMO) or its extension with a large number of antennas Massive MIMO (mMIMO) systems [15]. This evolution implies that part of the work done for SISO systems will have to be extended to these new systems. This is the case for the propagation models which have been created and modeled specifically for

SISO systems and their use is no longer consistent with other systems. It is therefore important to know how the propagation models used in SISO systems can be applied to MIMO systems and also understand what is the impact of that change. The great majority of the propagation models created for SISO systems use DT measures and since the realisation of DTs campaigns is a very time-consuming and expensive task, it would be useful to understand how the DTs collected in SISO systems can be applied in MIMO systems.

Another need of these systems is related to the performance of the telecommunication receivers that are used in devices since they influence the users' experience. These receivers need to have certain characteristics, such as being energy efficient in order to increase the battery life of the mobile devices [16].

## 1.2 Objectives

The coverage estimation is essential for the correct planning and operation of telecommunications networks, so this thesis intends to study the signal estimation and present a propagation model that can accurately represent the current state of the network, using real network measurements to predict the signal received for a given area. This model should be automatically triggered when certain network conditions are reached and should store the calculated information in order to enable its use in network optimisation tools.

Another objective is to present a methodology for using propagation models created for SISO systems in MIMO systems. This model extension methodology should be simple and should be capable of being used with any propagation model in order to allow for the use of these existing models without the need to create new ones.

Finally, the question of the efficiency of MIMO receivers should also be studied in order to present receivers that achieve good performance results with reduced

complexity. This improvement in performance allows an optimisation of the coverage when changing from a SISO system to a MIMO system.

### 1.3 Contributions of Research

The last years of research have allowed some research questions to be answered, which have resulted in several publications both in conferences and journals. This research not only allowed the development of other types of scientific materials with great relevance, like a new propagation model, but it was also the basis for parallel research in cellular planning and efficient network management. Although the most important articles resulting from this research are presented in the following chapters, it is important to highlight all the contributions of this research work in the next subsection. In summary, the work developed in the research for this thesis resulted in publications in International Journals (IJ), International Conferences (IC), National Conference (NC), Deliverable Reports (DR) and Prototype (PR). In terms of quantity these are:

- **IJ** - 4 publications as first author and 3 as co-author;
- **IC** - 4 publications as first author and 6 as co-author;
- **NC** - 1 publication as first author;
- **DR** - 5 publications as co-author;
- **PR** - 1 prototype as author.

Table 1.1 presents in chronological order the contributions achieved.

TABLE 1.1: Timeline of contributions.

---

June'17 ···•	<b>IC1</b> Iterative Receiver Combining IB-DFE with MRC for Massive MIMO Schemes.
--------------	---

Sept.'17 .. •	<b>IC2</b> Efficient frequency-domain detection for massive MIMO systems.
Sept.'18 .. •	<b>IC3</b> Combining Drive Tests and Automatically Tuned Propagation Models in the Construction of Path Loss Grids.
Nov.'18 .. •	<b>NC1</b> Enhanced MIMO Techniques for 5G.
Feb.'19 .. •	<b>DR1</b> Technical, Economical and Environmental Optimisation Modules.
Feb.'19 .. •	<b>DR2</b> Operation of the Technical Optimisation Modules.
Apr.'19 .. •	<b>DR3</b> Testing and Evaluation of Modules.
Apr.'19 .. •	<b>DR4</b> Tests and intermediate Evaluation of Module Integration.
Aug.'19 .. •	<b>DR5</b> Tests and Final Evaluation and Acceptance of the Prototype Produced.
Sept.'19 .. •	<b>IC4</b> Combining Measurements and Propagation Models for Estimation of Coverage in Wireless Networks.
Sept.'19 .. •	<b>IC5</b> Traffic Forecast in Mobile Networks: Classification System Using Machine Learning.
Nov.'19 .. •	<b>IC6</b> Integration of a Cloud-Based Realistic and Automatic Coverage Estimation Methodology in Metric SaaS.
Nov.'19 .. •	<b>IC7</b> Cloud-based Implementation of an Automatic Pixel-based Neighbour Identification System for Cellular Networks.
Nov.'19 .. •	<b>IC8</b> Cloud-based Cellular Network Planning System: Proof-of-Concept Implementation for GSM in AWS.
Nov.'19 .. •	<b>IC9</b> Cloud-based Implementation of a SON Automatic Planning System: a proof-of-concept for UMTS.
Nov.'19 .. •	<b>IC10</b> Assessment of Traffic Prediction Models for Mobile Communication Networks.
Dec.'19 .. •	<b>PR1</b> Automatically Calibrated Standard Propagation Model.
Mar.'20 .. •	<b>IJ1</b> Analytical Performance Evaluation of Massive MIMO Techniques for SC-FDE Modulations.
Apr.'20 .. •	<b>IJ2</b> Cloud-Based Implementation of an Automatic Coverage Estimation Methodology for Self-Organising Networks.
Apr.'20 .. •	<b>IJ3</b> Automatic Coverage Based Neighbour Estimation System: A Cloud-Based Implementation.

Apr.'20 ..	•	<b>IJ4</b> A Novel Way to Automatically Plan Cellular Networks Supported by Linear Programming and Cloud Computing.
July'20 ..	•	<b>IJ5</b> Comparison of Artificial Intelligence and Semi-Empirical Methodologies for Estimation of Coverage in Mobile Networks.
Sept.'20 ..	•	<b>IJ6</b> Estimating the performance of MIMO SC-FDE systems using SISO measurements.
Sept.'20 ..	•	<b>IJ7</b> Cloud-based Implementation of a SON Radio Resources Planning System for Mobile Networks and Integration in SaaS Metric.

---

The information of each of the contributions is now detailed, including the Scimago/Scopus Journal Ranking, beginning with the publications in peer reviewed International Journals (IJ):

- IJ1**     D. Fernandes, F. Cercas and R. Dinis, "**Analytical Performance Evaluation of Massive MIMO Techniques for SC-FDE Modulations**," Electronics, vol. 9, no. 3, p. 533, Mar. 2020, Quartile 2, Digital Object Identifier (DOI):10.3390/electronics9030533. [17].
- IJ2**     D. Fernandes, D. Clemente, G. Soares, P. Sebastião, F. Cercas, R. Dinis and L. S. Ferreira, "**Cloud-Based Implementation of an Automatic Coverage Estimation Methodology for Self-Organising Network**," IEEE Access, vol. 8, pp. 66456-66474, Apr. 2020, Quartile 1, DOI:10.1109/ACCESS.2020.2986437. [18].
- IJ3**     P. Pina, A. Godinho, D. Fernandes, D. Clemente, P. Sebastião, G. Soares and L. S. Ferreira, "**Automatic Coverage Based Neighbour Estimation System: A Cloud-Based Implementation**," IEEE Access, vol. 8, pp. 69671-69682, Apr. 2020, Quartile 1, DOI:10.1109/ACCESS.2020.2986755. [19].
- IJ4**     A. Godinho, D. Fernandes, G. Soares, P. Pina, P. Sebastião, A. Correia and L. S. Ferreira, "**A Novel Way to Automatically Plan Cellular**

- Networks Supported by Linear Programming and Cloud Computing,"** Applied Sciences, vol. 10, no. 9, p. 3072, Apr. 2020, Quartile 1, DOI:10.3390/app10093072. [20].
- IJ5** D. Fernandes, A. Raimundo, F. Cercas, P. Sebastião, R. Dinis and L. S. Ferreira, "**Comparison of Artificial Intelligence and Semi-Empirical Methodologies for Estimation of Coverage in Mobile Networks,**" IEEE Access, vol. 8, pp. 139803-139812, July 2020, Quartile 1, DOI:10.1109/ACCESS.2020.3013036. [21].
- IJ6** D. Fernandes, F. Cercas, R. Dinis and P. Sebastião, "**Estimating the performance of MIMO SC-FDE systems using SISO measurements,**" Applied Sciences, vol. 10, no. 21, p. 7492, Oct. 2020, Quartile 1, DOI:10.3390/app10217492. [22].
- IJ7** R. Cortesão, D. Fernandes, G. Soares, D. Clemente, P. Sebastião and L. S. Ferreira, "**Cloud-based Implementation of a SON Radio Resources Planning System for Mobile Networks and Integration in SaaS Metric,**" Submitted, under peer review in *IEEE Access*, Quartile 1, [23].

The publications in peer reviewed International Conferences (IC) are the following:

- IC1** D. Fernandes, F. Cercas and R. Dinis, "**Iterative Receiver Combining IB- DFE with MRC for Massive MIMO Schemes,**" Procedia Computer Science, vol. 109, June 2017, pp. 305–310, DOI:10.1016/j.procs.2017. 05.356. [24].
- IC2** L. Cabral, D. Fernandes, F. Cercas and R. Dinis, "**Efficient frequency-domain detection for massive MIMO systems,**" 2017 South Eastern European Design Automation, Computer Engineering, Computer Networks and Social Media Conference (SEEDA-CECNSM), Kastoria, 2017, pp. 1-5, DOI:10.23919/SEEDA-CECNSM.207.8088227. [25].

- IC3** D. Fernandes, L. S. Ferreira, M. Nozari, P. Sebastião, F. Cercas and R. Dinis, "**Combining Drive Tests and Automatically Tuned Propagation Models in the Construction of Path Loss Grids**," 2018 IEEE 29<sup>th</sup> Annual International Symposium on Personal, Indoor and Mobile Radio Communications (PIMRC), Bologna, 2018, pp. 1-2, DOI:10.1109/PIMRC.2018.8580708. [26].
- IC4** D. Fernandes, G. Soares, D. Clemente, R. Cortesão, P. Sebastião, F. Cercas, R. Dinis and L. S. Ferreira, "**Combining Measurements and Propagation Models for Estimation of Coverage in Wireless Networks**," 2019 IEEE 90<sup>th</sup> Vehicular Technology Conference (VTC2019-Fall), Honolulu, Hawaii, Sept, 2019, pp. 1-5, DOI:10.1109/VTCFall.2019.8891451. [27].
- IC5** D. Clemente, G. Soares, D. Fernandes, R. Cortesão, P. Sebastião and L. S. Ferreira, "**Traffic Forecast in Mobile Networks: Classification System Using Machine Learning**," 2019 IEEE 90<sup>th</sup> Vehicular Technology Conference (VTC2019-Fall), Honolulu, Hawaii, Sept, 2019, pp. 1-5, DOI:10.1109/VTCFall.2019.8891348. [28].
- IC6** D. Fernandes, G. Soares, D. Clemente, R. Cortesão, P. Sebastião, F. Cercas, R. Dinis and L. S. Ferreira, "**Integration of a Cloud-Based Realistic and Automatic Coverage Estimation Methodology in Metric SaaS**," 2019 22<sup>nd</sup> International Symposium on Wireless Personal Multimedia Communications (WPMC), Lisbon, Portugal, 2019, pp. 1-4, DOI:10.1109/WPMC48795.2019.9096207. [29].
- IC7** P. Pina, A. Godinho, D. Fernandes, D. Clemente, G. Soares, P. Sebastião and L. S. Ferreira, "**Cloud-based Implementation of an Automatic Pixel-based Neighbour Identification System for Cellular Networks**," 2019 22<sup>nd</sup> International Symposium on Wireless Personal Multimedia Communications (WPMC), Lisbon, Portugal, 2019, pp. 1-6, DOI:10.1109/WPMC48795.2019.9096084. [30].

- IC8** A. Godinho, D. Fernandes, D. Clemente, G. Soares, P. Sebastião, P. Pina and L. S. Ferreira, "**Cloud-based Cellular Network Planning System: Proof-of-Concept Implementation for GSM in AWS**," 2019 22<sup>nd</sup> International Symposium on Wireless Personal Multimedia Communications (WPMC), Lisbon, Portugal, 2019, pp. 1-5, DOI:10.1109/WPMC48795.2019.9096082. [31].
- IC9** R. Cortesão, D. Fernandes, D. Clemente, G. Soares, P. Sebastião and L. S. Ferreira, "**Cloud-based Implementation of a SON Automatic Planning System: a proof-of-concept for UMTS**," 2019 22<sup>nd</sup> International Symposium on Wireless Personal Multimedia Communications (WPMC), Lisbon, Portugal, 2019, pp. 1-6, DOI:10.1109/WPMC48795.2019.9096060. [32].
- IC10** D. Clemente, D. Fernandes, R. Cortesão, G. Soares, P. Sebastião and L. S. Ferreira, "**Assessment of Traffic Prediction Models for Mobile Communication Networks**," 2019 22<sup>nd</sup> International Symposium on Wireless Personal Multimedia Communications (WPMC), Lisbon, Portugal, 2019, pp. 1-4, DOI:10.1109/WPMC48795.2019.9096098. [33].

In terms of National Conference (NC), the contribution is:

- NC1** D. Fernandes, F. Cercas, and R. Dinis, "**Enhanced MIMO Techniques for 5G**," Poster presentation at Instituto de Telecomunicações, Aveiro, Portugal, Nov. 2018. [34].

The detailed information of the Deliverable Reports (DR), peer reviewed and approved by an independent commission is the following:

- DR1** Multivision, "**Technical, Economical and Environmental Optimisation Modules**," Deliverable Report D4.1, OptiNet-5G Project, Lisbon, Feb. 2019, (translated from Portuguese). [35].

- DR2** Multivision, "**Operation of the Technical Optimisation Modules**," Deliverable Report D4.2, OptiNet-5G Project, Lisbon, Feb. 2019, (translated from Portuguese). [36].
- DR3** Multivision, "**Testing and Evaluation of Modules**," Deliverable Report D6.1, OptiNet-5G Project, Lisbon, Apr. 2019, (translated from Portuguese). [37].
- DR4** Multivision, "**Tests and intermediate Evaluation of Module Integration**," Deliverable Report D6.2, OptiNet-5G Project, Lisbon, Apr. 2019, (translated from Portuguese). [38].
- DR5** Multivision, "**Tests and Final Evaluation and Acceptance of the Prototype Produced**," Deliverable Report D6.3, OptiNet-5G Project, Lisbon, Aug. 2019, (translated from Portuguese). [39].

Finally, the Prototype (PR) information is:

- PR1** D. Fernandes, D. Clemente, G. Soares, P. Sebastião, F. Cercas, R. Dinis and L. S. Ferreira, "**Automatically Calibrated Standard Propagation Model**," OptiNet-5G Project, Lisbon, Dec. 2019. [40].

## 1.4 Thesis Overview

In this subsection an overview of the thesis is presented, highlighting and interconnecting all the contributions identified in the former subsection 1.3. In order to demonstrate this, all the subjects addressed in this thesis and all their links are illustrated in Figure 1.1, which is composed of five layers and represents the vision of a cellular network. The lower layer, called the *Users layer*, is where all the Mobile Terminal (MT) using the services provided by the upper layer (the *RAN layer*) are found. In the *RAN layer*, there are the Base Station (BS), responsible for covering certain areas, which communicate with the MT, generating traffic that is exchanged between these two layers. The layer above the RAN is one of

the most important because it is in this layer, called the *OSS*, that the monitoring information and performance indicators are aggregated, also being possible to manage the network configurations. Since each manufacturer has an OSS with specific characteristics, it is important to ensure that data is standardised for future use. This normalisation and aggregation of data occurs in the *METRIC SaaS layer* where the ETL normalisation process is applied. Once all data is normalised, it is ready to be applied in the *Research Framework layer*. This last layer presents the investigation developed in this thesis and in the OptiNet-5G project, depicting the inputs, the algorithms identification, and the output. The information given by Figure 1.1 is detailed throughout this thesis.

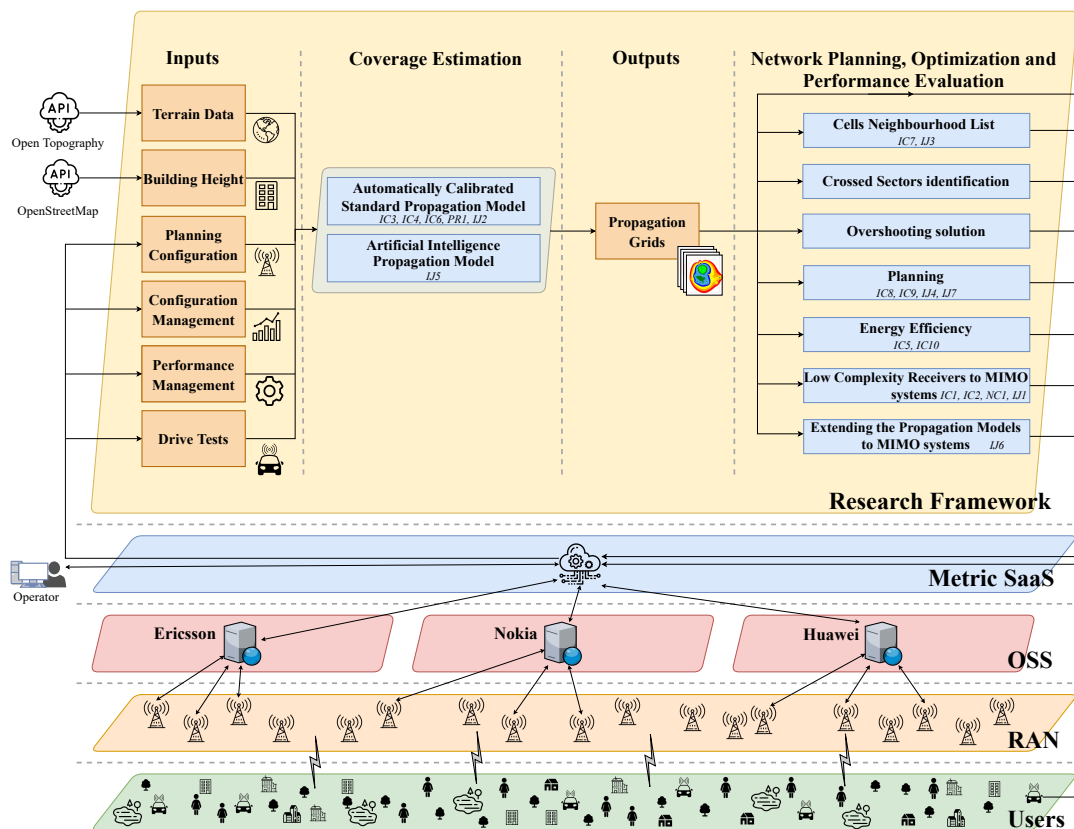


FIGURE 1.1: Synthesis of research identifying all contributions.

Part of this thesis is inserted in the OptiNet-5G project, which foresaw the precise estimation of the coverage. This estimation combines data from real networks, such as DT, and well-known propagation models, such as Standard Propagation Model (SPM) [12] and Walfish-Ikegami [41]. The estimation is always done in the

area that surrounds an antenna and always resulted in a grid where the propagation is represented. In Figure 1.2 it is possible to analyse the evolution of the results achieved from a Nordic 4G network, being initially a fairly rudimentary grid, as in [26], and later a more robust one, as in [18].

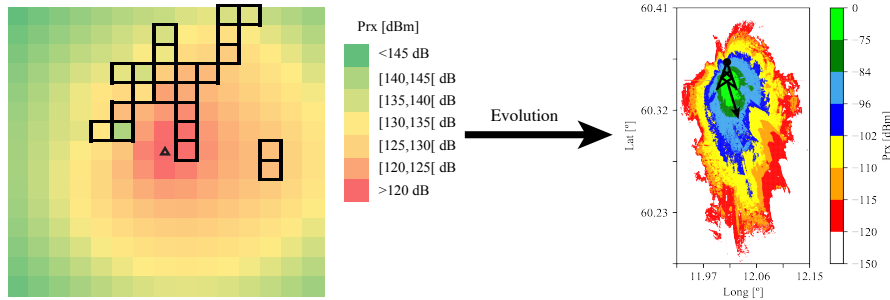


FIGURE 1.2: Evolution of the results achieved in coverage estimation.

The constant improvement in signal coverage estimation led to the development of a propagation model, called Automatically Calibrated Standard Propagation Model (ACSPM) [18], depicted in Figure 1.1 and detailed in **PR1** [40] and **IJ2** [18] which was implemented with AWS microservices and integrated into the METRIC platform. This new model computes the signal coverage in two different moments: Initially, a pre-grid with all the information in which temporal variation is quite reduced, such as the gain of the transmitter antenna at that point, the elevation of the terrain, among other parameters, is computed. At a second moment, the data resulting from the first step is combined with data from DTs in order to estimate the signal coverage in specific for that region. The implementation and integration of the model using microservices in the cloud allows not only a faster computation of results but also their faster representation. Initially, for the SISO systems, a propagation model was proposed which has been modified and refined several times. Each iteration is explained in **IC3** [26], **IC4** [27] and **IC6** [27]. The final version of the propagation model, its integration with the METRIC platform and the respective accuracy analysis is presented in **IJ2** [18] and described in Chapter 2.

Although the results achieved by the ACSPM were quite reasonable, they were only possible due to the use of large quantities of DTs for the same antenna, which

is not always possible. Initially, when the location of a new antenna is planned, the DT data does not exist, and even in an already implemented and functioning antenna, the cost associated with the realisation of DTs may be a prejudicial factor in its collection. Thus, the ACSPM may represent some gaps when assessing the impact of placing a new antenna.

In order to minimise the problem of using the ACSPM, a new solution was conceived, the Artificial Intelligence Propagation Model (AIPM) [21], identified in Figure 1.1 by **IJ5** [21], which, despite being based on DT data, presents some advantages. This new solution was based on Artificial Neural Networks (ANNs) and allowed to create a propagation model that can be applied in a given geographical area. This model is completely agnostic to any previous knowledge of radio propagation and is trained on the basis of DT information from antennas in a given geographical area. In this way, it can be used to verify the impact on the network when installing a new antenna in the geographical area with the same characteristics as the area where the DTs were collected. The creation of the AIPM, its validation, and comparison with the ACSPM is presented in **IJ5** [21] and in Chapter 3.

As mentioned before, the propagation models presented were validated using real network data obtained through the METRIC platform. Unfortunately, the operators who use this platform to manage their networks only use SISO systems and there are no scenarios in these networks where MIMO systems are used, even for the simplest ones where only two antennas are considered. Due to this situation, the large amount of DTs available are always related to SISO systems which are not valid for MIMO systems.

As it would be useful to understand how the DTs collected in SISO systems can be applied in MIMO systems the **IJ6** [22], identified in Figure 1.1, presents a methodology for extending the applicability of the SISO system propagation models to MIMO systems described in this thesis in Chapter 4, where for a given Bit Error Rate (BER) performance, the expressions that represent the impact experienced with this change of systems are presented. Once these impact expressions

are obtained, it is possible to use the results obtained from the coverage estimation by the propagation models for SISO systems and to calculate the new coverage estimation if that system is replaced by a MIMO system. In order to present the results of this system substitution it was considered one of the scenarios presented in Chapter 3, which was for a SISO system, and it is explained how the coverage area would be affected if this system was composed by a MIMO system. Of course, this analysis is only valid for the specific case under study and for the receiver considered, which in this case was the Iterative Block Decision Feedback Equalization (IB-DFE). The analysis of the results achieved led to the conclusion that the better the BER performance achieved by the receiver considered, i.e. the closer the BER performance is to Matched Filter Bound (MFB), the smaller the reduction in the coverage area when compared to the coverage area for the SISO system.

As explained, the new telecommunications technology may use MIMO systems, however, these systems may be expanded to massive MIMO systems, where the number of antennas is much higher. The receivers thought for MIMO systems present good a performance, however when these receivers are applied in mMIMO systems this performance is reduced since the complexity associated with the algorithms increase, reducing the coverage area when compared to a SISO system.

In order to enable the use of mMIMO systems with receivers that reach BER performances close to the MFB, it is important to reduce the complexity associated to the algorithms and in this case, contrary to what was studied in the first chapters of this thesis, the scenario considered is no longer the communication between BS and MT (downlink) but the uplink communication (MT-BS). This complexity of the algorithms is related to the type of receiver used and the performance it reaches, there must always be a trade-off between performance and complexity.

As presented in Figure 1.1 a comparative study of three receivers, the IB-DFE, the Maximum Ratio Combining (MRC), and a receiver that combines the IB-DFE and the MRC, is presented in **IJ1** [17], which joins and extends the works carried out along several International Conferences (**IC1** [24] and **IC2** [25]), and National

Conferences (**NC1** [34]). This comparison is detailed in Chapter 5. The complexity of each of these receivers is different, as is the BER performance achieved, which is also compared with the MFB performance.

As it can be observed in Figure 1.1, this research has introduced a new approach for network error correction such as cross sectors or overshooting and also to develop new planning algorithms such as the creation of cell neighbouring lists **IC7** [30], **IJ3** [19], planning of 2G, 3G and 4G networks **IC8** [31], **IC9** [32], **IJ4** [20], **IJ7** [23], and optimisation of energy resources in the networks **IC5** [28], **IC10** [33]. All these network optimisation algorithms, as well as the propagation model, were implemented and integrated into the METRIC platform, however before being fully integrated they were completely tested and the results were presented along the Deliverable Reports **DR1** [35], **DR2** [36], **DR3** [37], **DR4** [38] and **DR5** [39].

Finally, in Chapter 6, the thesis conclusions and future directions of research are discussed.



## Chapter 2

# Novel Semi-Empirical Propagation Model

The article presented in this chapter describes in detail the creation, implementation, and integration of a novel cloud-based framework of a semi-empirical propagation model which is validated in a real scenario. This model, to realistically portray the propagation environment, uses real measures in the estimation of the signal coverage. The implementation of this model using cloud services, the integration in the METRIC platform, and the triggers for its activation are also described.

Some paper details:

- **Title:** Cloud-Based Implementation of an Automatic Coverage Estimation Methodology for Self-Organising Network;
- **Date of publication:** April 2020;
- **Journal:** IEEE Access;
- **Scimago/Scopus Journal Ranking:** Quartile 1;
- **Publisher:** IEEE.

# Cloud-Based Implementation of an Automatic Coverage Estimation Methodology for Self-Organising Network

DANIEL FERNANDES<sup>1</sup>, DIOGO CLEMENTE<sup>1</sup>, GABRIELA SOARES<sup>2</sup>, PEDRO SEBASTIÃO<sup>1</sup>, (Member, IEEE), FRANCISCO CERCAS<sup>1</sup>, (Senior Member, IEEE), RUI DINIS<sup>3</sup>, (Senior Member, IEEE), AND LÚCIO S. FERREIRA<sup>2,4,5</sup>, (Senior Member, IEEE)

<sup>1</sup>Instituto Universitário de Lisboa (ISCTE-IUL)/IT—Instituto de Telecomunicações, Av. das Forças Armadas, 1649-026 Lisbon, Portugal

<sup>2</sup>Multivision—Consultoria, Rua Soeiro Pereira Gomes, Lote N.º 1, 3.º C, 1600-196 Lisbon, Portugal

<sup>3</sup>FCT—Universidade Nova de Lisboa, Monte da Caparica, 2829-516 Caparica, Portugal

<sup>4</sup>ISTEC, A. das Linhas de Torres 179, 1750-142 Lisboa, Portugal

<sup>5</sup>INESC—ID/COPELABS Lusófona University, Campo Grande, 376, 1749-024 Lisbon, Portugal

Corresponding author: Daniel Fernandes (dfsfs@iscte-iul.pt)

This work was supported in part by the OptiNET-5G project and co-funded by the Centro2020, Portugal2020, and European Union under Project 023304, in part by the Instituto de Telecomunicações, FCT/MCTES through national funds and co-funded by the EU funds under Project UIDB/EEA/50008/2020.

**ABSTRACT** One of the main concerns of telecommunications operators is related to network coverage. A weak coverage can lead to a performance decrease, not only in the user experience, when using the operators' services, such as multimedia streaming, but also in the overall Quality of Service. This paper presents a novel cloud-based framework of a semi-empirical propagation model that estimates the coverage in a precise way. The novelty of this model is that it is automatically calibrated by using drive test measurements, terrain morphology, buildings in the area, configurations of the network itself and key performance indicators, automatically extracted from the operator's network. Requirements and use cases are presented as motivations for this methodology. The results achieve an accuracy of about 5 dB, allowing operators to obtain accurate neighbour lists, optimise network planning and automate certain actions on the network by enabling the Self-Organising Network concept. The cloud implementation enables a fast and easy integration with other network management and monitoring tools, such as the Metric platform, optimising operators' resource usage recurring to elastic resources on-demand when needed. This implementation was integrated into the Metric platform, which is currently available to be used by several operators.

**INDEX TERMS** Cloud implementation, coverage estimation, drive tests, measurements, propagation model.

## I. INTRODUCTION

Nowadays, there is an increasing demand of mobile users, which also increases the use of telecommunication services, making network coverage estimation a concern for operators. According with [1], in 2018 75% of world population was covered by 4G technology and with a predicted increase to 90% in 2025. In 2025 it is also expected that about 65% of world population will be covered by 5G technology. A correct estimation allows operators, not only the guarantee of a better network coverage delivery to its users, but also to perform an efficient optimisation of their resources. This

estimation can be done by using several tools, from various vendors [2], [3], that are commercially available. These tools have important features that are very useful to telecommunication operators. However, most of these tools, like [4], require local installation on the operator's machine, and the network planning configuration tasks can be difficult and time-consuming.

To simplify the planning process of a network, this paper presents a novel cloud-based framework of a semi-empirical propagation that using Drive Test (DT) measurements, terrain morphology, buildings information and configurations of the network itself to estimate the coverage in a precise way. This optimised propagation model uses a cloud-based implementation, which allows its integration into a tool for

The associate editor coordinating the review of this manuscript and approving it for publication was Danping He<sup>1</sup>.

monitoring and management of telecommunications networks, called Metric.

Several studies [5], [6] combine propagation models with DT measurements in order to define a realistic propagation model, each time the telecommunications operator wants. We observe that these studies use propagation models that are only applicable to specific macro or micro cells scenarios. In the literature we can also find adaptive systems capable of performing automatic selection of the propagation model according to the scenario (micro and macro cells) [7]. We observe that these different propagation models can only be used under specific conditions, also specifying antenna distance or height. The proposed propagation model intends to overcome these situations and to be generally applicable, regardless of the scenario or antenna properties, for example. In addition, the main novelty of this propagation model is that it is automatically calibrated with drive tests as well as network Key Performance Indicators (KPIs), providing a realistic estimation of path loss without the need for this calibration to be triggered by the user.

This work extends the ideas presented in [8]–[10], where the cell reach value and the handover distance were considered in the calibration of the model. These authors, namely in [9] and [10], include the terrain morphology but they omit the possibility of a Line of Sight (LoS) between the Mobile Terminal (MT) and the Base Station (BS). Despite the cloud implementation, using Amazon Web Services (AWS), has already been used in [10], this proposed work presents further enhancements that generalise and increase its precision, mostly related with fine-tuning of our propagation model. Several aspects, such as the reuse of previous DT measurements and the application of LoS between the Mobile Terminal (MT) and the Base Station (BS) were also considered. One of the novelties of this work is the inclusion of an evaluation metric that allows to estimate the performance of the proposed propagation model. A very important feature of our propagation model is that it fully automates network coverage estimation, while maintaining a simple user intervention, and all aspects of it are carefully detailed. This model can be used by telecommunication operators not only for coverage estimation based in new DT measurements, but also for cell and KPI configurations.

Proposed semi-empirical propagation model, named Automatically Calibrated SPM (ACSPM) presents several innovations. This model integrates various types of KPIs, network configurations, different propagation models, terrain morphology data (as accurate as possible) and the LoS between the Mobile Terminal (MT) and Base Station (BS). The grid is dynamically created. In this paper, the implementation with cloud services, the integration in the Metric platform and the various application for this work, like the network coverage estimation, the crossed sectors identification, the 2G, 3G and 4G planning and the traffic prediction, are presented.

The cloud implementation of the ACSPM enables the Metric platform to have several users to access resources simultaneously, such as the coverage of an antenna. It is also

possible to execute multiple tasks at the same time, allowing the user to perform other actions while, e.g. the platform is computing a cell coverage. After the model is integrated into the Metric platform it is possible for telecommunications operators, not only to visualise the realistic area that a given cell covers, but also to optimise the entire network, namely in the establishment of neighbouring cells list.

The main contribution of this paper is the creation of a novel generalised and new semi-empirical propagation model that can be applied simultaneously in micro and macro cell scenarios. This propagation model introduces the innovation of being automatically calibrated with DTs as well as network KPIs, providing a realistic estimation of path loss each time data related to the antenna (tilt, azimuth, KPIs, DTs) is added or changed. The automation of the calibration process follows the Self-Organising Network (SON) paradigm, makes it possible to reduce the human effort, which results in a financial impact on the management of these networks. The overall accuracy achieved by using this ACSPM model, through the use of new measurements and the constant update and storage of results in the cloud, allows telecommunications operators to efficiently plan and optimise their 2G, 3G and 4G and 5G networks and to identify possible problems within their network configurations. The implementation of this methodology is based on cloud-services, efficiently providing elastic, on-demand and pay-per-use computation and storage resources. The resulting work pattern proves to be effective in the integration of various inputs and in the provision of realistic estimations of received signal levels around antennas, essential for network planning and optimisation.

The paper has the following structure: In Section II motivation for the use of cloud-based software as a service solutions, is presented, highlighting the tool Metric where this methodology is implemented and integrated. Key aspects related to the estimation of coverage in cellular networks are presented in Section III. In Section IV a unified coverage estimation methodology and use cases are presented, being the coverage estimation detailed in Section V. In Section VI, the implementation using AWS and its integration in Metric platform is presented. To test and evaluate the proposed model, Section VII presents a reference scenario and performance evaluation results are shown in Section VIII. Section IX highlights several applications where the proposed ACSPM is currently used and the conclusion of this paper is presented in Section X.

## II. PLANNING AND OPTIMISATION TOOLS, PARADIGMS AND CLOUD-SERVICES

This section presents an overview of the tools, paradigms and services related or useful for the management of telecommunication networks.

There is currently a growing demand for services accessed through mobile devices, which represents a problem for telecommunications operators due to the excessive usage of network resources. This demand, which is in constant growing, makes mobile networks more complex and dense,

resulting also in a more complex planning and optimisation requirements.

As each operator seeks to provide the best service for its customers, there is a major concern for proper planning and optimisation of mobile networks. Several vendors like Nokia [2] and Huawei [3], associated with the equipment they sell, provide planning and optimisation software. Each vendor has associated an Operations Support System (OSS), which congregates configuration parameters as well as KPIs. Still, these software products are proprietary, vendor-specific. Telecommunications operators must recur to these expensive tools from various vendors, not being able to have a unified vision of their network. Vendor-agnostic tools, like Atoll [4], installed on a local machine, enable the planning and optimisation of their network, independently of the vendor, as long as these follow the standards of each technology - Global System for Mobile Communications (GSM), Universal Mobile Telecommunication System (UMTS), or Long Term Evolution (LTE). These can be also associated to the OSS, although, this process requires additional configurations.

Besides the vendors' heterogeneity, telecommunications operators have heterogeneous networks as well. Within the same network, technologies such as 2G, 3G and 4G coexist and interact, each one with different specificities. The networks' densification, the increasing number of users, and the quality assurance demand for telecommunication operators force networks to continuously generate a huge amount of information per cell and per user. One way to monitor the network's performance is through the several available KPIs which results from a mathematical manipulation of several counters (component information). To increase the network's quality, it is possible to optimise the various cell's configuration parameters to reach the optimal configuration and the consequent optimal performance, required by operators.

Once there is a considerable amount of information per cell and per user through time, the generated data can be analysed through a big data approach. The concept of big data considers the volume and the variety of data, the value generated through analysis, the velocity at which the data is generated and processed. An example of big data application is to acquire dynamic data from different sources, in different formats [11]. Big data methods have been used in recent studies to implement Self-Organising Network [12]–[14]. SON aims to reduce operational costs, investment costs and offers a better Quality of Service (QoS) to users [15]. The description of some use cases related to SON is present in [16] and some of these implementations are presented below:

- Self-Planning - When a node is added to the network, the site location and hardware settings are selected;
- Self-Deployment - This implementation receives the data from Self-Planning and performs the installation and validation of the node;
- Self-Optimisation - Using data obtained from network users, such as MT, the network settings are automatically adjusted;

- Self-Healing - A set of preventive actions keeps the network operational and prevents disruptive network problems from arising.

These four use cases can associate the use of SON networks as networks with the “plug & play” feature. This feature can be useful for telecommunication operators, since it can simplify the implementation and maintenance of the network. Whenever an incident is detected, the network can minimise its effect until a permanent resolution decision is made.

With the advance of SON networks, the volume of data useful for the correct operation of the network has increased, and this data may no longer require human intervention in its handling. Ideally, the information should be collected and automatically made available to the SON algorithms [17]. In this paper, in order for this automation to be easily implemented, all the adjacent computing processes were migrated to a cloud-based implementation. This migration presents the advantages of a cloud-based implementation being very scalable and ready for big data manipulation. This implementation provide users with storage and processing services.

Cloud services are a solution based on a flexible, scalable and abstract infrastructure for the user. One of the main advantages of using cloud-based services is that the user can explore all the available resources and is only charged on the applications used in a per-second price basis, which corresponds to the effective running time of processing nodes. Another advantage of these services is that they are always available and accessible through any device connected to Internet. There are many public cloud providers such as Amazon Web Services (AWS) [18], Google Cloud [19], Microsoft Azure [20].

However, in order to be able to migrate the management of the telecommunications network to the cloud, it is necessary to make some changes to the core of the network. The functions performed by the Radio Access Network (RAN), namely the management of base stations, are now performed in a centralised component with a cloud-based architecture, called C-RAN or RAN-as-a-Service (RANaaS). This change allows for Network Functions Virtualisation (NFV) and scalability that was previously non-existent [21]. With C-RAN, the management of telecommunications networks can now move to a cloud environment and thus the concept of SON can be applied.

A Software-as-a-Service (SaaS) is a web-based application that does not require any local installation on any computer or server. This avoids machine limitations and constraints, and other operating system related restrictions. A SON solution for telecommunications networks, Metric [22], was developed by Multivision [23]. It is a web-based SaaS application that can be accessed by any browser on any device, enabling the monitoring and maintenance of a network, allowing SON implementation and quick access to information on the current status of the network. Being one of the main objectives the aggregation of data in a single platform, Metric platform is based on a set of modules. These modules allow the upload of data, regardless of the hardware vendors or network data

source. A subsequent manipulation of the data allows them to be visualised on a map, in the form of a table or even in the form of a report. This analysis allows critical situations to be immediately identified in the network, namely crossed feeders, cell in overshooting, missing neighbours and consistency checks. Finally, this platform allows the scheduling of network validation tasks that, depending on the input data, can trigger correction/improvement actions in the network.

### III. ESTIMATION OF COVERAGE IN CELLULAR NETWORKS

The estimation of coverage is of key importance in cellular networks planning. These wireless networks must rely in realistic predictions of coverage of their antennas to efficiently provide service within specific geographical areas, taking into account service requirements and offered traffic load predictions. Several methodologies and procedures are available to estimate coverage in cellular networks and are presented and detailed in this section.

#### A. WIRELESS COVERAGE

Wireless coverage allows MTs to access services and features provided by BSs cells. The aggregation and control of these BS is the responsibility of the RAN. The coverage area of a cell depends on several parameters. Among these parameters are those that defines the transmitted signal such as the position of the antenna, its radiation diagram, the azimuth, the tilt, and the transmission power. The signal received by the MT is the result of the transmitted signal by BS and the path loss attenuation. The location vector  $\mathbf{p}$ , identifying a position with its latitude, longitude and height, the received signal level from antenna  $\mathbf{a}$  operating at frequency  $f$  is given by [24]:

$$P_{rx[\text{dBm}]}(f, \mathbf{a}, \mathbf{p}) = P_{tx[\text{dBm}]}(\mathbf{a}) + G_{tx}(\varphi_p - \varphi_a, \theta_p - \theta_a)_{[\text{dB}]} - L(f, \mathbf{a}, \mathbf{p})_{[\text{dB}]}, \quad (1)$$

where,

- $P_{tx}$  [dBm]: Transmitted power;
- $G_{tx}$  [dB]: Transmitted antenna gain, considering the antenna's vertical and horizontal diagrams, for the vertical  $\theta$  and horizontal  $\varphi$  direction between antenna location vector  $\mathbf{a}$  (antenna latitude, longitude and height,  $h_a$ ), and position  $\mathbf{p}$ , using the deviation of the antenna azimuth  $\varphi_a$  and tilt  $\theta_a$ ;
- $L$  [dB]: Path loss attenuation between  $\mathbf{a}$  and  $\mathbf{p}$  ( $x, y, z$ ) positions.

In order to simplify the process, it is considered that the gain of the receiving antenna is 0 dB.

For an antenna located at vector location  $\mathbf{a}$  its coverage area  $C_a$  is given by the set of points of the service area  $A$  that satisfy the condition:

$$C_a = \{\mathbf{p} \in A : P_{rx[\text{dBm}]}(f, \mathbf{a}, \mathbf{p}) \geq P_{rxmin[\text{dBm}]}\}, \quad (2)$$

where  $P_{rxmin}$  is the system's sensitivity, i.e., the minimum received signal level required to establish a connection with a terminal.

In order for telecommunication operators to provide their services to customers, a preliminary study is carried out on

the locations where the antennas should be placed to obtain a large coverage area. These antennas can be divided according to their function, having macro-cells that are responsible for the coverage, the micro-cells responsible for the capacity and the femto-cells that provide the capacity to specific zones.

A weak cellular planning can lead to gaps in coverage and the proper provision of services to users is impossible. It is therefore essential to correctly estimate coverage in order to allow a correct configuration of parameters such as identification of neighbouring cells and identification of overshooting or crossed sectors problems.

#### B. PROPAGATION MODELS

A propagation model attempts to represent how an electromagnetic signal propagates, and has two types of application [25]:

- 1) Plan, design, test and validate a wireless system;
- 2) Optimisation of wireless systems. Operators use these models, which represent reality accurately as possible, to simulate the impact in the network when certain parameters are modified.

According to [26], [27], propagation models can be classified according to the type of information used. They can be classified as:

- *Empirical*: Empirical models are created through field measurements, while not considering the terrain information. They represent a particular propagation environment. This has the advantage that these models are simple and efficient to use. However, it has the disadvantage that it cannot be used in another environment without being updated.
- *Semi-Empirical*: While empirical models are specific to a particular propagation environment, semi-empirical models use terrain information such as the elevation and height of buildings, which makes these models much more specific to a particular region.
- *Deterministic*: Deterministic models combine the laws of electromagnetic wave propagation with terrain information. These models present more realistic results but have strong computational requirements.

In general, telecommunication operators use Empirical models for the design and comparison of systems and the Semi-Empirical and Deterministic models for network planning and deployment. Some of the most well-known propagation models are empirical models such as Okumura-Hata [28], Mishra [29] and Mishra [29] applied to macro and micro-cells, respectively. There are other models that extend these like Standard Propagation Model (SPM) [4].

In order to make propagation models more realistic, it is possible to calibrate them using real data. These calibrations can be performed through Artificial Neural Networks (ANNs) and they are strongly discussed in [30]–[32]. Despite the use of ANNs, the limitations of the propagation models still exist. For example, on an Okumura-Hata implementation (using ANNs or not), can only be applied at distances greater than 1 km, for a given frequency and

**TABLE 1.** Conditions under which the models are applicable.

Parameter	Range	
	Walfish-Ikegami	SPM
Frequency, $f$ [MHz]	800 – 2000	150 – 2000
Distance, $d_{BS}$ [km]	0.02 – 5	1 – 20
BS height, $h_{BS}$ [m]	4 – 50	30 – 200
MS height, $h_{MS}$ [m]	1 – 3	1 – 10

for a given propagation environment. For heterogeneous networks, where several technologies working simultaneously at different frequencies, the calibrated models cannot be used. In order to reduce the limitation presented above, a calibrated propagation model was presented in [33], whose main disadvantage is that it requires the type of environment and its specifications in the calibration process.

In order to generate a propagation model that can be used in heterogeneous networks regardless of the type of propagation environment, this research uses the Walfish-Ikegami and SPM propagation models, used in micro cell and macro cell scenarios, respectively.

One propagation model typically used in micro cell scenarios is the Walfish-Ikegami model [29]. Table 1 presents the conditions under which it is applicable.

For this research, in the distance where the model is applied, considering LoS, its path loss is given by:

$$L_{Walfish_{(dB)}} = 42.6 + 26\log(d_{BS_{[km]}}) + 20\log(f_{[MHz]}), \quad (3)$$

where  $d_{BS}$  is the distance between BS and the MT and  $f$  is the frequency.

A macro cell model is the SPM [4]. The SPM is an extension of the Okumura-Hata propagation model and its extension COST 231-Hata. The validity intervals, Table 1, must be observed.

The SPM [4] is an extension of the Okumura-Hata propagation model and its extension COST 231-Hata, being a macro cell model. The validity intervals, Table 1, must be observed. The path loss calculation of the SPM model is given by:

$$L_{SPM_{(dB)}} = K_1 + K_2\log(d_{BS_{[m]}}) + K_3\log(h_{BS_{[m]}}) + K_4L_{dif} + K_5\log(d_{BS_{[m]}})\log(h_{BS_{[m]}}) + K_6(h_{MT_{[m]}}) + K_7\log(h_{MT_{[m]}}) + K_{clutter}f(clutter), \quad (4)$$

where,

- $K_1$  [dB]: Constant offset;
- $K_2$ : Coefficient for  $\log(d_{BS})$ ;
- $d_{BS}$  [m]: Distance between BS and the MT;
- $K_3$ : Coefficient for  $\log(h_{BS})$ ;
- $h_{BS}$  [m]: Height of BS;
- $K_4$ : Coefficient for diffraction calculation;
- $L_{dif}$  [dB]: Loss due to diffraction over an obstructed path;
- $K_5$ : Coefficient for  $\log(d_{BS})\log(h_{BS})$ ;
- $K_6$ : Coefficient for  $h_{MT}$ ;
- $h_{MT}$  [m]: Height of MT;

**TABLE 2.** Typical values for the SPM coefficient parameters.

	Minimum	Typical	Maximum
$K_2$	20	44.9	70
$K_3$	-20	5.83	20
$K_4$	0	0.5	0.8
$K_5$	-10	-6.55	0
$K_6$	-1	0	0
$K_7$	-10	0	0

- $K_7$ : Coefficient for  $\log(h_{MT})$ ;
- $K_{clutter}$ : Coefficient for  $K_{clutter}$ ;
- $f(clutter)$ : Average of weighted losses due to clutter;

The coefficients parameters explained above are limited to the presented in Table 2. Although the frequency of the antenna and the attenuation coefficient is not present in 8, this is considered in the  $K_1$  factor.

Although this model is based from the Okumura-Hata model, the SPM allows values of elevation, diffraction loss, among other parameters in the calculation of path loss, making the model more accurate and realistic.

### C. COVERAGE MONITORING

In order to enable telecommunications operators to collect data with network quality information, some field measurements, called Drive Tests (DT), are made. As a rule, these DTs are collected using a vehicle with radio equipment that travels along a predefined route, collecting data from a certain area and each geolocated measuring point. The analysis of the DTs allows operators to understand network failures, such as areas with weak coverage, making it possible for operators to perform corrective measures (like the placement of a new base station). The reception signal suffers some effects like shadowing, slow and fast fading [25]. When working with discrete areas, each one of the sub-areas considered, the signal suffers from fast fading. The use of DTs measurements allows the neutralisation of this effect.

Despite the precise information revealed by the DTs, their execution can be expensive and requires allocation of human resources. The information collected only refers to areas with roads, which limits the true perception of the entire network.

In order to make use of DTs data more efficiently, a standardisation was proposed. This would reduce the costs associated with their execution, allowing them to be made by a MT. This standardisation is called Minimisation of Drive Tests (MDT) and in addition to the objectives mentioned above for DTs, these are triggered whenever there is the implementation of a new base station, the construction of new roads or buildings and if there are complaints from customers [34]. MDT is available in the vast majority of devices, and it is operators' decision to activate this functionality. For the user, the only drawback is the additional power consumption. However, and if the measurements are geolocated, it is possible to create a realistic view of the signal at various points in a cell. By using this data in the proposed

model, signal estimation over an entire cell area will become more precise and accurate.

#### D. AVAILABLE NETWORK PERFORMANCE INDICATORS RELATED TO COVERAGE

In the OSS are available, for the operators, performance indicators, KPIs. These indicators, such as Cell Reach can help in estimating coverage. When an MT connects to a BS, the BS estimates the propagation delay of the communication and sends this value to MT allowing for adjustment in the transmission time ensuring that all communications from different MTs in different places and at different times arrive at BS at the same time. This setting in the transmissions allows the minimisation of interference in the uplink signals of MTs.

Depending on the technology used, the propagation delay presents different denominations. For 2G is referred to the timing advance indicator and for 3G and 4G the propagation delay indicator. These indicators are discrete values defined by each of the vendors. After the information is collected, it is stored and made available in the OSS in the form of counters, which registers the number of occurrences within a given time period [35], allowing an understanding overview of the geographical distribution of MTs within rings of specific ranges.

The propagation delay can be used to estimate the distance between the BS and MT. Considering that an electromagnetic signal propagates at the speed of light,  $c$ , and the propagation delays,  $t_{prop}$ , the distance is given by:

$$d_{prop[m]} = c \times t_{prop[s]} \quad (5)$$

When network planning is performed, telecommunications operators combine some configuration parameters in order to obtain a certain cell size or a planned cell size. This size can be considered as the maximum range of the cell where communications can occur.

#### IV. NOVEL CELLS COVERAGE ESTIMATION WORK PATTERN

Several methodologies currently used by operators related to cell coverage estimation were presented in the former section. The present work aims to propose a unified methodology to integrate them all and reach a realistic estimation of coverage for any antenna, based on a varied set of information: terrain information, antenna configurations, propagation models, DT measurements, and KPIs. To present it, first a motivation is presented, highlighting the identified needs as requirements for a new methodology. Then, a small use case that exemplifies the way the proposed methodology can be used. Finally, the overall architectural framework is presented, its components being detailed in later sections.

##### A. MOTIVATION AND REQUIREMENTS

In this section, a motivation and requirements for a unified coverage estimation methodology are presented, based on current practices of operators.

Within the planning and optimisation activities of a telecommunication operator, a key task is the estimation of the coverage area of the cells of its network. For example, given a cell of, e.g., expected 7 km range, the receive power level within the surrounding geographical area of the antenna must be estimated in order to evaluate how it fits with the neighbouring cells. For it, considering the currently used models, the operator will need to apply two distinct propagation models, as the range of micro-cell models (Walfish-Ikegami) only applies up to 5 km, while a macro cell model (SPM) only applies from 1 km on. In this sense, a unified model capable of predicting coverage would be very useful for operators.

To achieve a more realistic estimation of the signal level, the operator recurs to DTs. Still, the criteria to determine the specific areas for the measurement campaign is many times random, which may question from the start the usability of such campaigns. These measurements, once collected, are manually processed by the engineers following arbitrary procedures. They aim at manually fitting certain parameters of the propagation models in order to adapt the model's prediction to the real measurements. This curve fitting is time consuming and erroneous, as statistical indicators of DT measurements (average, standard deviation of measurements) are used, still not taking into account the specific geographic location of them. In fact, propagation conditions of a geographical area where DTs are done may not be representative for another area. Some operators tend to regularly do extensive and expensive DT campaigns to evaluate the quality of the network. Still, they do not have tools to process this large amounts of data nor integrate them in their planning and optimisation tools. In this sense, a coverage prediction model automatically calibrated with available DT measurements would be of key value. A model that would take into consideration the geographical position of each DT, using these geolocated measurements to weight a propagation model to build a complete map of estimated coverage (to estimate coverage in a given position, DTs that would be nearby, in similar propagation conditions, would have more weight than farther DTs). This model would be able to easily integrate MDT measurements, enabling to build a realistic picture of the received signal level around any antenna. This would require an efficient infrastructure for the storage and processing of DT measurements, and computation of propagation grids for each antenna. We think that the use of cloud-services enables an elastic and efficient storage and processing of resources on-demand.

The operator also has available several KPIs. In particular, as formerly discussed, the availability of propagation delay measurements for every connection of each cell is of precious value, enabling to characterise the spatial statistical distribution of users using the cell. In particular, it enables to determine the cell reach. Combined with signal level configurations that trigger handover procedures, these are important indicator that should be integrated in a realistic coverage estimation model of a given cell.



processing module, which is the most relevant element in the proposed framework, namely the generation of the Propagation Model. In the Output module, for a given cell the received signal power grid is stored on the Metric server and becomes available to the user.

In the following section, the various components of the processing module represented in the architectural framework are detailed.

## V. MODULES OF THE AUTOMATIC COVERAGE ESTIMATION FRAMEWORK

In this section, a semi-empirical propagation model that accurately represents reality is detailed. It details and largely extends initial ideas drafted over [8]–[10].

### A. INPUTS MODULE

This subsection describes in detail each of the Input submodules of the architectural framework depicted in Fig. 1.

The *Drive Tests submodule* is an important input in the presented architecture. DTs in this context are used to calibrate the propagation model to a particular geographical area allowing the propagation model to accurately represent reality. DTs data comes directly from the Metric server and is made available to an antenna at a given time for certain antenna characteristics over a given time period. The DT for a given position provides the receiving power, being represented as  $P_{rxDT}$  [dBm].

There are configurable network parameters, which are received through the OSS and serve to calibrate the model. These parameters are aggregated in the *Configuration Management module*. Some of these parameters are related to the antenna such as its model, the height ( $h_{BS}$ ), the mechanical and electrical tilt ( $\theta_{mecBS}$  and  $\theta_{eleBS}$ ), the azimuth ( $\varphi_{BS}$ ), the position and the transmitting power ( $P_{tx}$ ). Other parameters are related to the technology, frequency, the MT sensitivity ( $P_{rxmin}$ ) and the geohash length,  $Geo_{hash}$ . The geohash is an encoder that transforms coordinates in a unique hash, where each length of geohash is associated with a certain cell size [36]. Due to the projection systems considered, the geohash has different cell size values depending on the location on the globe. After choosing the length of the geohash and depending on the antenna location, pixel size is defined which is used in the grid construction. For example, if an antenna is located near the Equator line, the cell size is smaller in terms of height when compared to an antenna located in northern Europe.

This information is essential for describing the characteristics of the BS. The handling of this data needs special attention since it is manually entered by the user. This may cause problems if it is not entered correctly.

The *Planning Management submodule* corresponds to counters collected by the OSS which monitors the operation of various aspects. An example of this data type is the cell reach which allows obtaining the  $P_{rxho}$  value.

The *Terrain Data submodule* is divided into two steps. Initially, information on the terrain morphology of a given

TABLE 3. Parameters used in the propagation model.

Parameter	Description	
Antenna	$h_{BS}$	Height of BS [m].
	$G(p)$	Antenna gain for pixel $p$ [dB].
	$\theta_{mecBS}$	Antenna mechanical tilt [°].
	$\theta_{eleBS}$	Antenna electrical tilt [°].
	$\varphi_{BS}$	Antenna azimuth [°].
Network	$P_{tx}$	Transmitting power [dBm].
	$P_{rxDT}$	Receiving power for a DT [dBm].
	$P_{rxmin}$	Minimum reception power to be considered [dBm].
	$P_{rxho}$	Handover power [dBm].
	$d_{ho}$	Handover distance [m].
	$L(d_{ho})$	Loss at handover distance [dB].
	$Geo_{hash}$	Length of the geohash, when combined with antenna positions define the pixel size.
Model	$d_{wal}$	Minimum distance for application of the Walfish-Ikegami propagation model [m].
	$L(d_{wal})$	Loss at $d_{wal}$ [dB].
	$K_1$	SPM offset.
	$K_2$	SPM for $\log(d_{BS})$ [dB].
	$L_{dif}$	Diffraction loss due an obstructed path [dB].
	$h_{MT}$	Height of MT [m].
	$d_{BS}$	Distance between BS and the MT [m].

work area is requested through the Application Programming Interface (API) provided by *OpenTopography* [37]–[39]. This API returns elevation information for the considered area in raster format 30m by 30m pixels. This information is then integrated into the architecture displayed according to the size of the pixel, defined by the user in the grid generation. For each of the pixels created, the elevation value is searched in the API result. The next step is to add information about buildings and large structures that are requested through the Overpass API [40]. This API returns information from *OpenStreetMap* [41], where data is available under the Open Database License (ODbL), and for a given workspace, it returns the height information of the existing buildings. For each of the pixels of the generated grid, the average of the heights of the buildings in that pixel is calculated. These two steps allow to obtain data similar to Light Detection and Ranging (LiDAR) data and thus realistically portrays the propagation environment.

Table 3 shows some of the parameters used in the propagation model.

### B. PROCESSING MODULE

The core module of our framework is the novel *Propagation Model* implemented in the cloud where, for a given cell, based on available inputs, it automatically estimates the cell's path loss within an area of interest. It results from the combination of various aspects. In Fig. 2 it is possible to verify the basic idea of the proposed propagation model, ACSPM. The ACSPM is calibrated with the Walfish-Ikegami model, power level at the handover distance. This calibration allows adjusting SPM to a distance of less than 1 km and adjust to the reality of the antenna, using not only the handover information, but also the DT information. In Fig. 2,  $d_{max}$  corresponds to the maximum distance returned by the

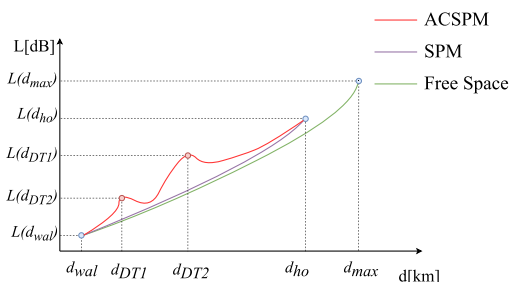


FIGURE 2. Illustration of the combination of various aspects for the construction of the ACSPM.

free space attenuation expression for a given power considered. The remaining variables are defined in Table 3.

The needed inputs to obtain the propagation loss grid are listed in Table 3. Many of these are obtained along the steps detailed in Section V-A. Taking as input the parameters discussed in Section V-A and presented in the Table 3, the calibration of the propagation model and computation of propagation loss grids follows the methodology illustrated in Fig. 3, which is detailed furthermore.

### 1) DIMENSIONING THE GRID

The proposed methodology aims to estimate propagation loss around a given cell. For that estimation, a rectangular area of interest around the cell area must be identified. Within this area, a grid of pixels is defined. For each pixel the path loss from the antenna shall be estimated.

The maximum communication range,  $d_{max}$ , is computed for the antenna. Using the free space propagation model, it corresponds to the distance where, for the antenna's  $P_{tx}$  and  $G_{tx}$ , the received power reaches the MT sensitivity,  $P_{rxmin}$ . This range will define the initial size of the grid, centred in the antenna position. The grid dimensions are then reduced following a binary search iterative procedure for each of the borders of the grid. In each step, once there is no terrain elevation information, the SPM model, with no diffraction is used to evaluate  $P_{rx}$  along the border, determining if, in the next step of the binary search, one should search nearer or farther from the current border. If for a given position the

received power is equal to a minimum power  $P_{rxmin}$  it becomes one of the grid limits. This procedure is applied to each border of the grid.

Once the dimension of the grid of the cell is defined, it is filled with geolocated pixels. The size of the pixels is specified by the  $Geo_{hash}$ . Each of the geolocated pixel in the grid will be used to store various information useful to the model and specific for its position. This information is obtained throughout the process illustrated in Fig. 3 and is detailed in the next sections. For each pixel, the following information shall be obtained:

- Terrain height information,  $h_{MT}$ , of the pixel and the distance to the BS,  $d_{BS}$ ;
- Existence of LoS, expressed as diffraction losses,  $L_{dif}$ ;
- Gain introduced by the antenna in that pixel,  $G(p)$ ;
- Power information received from DTs,  $P_{rxDT}$ ;
- Specific SPM calibration parameters,  $K_1$  and  $K_2$ ;
- Estimated path loss value for that pixel.

### 2) INCLUSION OF TERRAIN MORPHOLOGY INFORMATION

The terrain morphology and the building heights are added to each pixel. In order to validate if line of sight exists between the pixel and the BS, the Bresenham's line algorithm [42] is initially used to find all pixels, in a straight line, between the pixel and the pixel where the BS is located, depicted in Fig. 3.

### 3) COMPUTATION OF DIFFRACTION LOSS FOR EACH PIXEL

The Knife-Edge Diffraction model [43], [44] is used for each pixel of the line between the antenna and the pixel, to estimate the diffraction losses in that path. For each pixel in the path, a parameter  $\nu$  is calculated according to the following equation:

$$\nu = h \sqrt{\frac{2}{\lambda} \left( \frac{1}{d_1} + \frac{1}{d_2} \right)} \quad (6)$$

where  $h$  is the obstruction height, i.e., height from the obstacle top to the Tx-Rx axis (straight line between transmitter and receiver antennas),  $\lambda$  is the wavelength and  $d_1$  and  $d_2$  is the distance between each side of the path and the obstacle. After calculating the parameter  $\nu$  for each pixel of the line, the pixel with the highest value of  $\nu$  is the pixel with the highest diffraction loss. So if the value of  $\nu < -0.78$ ,  $L_{dif} = 0$  dB

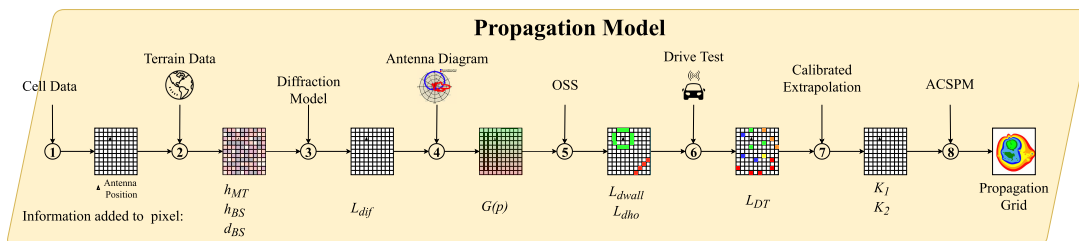


FIGURE 3. Steps for the computation of a propagation grid.

else the  $L_{dif}$  is given by [43]:

$$L_{dif} = 6.9 + 20 \log \left( \sqrt{(v - 0.1)^2 + 1} + v - 0.1 \right) \quad (7)$$

For each pixel, the  $L_{dif}$  value is stored in the grid, depicted in Fig. 3, and this value is considered into the ACSPM algorithm.

#### 4) INCLUSION OF BS ANTENNA GAIN FOR EACH PIXEL

According to Fig. 3, other information that is stored in each pixel is the antenna gain perceived at the position of each pixel,  $G_{tx}(\varphi_p - \varphi_{BS}, \theta_p - \theta_{mec_{BS}})$  according to its radiation pattern and its azimuth. This information is relevant to make the estimation of path loss independent of the characteristics of the antennas, when DT measurements are available and used to estimate the path loss for that pixel. In fact, by removing to  $P_{rxDT}$  the  $P_{tx}$  and  $G_{tx}$ , a path loss,  $L(dt)$ , independent of the antenna configuration is obtained from (1).

#### 5) ESTIMATION OF PATH LOSS IN PIXELS OF CELL EDGES

By knowing the antenna's operating frequency, from OSS information it is possible to estimate, using (3), the value of path loss,  $L(d_{wal})$ , for distance,  $d_{wal}$  from the antenna, according to Fig. 3.

In a scenario where the cells are placed side by side, in order to cover a large area, the cell reach may be associated with the handover power, ( $Prx_{ho}$ ).  $Prx_{ho}$  is a parameter defined by the operator in the planning phase of a network, where is considered that handover shall occur and it is related to the distance between cells. It is a minimum received power that the network shall guarantee in the service area. A handover to a new cell is triggered when signals are below the  $Prx_{ho}$ . The cell reach information identifies distance ranges within which communicating MTs are monitored/recorded by the OSS. The last ring represents the farthest area where MTs are connected to the BS, where  $Prx = Prx_{ho}$ .

Combining this two aspects, it is possible to calculate at a distance,  $d_{ho}$ , the path loss,  $L(d_{ho})$ , using (1) and the  $Prx_{ho}$  value. For each pixel that is at  $d_{ho}$  distance from the antenna, the value of  $L(d_{ho})$  is considered.

#### 6) ESTIMATION OF PATH LOSS IN PIXELS WITH DTs

The next step, according Fig. 3, is to register  $P_{rx}$  from DT measurements in the corresponding pixels. If, for a given pixel, there is more than one DT, then the value considered is the mean value of DTs in that pixel. The DT values considered are obtained from the Metric platform and are used to calibrate the propagation model.

Once the DTs are registered in the corresponding pixels, it is possible to compute and store for each of these pixels the corresponding perceived path loss, through (1), removing the antenna gain for that pixel as well as the  $P_{tx}$  of the antenna.

#### 7) CALIBRATION OF PROPAGATION PARAMETERS OF EACH PIXEL

Initially, the  $K_2$  parameter is estimated for all pixels, using the information,  $L(d_{wal})$  and  $L(d_{ho})$ , calculated in V-B.5. Then, once path loss is registered in pixels with DTs or in cell edges, values of  $K_1$  SPM parameter are estimated as follows:

- **Pixels with estimated path loss:** For each of these pixels, (4) is used to extrapolate values of  $K_1$  parameters, taking for the remaining parameters of the equation the values presented in Table 2. If a pixel already has a value for  $K_1$  (e.g., previous DT), then the average is taken between the two.
- **Pixels without estimated path loss:** Equation (8) is used to calculate the value of  $K_1(p)$ , for a pixel  $p$  without estimated path loss:

$$K_1(p) = \frac{\sum_{m=1}^N K_1(m)\alpha(p, m)}{\sum_{m=1}^N \alpha(p, m)}, \quad (8)$$

weighted by the  $N$  pixels with estimated path loss,  $K_1(m)$ . The parameter  $\alpha(p, m)$  uses the distance between pixels  $p$  and  $m$ , given by

$$\alpha(p, m) = \frac{1}{[d(p, m)]^2}. \quad (9)$$

If the antenna has been characterised before, a file containing a list of all DTs previously converted to  $K_1$  values is available. These values are distributed over the grid pixels the same way DTs are distributed.

#### 8) ESTIMATION OF PATH LOSS FOR EVERY PIXEL

After calculating a value of  $K_2$  and a value of  $K_1$  for each pixel, it is possible to obtain the path loss value for each pixel using (4) and the remaining parameters presented on Table 2.

#### C. OUTPUT MODULE

After the processing task, some output files are generated with diversified information that can have many uses.

- **Path Loss File:** This JSON file is created directly from the antenna grid information without further processing. This file maps the path loss value to each of the grid pixel coordinates. The created text file is later represented in the Metric platform.
- **Receive Power File:** From the information present in the antenna grid, it is possible to convert the path loss values of each pixel into received power values, using (1) and the antenna gain values for that same pixel. This information is stored in this JSON file and can later be represented in the Metric platform.
- **$K_1$  File:** This JSON file stores the information regarding the used DTs. For each DT, the geographical location and the calculated  $K_1$  values are stored. In this way, information related to the DT is stored, regardless of the

characteristics of the scenario under study. This information can later be reused for the same antenna.

#### D. EVALUATION METRICS

To evaluate the ACSPM, a common metric used in estimation models was applied. This metric allows not only to quantify the accuracy of the model but also to validate the improvement in signal estimation.

One way to visualise the performance of the model is to make a direct comparison between the SPM estimated values and the proposed model values. This analysis can be done visually by representing the coverage estimation by each model and comparing it or, for a more precise comparison, for a location where there are DT values.

In order to evaluate the proposed model estimation against the SPM model, a performance metric can be used to calculate the error between real values,  $y_i$ , and estimated ones,  $\hat{y}_i$ . The Mean Absolute Error (MAE) metric was applied in both models, using (10) [45].

$$MAE = \frac{1}{N} \sum_{i=1}^N |y_i - \hat{y}_i|, \quad (10)$$

where  $N$  refers to the number of considered values.

To calculate the accuracy of the model, for a certain point where DTs exist, DT value is ignored at the time of model calibration and its value is then compared with the value estimated by the model, by using the absolute error. This process is called “blind calibration”.

#### VI. IMPLEMENTATION AND INTEGRATION OF A COVERAGE ESTIMATION WORK PATTERN

After an exhaustive presentation of all the elements and mechanisms of the proposed propagation model, this section discusses the microservices provided by AWS used in the implementation of the architectural framework. The implementation and integration in the Metric platform is also presented and detailed.

##### A. METRIC SaaS PLATFORM

As previously mentioned, the Metric platform allows bringing together in a single platform all the management of telecommunications networks. The Metric platform collects KPIs from the OSS of various manufacturers and technologies, presenting a unified view of network performance.

Several features of the Metric platform were implemented in the cloud using AWS microservices. An example of these features is the processing of performance indicators and DTs. Another example of using AWS microservices is when the data from multiple operators is received and integrated into the platform to make it available in the ETL process.

Using the AWS microservices allows the Metric platform to automatically respond to user actions, such as processing cell information. The Metric platform shows the characteristics of each of the cells, like the antenna model, azimuth and other information. Whenever the user uploads a file with

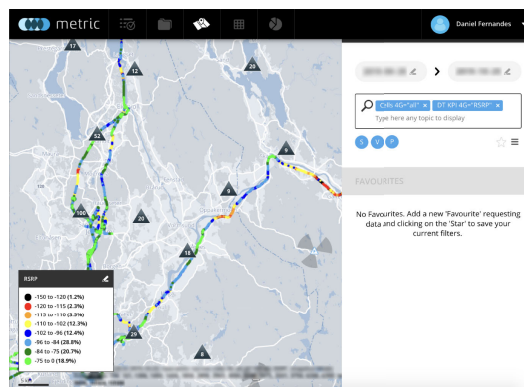


FIGURE 4. Drive Test to a given cell, obtained through the Metric platform.

new cell information, a microservice on AWS is triggered and allows to validate the cells with changed information and make it available through the platform.

Multivision company is currently migrating the services available on the Metric platform to an implementation using AWS. The new features developed will provide the platform with new services using AWS microservices. Using AWS cloud microservices allows Multivision to expand scalability and speed of the product developed to any device, in particular in the processing of data through the ETL process.

In Fig. 4 a search result to a given cell, obtained through the Metric platform is presented. The search result includes the DTs in a given time period.

##### B. AMAZON WEB SERVICES

The AWS provides services for performing computing tasks, such as Amazon Elastic Compute Cloud (Amazon EC2) and AWS Lambda. For database and storage purposes, microservices like Amazon Relational Database Service (Amazon RDS), Amazon DynamoDB, or Amazon Simple Storage Service (Amazon S3) can be used.

Amazon EC2 is a product that was developed with the aim of simplifying web-scale cloud computing. However, its actions cannot be triggered in response to an event, which makes this product unattractive to the solution to be implemented, since it is intended that the presented models run each time there is new cell information in a particular repository. This feature is supported by AWS Lambda which is a service that executes code in response to multiple events and supports multiple programming languages. It runs only when needed, which allows being automatically scalable. It can be used whenever the computing time is less than 15 minutes and the virtual memory required is less than 500 MBytes. In terms of memory, Lambda only provides 3 GBytes.

For database and storage purposes, AWS provides the Amazon RDS, which is a relational database that supports different commercial and open-source products, and does not require users to install, configure, and manage them.

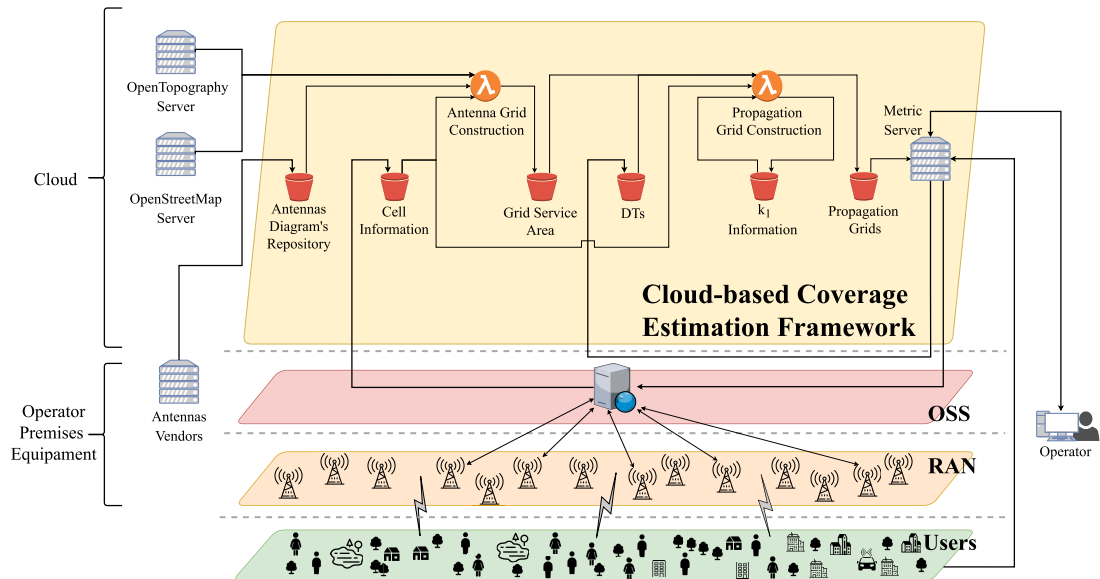


FIGURE 5. Mobile network monitoring and optimisation architecture, with work pattern using AWS services that implements the ACSPM.

In case of non-relational databases, Amazon also offers a user-friendly service, called Amazon DynamoDB. A storage service provided by AWS is Amazon S3, which allows users to store files regardless of their size (each file can have a maximum of 5 TBytes), and is highly scalable. The internal management of Amazon DynamoDB and Amazon S3 is done by AWS without the need for user intervention.

To implement the architectural framework presented in Fig. 1, the microservices AWS Lambda and Amazon S3 were used. Amazon S3 has an internal function that triggers whenever a new cell configuration file is received, starting the whole process.

The system architecture developed and implemented in AWS is depicted in Fig. 5.

### C. IMPLEMENTATION OF THE SYSTEM ARCHITECTURE

A new model for estimating coverage, that combines various types of information present in the architecture, is shown in Fig. 1. A proof of concept of this architecture and its implementation using AWS is presented in Fig. 5. This figure also identifies the functions that are performed in the cloud and the resources used at the telecommunications operator premises. This subsection explains the details of each of the components of the proposed system architecture.

#### 1) OVERVIEW

Using AWS, a proof of concept for a coverage estimation model was implemented. This implementation of the model was performed in Java [46] programming language.

The function of each element of the architecture is explained below.

The implementation of this proof of concept allows adding a new dimension in the scope of SON technology to the Metric platform, specifically for planning purposes. The use of this technology allows the decrease of overall operational costs, due to the reduction of human resources allocated to network planning tasks.

#### 2) AMAZON S3

This implementation uses 6 independent Amazon S3 storage location. Each location stores distinct information, which may be used in the various stages of the process, or final information to be made available to the user. This location is also called a *bucket*.

- **Antennas Diagram's Repository** - For each antenna model, frequency and tilt, an ".msi" file containing the vertical and horizontal gain of that antenna are stored. This information is provided by the suppliers of the various antennas.
- **Cell Information** - For each cell of the network there is a JSON file that contains various information necessary for the process. Examples of this information are the technology, the location and model of the antenna, the electric and mechanical tilt, the  $P_{tx}$ [dBm] among others. The presence of a file in this Amazon S3 *bucket* triggers the process.
- **Grid Service Area** - Stores a JSON file with a pre-computed grid for a cell. This grid contains for each pixel ground elevation and building information, antenna gain, antenna distance and the diffraction loss value.
- **DTs** - Cell DTs, whenever processed by Metric, are sent in form of a JSON file to this Amazon S3 *bucket*, and

they can be used whenever necessary, allowing calibration of the propagation model.

- **$K_1$  Information** - For each of the studied cells, a JSON file that compiles all the DTs performed for that cell is stored. Also the information of their coordinates and the value of the corresponding  $K_1$  factor are stored. This file have the same usage as the DT file.
- **Propagation Grids** - In this Amazon S3 bucket, the propagation grids of each of the studied cell are stored in a JSON file. This bucket directly serves as input to Metric platform, making it possible to represent the propagation of a cell.

### 3) AWS LAMBDA FUNCTIONS

For processing purposes, AWS Lambda features the execution of code. This independent code executions are called AWS Lambda *functions*. For this implementation, 2 AWS Lambda *functions* are used and makes use of the data stored in the different Amazon S3 *buckets* as inputs. After the processing, the resulting information is stored in another *bucket* for later use.

- **Antenna Grid Construction** - From the information file present in *Cell Information bucket*, a AWS Lambda *function* creates a grid with the maximum propagation distance of the cell. Each pixel of the grid has user-defined dimensions, and for each one, the antenna gain considering the *Antennas Diagram's Repository bucket* files, antenna azimuth and tilts are calculated and stored. Elevation information requested from an external server is added to the grid, as explained in the module terrain data detailed in V-A. Once the elevation for each pixel is obtained, it is possible to calculate the existence or nonexistence of a LoS and the corresponding diffraction loss between a given pixel and the antenna. This information is also stored in the pixel. When all these computations are completed, the grid is stored in a JSON file in *Grid Service Area bucket* for later use.
- **Propagation Grid Construction** - For each JSON files in *Cell Information bucket* the corresponding JSON file is searched in *Grid Service Area bucket*. When the file is found, all the information is loaded as well as the existing DTs for that cell. If that cell has already been analysed before, processed information from old DT values can be found in  *$K_1$  Information bucket*. This *function* uses all these information to fine tune the propagation model in order to generate a JSON file with the path loss. This file is stored in *Propagation Grids bucket*.

### D. INTEGRATION WITH METRIC

In order to proceed with the integration in the Metric platform, AWS services were used, as explained above.

When a user wants to obtain the propagation of a certain cell through the Metric platform, the user must input "Propagation" in the search box (represented in red in Fig. 6). This action will show the propagation grid for the given cell. If the propagation grid does not exist, the process shown

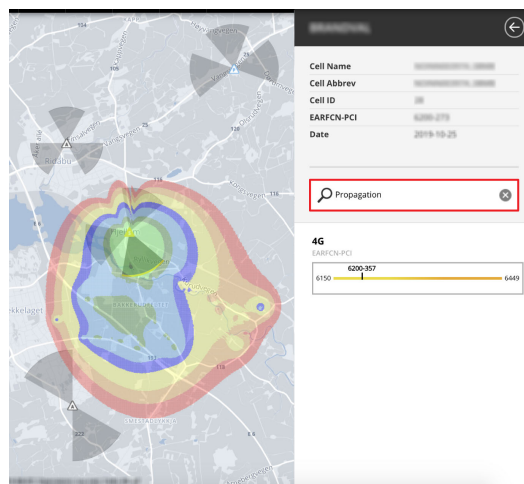


FIGURE 6. Cell coverage estimation module integrated in the Metric platform.

in Fig. 5 will be triggered, and after process completion, the propagation grid will be shown to the user. An example of this situation is shown in Fig. 6, where the propagation of a cell is presented to the user. This representation is the result of an initial implementation.

This integration in the Metric platform provides it with new features and allows users to explore, visualise and detect problems in their networks. These features can be categorised into three sets:

- **Planning** - With the propagation analysis, it is possible to perform the planning of Broadcast Control Channel (BCCH), Scrambling Codes (SC) and Physical Cell ID (PCI).
- **Evaluation and Optimisation** - Each time a new cell is implemented, it is possible to validate the coverage of this cell and the interference with the existing cells. To implement a new cell, it is necessary to initially generate the propagation grid of that cell, place this antenna in a map with the other antennas, and validate the impacts on the network already implemented. It is also possible through the analysis of coverage to optimise the network.
- **Malfunction Detection** - It is possible to detect some failures in the functioning of the network related to planning. These failures can be the identification of cross sectors and overshooting.

### VII. REFERENCE SCENARIO

In order to test the presented architecture, a test scenario was chosen. In this scenario, a macro cell with a 4G antenna implemented in a northern European country is chosen. This antenna has a transmission power,  $P_{tx}$ , of 46 dBm and an azimuth value of  $150^\circ$ . The chosen antenna is from Kathrein

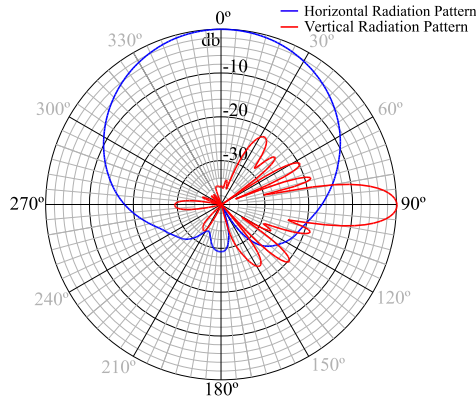


**FIGURE 7.** Horizontal and vertical radiation pattern of the reference antenna.

brand and the model is *80010665v01* configured with the mechanical and electrical tilt of  $0^\circ$ . The horizontal and vertical radiation patterns are depicted in Fig. 7. The E-UTRA Absolute Radio Frequency Channel Number (EARFCN) of the antenna is 6200, that corresponds to a downlink frequency of 796 MHz.

For this scenario, a *Geohash* parameter of 8 was chosen due to the fact that the reference scenario is located in a northern European region, where latitude presents higher values. This parameter allows the generated grid to have the dimensions of  $38.2 \text{ m} \times 19.1 \text{ m}$  (width  $\times$  height, approximately 2 : 1 pixel ratio) instead of using 1 : 1 pixel ratio (square pixels), which represents a more accurate approximation for geographic representation.

In Fig. 8 it is possible to visualise the scenario under study represented in the Metric platform. It is also represented in Fig. 8 the distance of the cell reach, which in this case is about 12 km, and the DTs associated with this antenna. The distance from the cell reach is associated with a certain receiving power that, in this case, was  $-85 \text{ dBm}$  and up to this distance is where more than 95% of the cell activity is performed, that is, after this distance, the activity that involves the cell is practically residual.

For the scenario under study, the DTs performed over a 6 month period were considered, which contains a total of 248 measurement points. During these 6 months, the antenna configurations were not changed.

The grid generated, also represented in Fig. 8, covers an area of approximately  $625 \text{ km}^2$  and the terrain elevation is depicted in Fig. 9. The antenna and its azimuth is represented as well.

### VIII. PERFORMANCE RESULTS

This section presents the results obtained with the propagation model proposed in Fig. 3 and implemented as detailed in Fig. 5.

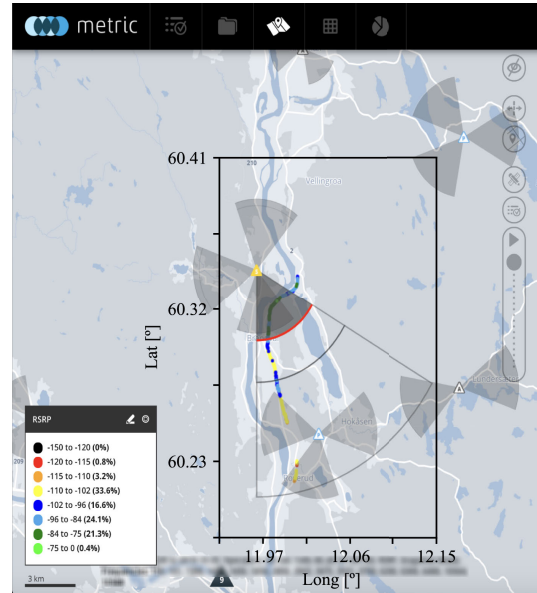


**FIGURE 8.** Propagation of a cell represented in the Metric platform.

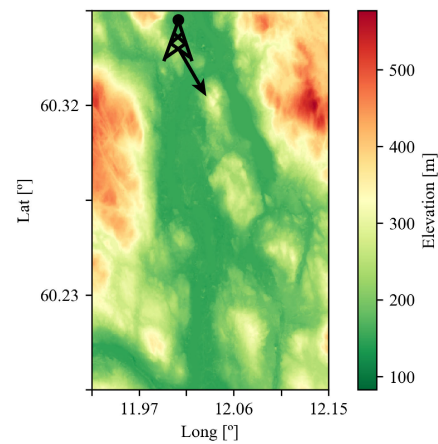


**FIGURE 9.** Terrain elevation of the reference scenario, with indication of the antenna's azimuth.

#### A. CELL COVERAGE

Following the model depicted in Fig. 3 and once the grid has been calculated, the attenuations due to obstacles and the gain for each of the pixels are calculated. Later, the DTs are distributed among the various pixels of the grid. The 248 DTs were distributed over 247 pixels, where one pixel contains 2 DTs.

Through the analysis of Fig. 8, it is perceptible that as the distance to the antenna increases, the value of the received power decreases.

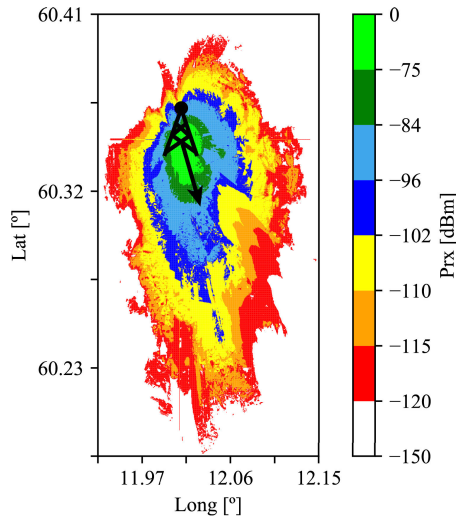


**FIGURE 10.** Estimated received signal level using the proposed propagation model.

With the tuning of the propagation model, either through cell reach or through the DTs, the result is depicted in Fig. 10.

It is possible to verify that there are areas strongly influenced by DTs, which is the case of the lower zone where this influence can be seen. In this zone, the region between  $-102$  dBm and  $-110$  dBm (represented in yellow color), there is an area with a higher power signal received between  $-96$  dBm and  $-102$  dBm (represented in dark blue). This influence is due, not only by the values obtained with DTs, but also by the morphology of the terrain, which clearly shows that, in this area, there is an terrain elevation.

Although the SPM model is used for distances bigger than 1 km, in order to establish a comparison between the proposed model and a classical model, the SPM model was applied, with the parameters presented on Table 2. For the same scenario, the result of the coverage estimation is presented in Fig. 11.

For each pixel built with data from DTs, the received power value is compared with the estimated power value for the proposed model for the SPM model as explained in V-D.

Since the proposed model is calibrated with DT values, the MAE between the estimated values and the DT values is zero for that pixel. However, there may be some small oscillations for pixels with more than one DT, since the mean value for the received power is considered.

The comparison of the proposed ACSPM with the SPM can also be calculated. To simplify the process, for each propagation model, the MAE between the estimated values and the DT values is calculated and shown in Table 4.

The results of “blind calibration”, present in V-D, is also depicted in Table 4.

As already mentioned, the absolute error between the values estimated through the proposed model and the DT values

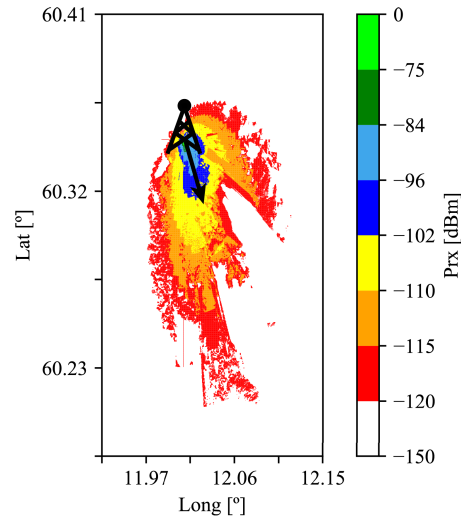


**FIGURE 11.** Estimated received signal level using the SPM model.

**TABLE 4.** Absolute error between estimated values and DT values for the 247 DT pixels.

	ACSPM	Error [dB]	
		SPM	"Blind Calibration"
Maximum	0.0	30.0	11.1
MAE	0.0	13.6	5.2
Minimum	0.0	1.9	0.0

is zero. When looking at a SPM model, the situation is different. The absolute error between the value estimated by the SPM and the DTs is quite variable and the MAE value is about 14 dB. The maximum error can reach 30 dB.

For the accuracy of the proposed model, is visible that the MAE value, 5 dB is about 8 dB lower when compared with the SPM model. The maximum value is also lower, almost one-third the value of SPM model.

#### B. IMPACT OF DT ON THE PROPOSED MODEL

Since the proposed model is calibrated using DTs values, it is important to validate the impact on the number of DTs used in the model calibration. Not only the amount of DTs is important but also their distribution around the antenna as the propagation conditions are variable even for the same distance due to the different angles.

Fig. 12 depicts the MAE values, between the values estimated through the proposed model and the DT values, for the set used for evaluation of the methodology. A second order polynomial regression is also shown to visualise MAE trend when DTs measurements increase. As expected, MAE values decrease when more DTs are considered. The increase of available DT measurements, namely with MDT, make the proposed model more robust to outliers, automatically improving the quality of the achieved coverage predictions.

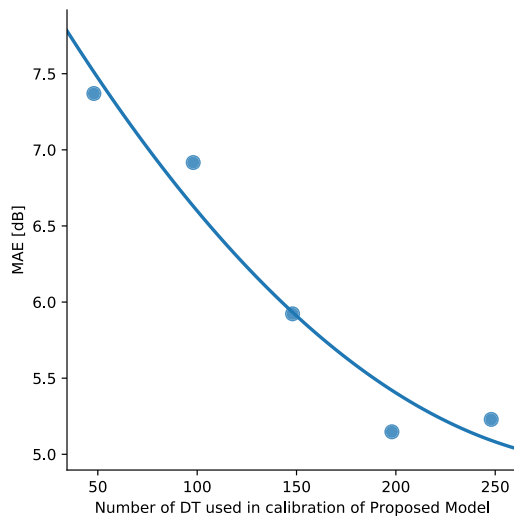


FIGURE 12. Polynomial regression for MAE values.

Once the various network measures are integrated into this model, if mobile phones had the option of monitoring the active network quality by reporting such data, network knowledge would be more realistic as well as its estimation.

### C. PLATFORM PERFORMANCE

By splitting the computational effort into two distinct Lambda functions, the waiting time for the end-user when making the request is drastically reduced. Initially, the Lambda function that needs more computational power is calculated for further reuse. Then, after user request, that information is used to generate the final propagation grid.

The computation of these tasks in a cloud environment allows quick access to the files, fast processing of the pre-defined tasks through computational parallelization. The result of this process can be further accessed simultaneously by several users.

Considering a network with 3 304 cells, the implementation in AWS of the proposed propagation model was tested. Table 5 refers to the computation times using AWS implementation and “No AWS” implementation, of each of the Lambda functions as well as the total elapsed time.

The results achieved by the AWS implementation are due to the parallelization feature that AWS services provide in their Lambda function execution. The case where parallelization is not considered, being the calculations sequential, was considered to be “No AWS” implementation.

In the case of Lambda function, **Antenna Grid Construction**, each cell needs on average 9 minutes and 8 seconds to be computed and in the case of Lambda function, **Propagation Grid Construction**, only 62 seconds are needed, being the time that user, in the worst case scenario, can expect to obtain propagation results from a cell.

TABLE 5. Computing time of the ACSPM, for 3 304 cells, on the AWS and not on the AWS. The format of the values is hh:mm:ss.

	Antenna Grid Construction	Computation Time Propagation Grid Construction	Total
AWS	05:01:49	00:37:56	05:39:45
No AWS	502:32:26	56:34:07	559:06:33

In the scenario where the user wants to get the propagation information for 3 304 cells, the use of AWS implementation allows a 89.7% time reduction when compared with not using AWS implementation.

### IX. MECHANISMS OF METRIC IMPROVED BY THE PROPOSED METHODOLOGY

The proposed work pattern for estimation of signal level around any cell simplifies the process of planning and optimisation of telecommunication networks, making the process simpler, faster and more accurate. The grids generated have been integrated in several mechanisms that have been developed, implemented and integrated in Metric platform:

- **Network (Cells Deployment) Coverage:** One of the applications where the information from the ACSPM is used is when it is intended to have a coverage overview in a given region. For each of the antennas in the region, a propagation grid is generated, and then all this information is combined. An example of the coverage of a given area is depicted in Fig. 13. This mechanism has been implemented in Metric platform [47]. Through the analysis of this area, it is possible to identify, for example, areas with weak coverage, as discussed in Section IV-B.
- **Cells Neighbourhood List:** The list of neighbouring cells is essential in the operation of the network, helping in the handover of mobile users, as well as in the planning of the 2G, 3G and 4G network resources. Through the superposition of grids, within the coverage area of a cell are calculated the amount of pixels covered by each neighbouring cell. This results in a list of neighbouring cells sorted by estimates of shared coverage, a mechanism that has been implemented in Metric platform, as detailed in [47].
- **Crossed Sectors identification:** When an anomaly occurs in the installation of the transmission cables supplying a certain cell, the signal emitted by that cell is not as planned. These situations can be easily identified by comparing the estimated signal with the DT data taken from the study area. The generation of a path loss grid for a given cell is transparent to the antenna characteristics, so the proposed model is used to estimate the signal with the planned characteristics. This mechanism has been implemented in Metric platform.
- **Overshooting solution:** One problem that also exists in telecommunication networks is the overshooting cells. This type of problems means that the cell in question has a signal outside its normal area of coverage.

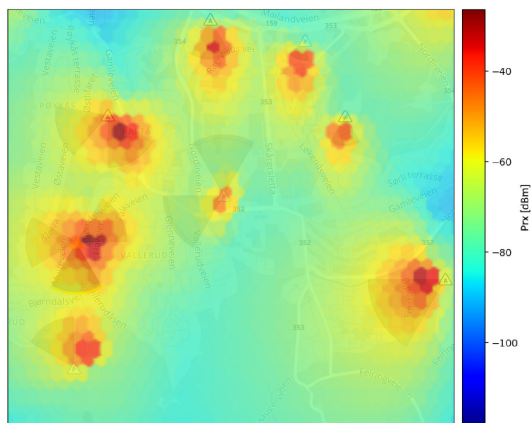


FIGURE 13. Signal received in a certain area.

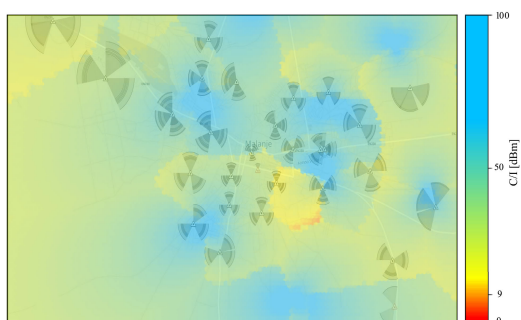


FIGURE 14. Carrier to Interference ratio in a certain area.

This problem drastically reduces the quality of the network. The analysis between the planned area of propagation and the DT quickly detects this problem. This mechanism has been implemented in Metric platform.

- **Planning:** With the generation of the received power grids, it is possible not only to elaborate a coverage map for an area but also a map with the interference of the various antennas, represented in Fig. 14. This information allows the planning of BCCBs and is detailed in [48]. This mechanism has been implemented in Metric platform. On the other side, through the power grids per cell, the lists of neighbors are then created, which are then used for SC and PCI planning (presented in [49]).
- **Energy Efficient Management of Resources:** Based on traffic predictions per cell, the cellular coverage area can be energy-efficiently optimised by a novel mechanism, as detailed in [24], [50], [51]. This proposed mechanism starts with grids of  $P_{rx}$  for each of the cells. This mechanism has been implemented in Metric platform.

## X. CONCLUSION

This paper presents a cloud-based framework of a novel semi-empirical propagation model that portrays, as accurately as possible, the propagation of an antenna. This model uses samples and antenna configuration data to automatically calibrate the model, making it more accurate. The automation of the calibration process makes it possible to reduce the human effort, which results in a financial impact on the management of these networks. This implementation, allows greater flexibility in the use of this model. This flexibility is related, not only to the ease of integration of the model in the Metric platform, for management and monitoring of telecommunications networks, but also to the features given by cloud services, namely in terms of processing and memory usage, and the availability of elastic resources on-demand, when needed.

The ACSPM was implemented and tested for a telecommunications network located in the northern European region, specifically, in a scenario where an antenna and its DTs were considered. The results obtained present about 13 dB gain when compared with SPM, and a MAE of about 5 dB in terms of model accuracy, which is about 8 dB lower than that obtained by SPM.

This work also shows what happens to the accuracy of the model when the number of DTs used for calibration changes. In fact, our model shows that, as the number of DTs used for model calibration increases, the MAE decreases, which makes our model more accurate, realistic and more robust to outlier samples.

This paper also highlights the importance of a precise propagation model for the correct implementation and optimisation of a telecommunications network. This has been integrated and implemented with other algorithms previously available in the tool, and is now in use allowing to build a neighbours list for a given cell, to plan resources of a 2G, 3G and 4G network and change configurations (overshooting or crossed sectors), as well as for more refined energy efficient mechanisms of radio resources.

The implementation and model described in this paper shows that the integration of MDT, to obtain more data describing the propagation environment, can be done in a fully automatic way, provided that operators make the data available, as it increases the responsiveness of the proposed model to the propagation environment. For future work, it would be interesting to explore a scenario with available MDT data for the calibration of the model, since it allows an even more realistic signal estimation.

## REFERENCES

- [1] *Ericsson Mobility Report 2019*, Ericsson, Stockholm, Sweden, Nov. 2019.
- [2] *Nokia*. Accessed: Jul. 15, 2019. [Online]. Available: <https://www.nokia.com>
- [3] *Huawei*. Accessed: Jul. 15, 2019. [Online]. Available: <https://consumer.huawei.com>
- [4] *Atoll 3.3.0 Technical Reference Guide for Radio Networks*, Forsk, Jaipur, Rajasthan, 2015.

- [5] Z. O. N. Martinez, C. Rodriguez, and O. M. Arias, "Propagation characteristics of managua city based on standard propagation model (SPM) at 850 MHz for 3G-WCDMA systems," in *Proc. IEEE Central Amer. Panama Conv. (CONCAPAN)*, Nov. 2014, pp. 1–6.
- [6] S. I. Popoola, A. A. Atayero, N. Faruk, C. T. Calafate, E. Adetiba, and V. O. Matthews, "Calibrating the standard path loss model for urban environments using field measurements and geospatial data," *Lect. Notes Eng. Comput. Sci.*, vol. 2229, no. July, pp. 513–518, 2017.
- [7] L. M. Correia, *Mobile Broadband Multimedia Networks*. Amsterdam, The Netherlands: Elsevier, 2007.
- [8] D. Fernandes, L. S. Ferreira, M. Nozari, P. Sebastiao, F. Cercas, and R. Dinis, "Combining drive tests and automatically tuned propagation models in the construction of path loss grids," in *Proc. IEEE 29th Annu. Int. Symp. Pers., Indoor Mobile Radio Commun. (PIMRC)*, Sep. 2018, pp. 1–2.
- [9] D. Fernandes *et al.*, "Combining measurements and propagation models for estimation of coverage in wireless networks," in *Proc. IEEE 90th Veh. Technol. Conf. (VTC-Fall)*, Honolulu, HI, USA, 2019, pp. 1–5.
- [10] D. Fernandes, G. Soares, D. Clemente, R. Cortesão, P. Sebastião, F. Cercas, R. Dinis, and L. S. Ferreira, "Integration of a cloud-based realistic and automatic coverage estimation methodology in metric SaaS," in *Proc. 22nd Int. Symp. Wireless Pers. Multimedia Commun. (WPMC)*, Lisbon, Portugal, Nov. 2019, pp. 326–329.
- [11] A. De Mauro, M. Greco, and M. Grimaldi, "What is big data? A consensual definition and a review of key research topics," *AIP Conf. Proc.*, vol. 1644, pp. 97–104, Feb. 2015.
- [12] K. Zheng, Z. Yang, K. Zhang, P. Chatzimisios, K. Yang, and W. Xiang, "Big data-driven optimization for mobile networks toward 5G," *IEEE Netw.*, vol. 30, no. 1, pp. 44–51, Jan./Feb. 2016.
- [13] A. Imran and A. Zoha, "Challenges in 5G: How to empower SON with big data for enabling 5G," *IEEE Netw.*, vol. 28, no. 6, pp. 27–33, Nov. 2014.
- [14] E. Bastug, M. Bennis, E. Zeydan, M. A. Kader, I. A. Karatepe, A. S. Er, and M. Debbah, "Big data meets telcos: A proactive caching perspective," *J. Commun. Netw.*, vol. 17, no. 6, pp. 549–557, Dec. 2015.
- [15] M. Frankel, N. Shacham, and J. E. Mathis, "Self-Organizing Networks," *Future Gener. Comput. Syst.*, vol. 4, no. 2, pp. 95–115, 9 1988.
- [16] *NGMN Use Cases related to Self Organising Network, Overall Description*, Berlin, Germany, NGMN, p. 17, 2008.
- [17] P. V. Klaine, M. A. Imran, O. Onireti, and R. D. Souza, "A survey of machine learning techniques applied to self-organizing cellular networks," *IEEE Commun. Surveys Tuts.*, vol. 19, no. 4, pp. 2392–2431, 4th Quart., 2017.
- [18] AWS. Accessed: Jul. 15, 2019. [Online]. Available: <https://aws.amazon.com>
- [19] Google Cloud. Accessed: Jul. 15, 2019. [Online]. Available: <https://cloud.google.com>
- [20] Microsoft Azure. Accessed: Jul. 15, 2019. [Online]. Available: <https://azure.microsoft.com>
- [21] D. Sabella, P. Rost, Y. Sheng, E. Pateromichelakis, U. Salim, P. Guitton-Ouhamou, M. Di Girolamo, and G. Giuliani, "RAN as a service: Challenges of designing a flexible RAN architecture in a cloud-based heterogeneous mobile network," *Future Netw. Mobile Summit*, no. 2, pp. 1–8, Jun. 2013.
- [22] Metric. Accessed: Jul. 16, 2019. [Online]. Available: <https://metric.pt>
- [23] Multivision. Accessed: Jul. 16, 2019. [Online]. Available: <https://multivision.pt>
- [24] D. Clemente, L. Ferreira, G. Soares, N. Valente, and P. Sebastiao, "Implementation of a cloud-based, traffic aware and energy efficient management of base Stations' activity," in *Proc. 21st Int. Symp. Wireless Pers. Multimedia Commun. (WPMC)*, Nov. 2018, pp. 600–605.
- [25] A. F. Molish, *Wireless Communication*, 2nd ed. Hoboken, NJ, USA: Wiley, 2010.
- [26] M. F. Iskander and Z. Yun, "Propagation prediction models for wireless communication systems," *IEEE Trans. Microw. Theory Techn.*, vol. 50, no. 3, pp. 662–673, Mar. 2002.
- [27] F. Letourneux, S. Guivarch, and Y. Lostanlen, "Propagation models for heterogeneous networks," *Proc. 7th Eur. Conf. Antennas Propag. (EuCAP)*, Jan. 2013, pp. 3993–3997.
- [28] M. Hata, "Empirical formula for propagation loss in land mobile radio services," *IEEE Trans. Veh. Technol.*, vol. 29, no. 3, pp. 317–325, Aug. 1980.
- [29] A. R. Mishra, *Advanced Cellular Network Planning and Optimisation*, A. R. Mishra, Ed. Chichester, U.K.: Wiley, 2006.
- [30] J. M. Mom, C. O. Mgbe, and G. A. Igwe, "Application of artificial neural network for path loss prediction in urban macrocellular environment," *Amer. J. Eng. Res.*, vol. 3, no. 2, pp. 270–275, 2014.
- [31] E. Ostlin, H. Zepernick, and H. Suzuki, "Macrocell path-loss prediction using artificial neural networks," *IEEE Trans. Veh. Technol.*, vol. 59, no. 6, pp. 2735–2747, Jul. 2010.
- [32] I. Popescu, I. Nafornita, G. Gavriloiu, P. Constantinou, and C. Gordan, "Field strength prediction in indoor environment with a neural model," in *Proc. 5th Int. Conf. Telecommun. Modern Satell.*, 2001, pp. 640–643.
- [33] M. Ayadi, A. Ben Zineb, and S. Tabbane, "A UHF path loss model using learning machine for heterogeneous networks," *IEEE Trans. Antennas Propag.*, vol. 65, no. 7, pp. 3675–3683, Jul. 2017.
- [34] W. A. Hapsari, A. Umesh, M. Iwamura, M. Tomala, B. Gyula, and B. Sebire, "Minimization of drive tests solution in 3GPP," *IEEE Commun. Mag.*, vol. 50, no. 6, pp. 28–36, Jun. 2012.
- [35] *Telecom Hall*. Accessed: Aug. 1, 2019. [Online]. Available: <http://www.telecomhall.com/analyzing-coverage-with-propagation-delay-pd-and-timing-advance-ta-gsm-wcdma-lte.aspx>
- [36] R. Moussalli, M. Srivatsa, and S. Asaad, "Fast and flexible conversion of geohash codes to and from Latitude/Longitude coordinates," in *Proc. IEEE 23rd Annu. Int. Symp. Field-Program. Custom Comput. Mach.*, May 2015, pp. 179–186.
- [37] *OpenTopography—High-Resolution Topography Data and Tools*. Accessed: Aug. 1, 2019. [Online]. Available: <https://opentopography.org>
- [38] J. Takaku, T. Tadono, and K. Tsutsui, "Generation of high resolution global DSM from ALOS PRISM," *Int. Arch. Photogramm., Remote Sens. Spatial Inf. Sci.*, vols. XL–4, pp. 243–248, Apr. 2014.
- [39] T. Tadono, H. Ishida, F. Oda, S. Naito, K. Minakawa, and H. Iwamoto, "Precise global DEM generation by ALOS PRISM," *Ann. Photogramm., Remote Sens. Spatial Inf. Sci.*, vol. 4, no. 5, pp. 71–76, Apr. 2014.
- [40] *Overpass API*. Accessed: Aug. 1, 2019. [Online]. Available: <http://overpass-api.de>
- [41] *OpenStreetMap*. Accessed: Aug. 1, 2019. [Online]. Available: <https://www.openstreetmap.org/>
- [42] M. Abrash, *Michael Abrash's Graphics Programming Black Book: The Complete Works of Graphics Master, Michael Abrash*, 10th ed. Stockbridge, GA, USA: Coriolis Group Books, 1997.
- [43] *Propagation by Diffraction*, document ITU-R P.526-14, 2018.
- [44] S. Saunders and A. Aragón, *Antennas and Propagation for Wireless Communication Systems*, 2nd ed., Hoboken, NJ, USA: Wiley, 2007.
- [45] C. Willmott and K. Matsuura, "Advantages of the mean absolute error (MAE) over the root mean square error (RMSE) in assessing average model performance," *Climate Res.*, vol. 30, pp. 79–82, Jun. 2005.
- [46] *Java Platform Standard Edition 7 Documentation*. Accessed: Aug. 1, 2019. [Online]. Available: <https://docs.oracle.com/javase/7/docs/index.html>
- [47] P. Pina, A. Godinho, D. Fernandes, D. Clemente, G. Soares, P. Sebastião, and L. S. Ferreira, "Cloud-based implementation of an automatic pixel-based neighbour identification system for cellular networks," in *Proc. 22nd Int. Symp. Wireless Pers. Multimedia Commun. (WPMC)*, Lisbon, Portugal, Nov. 2019, pp. 305–310.
- [48] A. Godinho, D. Fernandes, D. Clemente, G. Soares, P. Sebastião, P. Pina, and L. S. Ferreira, "Cloud-based cellular network planning system: Proof-of-concept implementation for GSM in AWS," in *Proc. 22nd Int. Symp. Wireless Pers. Multimedia Commun. (WPMC)*, Lisbon, Portugal, Nov. 2019, pp. 311–315.
- [49] R. Cortesão, D. Fernandes, D. Clemente, G. Soares, P. Sebastião, and L. S. Ferreira, "Cloud-based implementation of a SON automatic planning system: A proof-of-concept for UMTS," in *Proc. 22nd Int. Symp. Wireless Pers. Multimedia Commun. (WPMC)*, Lisbon, Portugal, Nov. 2019, pp. 316–321.
- [50] D. Clemente, G. Soares, D. Fernandes, R. Cortesao, P. Sebastiao, and L. S. Ferreira, "Traffic forecast in mobile networks: Classification system using machine learning," in *Proc. IEEE 90th Veh. Technol. Conf. (VTC-Fall)*, Honolulu, HI, USA, 2019, pp. 1–5.
- [51] D. Clemente, D. Fernandes, D. Clemente, R. Cortesão, G. Soares, P. Sebastião, and L. S. Ferreira, "Assessment of traffic prediction models for mobile communication networks," in *Proc. 22nd Int. Symp. Wireless Pers. Multimedia Commun. (WPMC)*, Lisbon, Portugal, Nov. 2019, pp. 322–325.



**DANIEL FERNANDES** received the B.S. and M.S. degrees in telecommunications and computer engineering from ISCTE-IUL, Lisbon, Portugal, in 2012 and 2017, respectively, where he is currently pursuing the Ph.D. degree in information science and technology. He is currently working as a Researcher with Multivision—Consultoria Informática. He has four scientific publications as author in international conferences and seven scientific publications as coauthor.



**DIOGO CLEMENTE** received the B.S. degree in electrical and computer engineering from the Branch of Renewable Systems and Power Systems, Escola Superior de Tecnologia de Setúbal-ESTSetúbal/IPS, and the M.S. degree in telecommunications and computer engineering from the University Institute of Lisbon (ISCTE-IUL), Lisbon, Portugal, where he is currently pursuing the Ph.D. degree in information science and technology. He is currently working as a

Researcher with Multivision—Consultoria Informática. He has eight scientific publications in international conferences.



**GABRIELA SOARES** received the B.S. degree in computational mathematics from the Universidade Federal de Minas Gerais (UFMG), Belo Horizonte, Brazil, the M.S. degree in mathematical and computational modeling from the Centro Federal de Educação Tecnológica de Minas Gerais (CEFET-MG), Belo Horizonte, and the Ph.D. degree in computer science from the Universidade de São Paulo (USP), São Paulo, Brazil. She is currently working as a Data Scientist Researcher

with Multivision. She participated as a Researcher in three Research and Development projects funded by FAPESP, CAPES, and CNPQ focused on optimization, evolutionary computing, complex networks, and data science. She has 17 scientific publications in journal articles and international conferences.



**PEDRO SEBASTIÃO** (Member, IEEE) received the Ph.D. degree in electrical and computer engineering from IST. He is currently a Professor with ISCTE-IUL's Information Science and Technology Department. He is also the Board Director of AUDAX-ISCTE-Entrepreneurship and Innovation Center, ISCTE, and responsible for the LABS LISBOA incubator and researcher, Institute of Telecommunications. He developed his professional activity at the National Defense Industries,

initially with the Office of Studies and later as the Board Director of the Quality Department, Production of New Products and Technologies. He was also responsible for systems of communications technology at the Nokia-Siemens business area. He has organized or co-organized more than 50 national and international scientific conferences. He planned and developed several postgraduate courses in technologies and management, entrepreneurship and innovation, and transfer of technology and innovation. He has supported several projects involving technology transfer and creation of start-ups and spin offs of value to society and market. He has oriented several master's dissertations and doctoral theses. He has been an expert and evaluator of more than 100 national and international civil and defense Research and Development projects. It has several scientific, engineering, and pedagogical awards. He is the author or coauthor of more than 200 scientific articles. He has been responsible for several national and international Research and Development projects. His main research interests are in monitoring, control and communications of drones, unmanned vehicles, planning tools, stochastic process (modeling and efficient simulations), the Internet of Things, and efficient communication systems.



**FRANCISCO CERCAS** (Senior Member, IEEE) received the Ph.D. degree from the Instituto Superior Técnico, Lisbon University, Portugal, in 1996, and the ISCTE-University Institute of Lisbon. He was Researcher with INESC, from 1984 to 1985, and CAPS, from 1986 to 1993. He was also a Visiting Researcher with the University of Plymouth, U.K., from 1987 to 1992. Since 1994, he has been a Researcher with the Instituto de Telecomunicações. He is currently a Full Professor

with more than 36 years of professional experience, including Research and Development at the industry and 35 years of university teaching with the Instituto Superior Técnico. He also supervised many Ph.D. and M.Sc. students. He has participated in more than a dozen European projects in the telecommunications area, namely as the Portuguese delegate in European Cooperation in Science and Technology (4 COST) actions. He has authored and/or coauthored of a new class of codes, Tomlinson, Cercas, Hughes (TCH), one patent, and about 200 publications including book chapters, journal articles and conference papers. His research interests include satellite and mobile communications, coding theory, spread spectrum communications and related topics.



**RUI DINIS** (Senior Member, IEEE) received the Ph.D. degree from the Instituto Superior Técnico (IST), Technical University of Lisbon, Portugal, in 2001, and the Habilitation degree in telecommunications from the Faculdade de Ciências e Tecnologia (FCT), Universidade Nova de Lisboa (UNL), in 2010. From 2001 to 2008, he was a Professor with IST. He was a Researcher with the Centro de Análise e Processamento de Sinal (CAPS), IST, from 1992 to 2005, and a Researcher

with the Instituto de Sistemas e Robótica (ISR), from 2005 to 2008. In 2003, he was an Invited Professor with Carleton University, Ottawa, ON, Canada. Since 2009, he has been a Researcher with the Instituto de Telecomunicações (IT). He is currently an Associate Professor with FCT-UNL. He has been actively involved in several national and international research projects in the broadband wireless communications area. His research interests include transmission, estimation, and detection techniques. He is a VTS Distinguished Lecturer. He is or was an Editor of the IEEE TRANSACTIONS ON WIRELESS COMMUNICATIONS, the IEEE TRANSACTIONS ON COMMUNICATIONS, the IEEE TRANSACTIONS ON VEHICULAR TECHNOLOGY, the IEEE *Open Journal on Communications*, and the *Elsevier Physical Communication*. He was also a Guest Editor of the *Elsevier Physical Communication* (Special Issue on Broadband Single-Carrier Transmission Techniques).



**LÚCIO S. FERREIRA** (Senior Member, IEEE) received the Licenciado and Ph.D. degrees in electrical and computer engineering from the IST/Technical University of Lisbon, Portugal. He worked as a Researcher with Deutsche Telekom Innovation Laboratories, in 1998, Instituto de Telecomunicações, from 1999 to 2012, and INOV-INESC, from 2012 to 2015. He has worked as an Assistant Professor with the Universidade da Beira Interior, Universidade Lusitana de Lisboa,

and ISTE, in the areas of computer science and telecommunications. He has been with INESC-ID, since 2016. He is currently a Project Manager with Multivision—Consultoria Informática. He participated, as a Project Manager and a Researcher, in 17 Research and Development projects funded by the European Commission. At the National Level, he has worked as a Consultant for mobile providers and ANACOM national regulator. He has more than 50 scientific publications in books, journal articles, and international conferences. He is an editor and coauthor of 63 technical reports for the European Commission. He reviewed 29 journal articles and conference papers, and participated in eight organisational committees and 15 technical committees of international conferences. He has supervised 12 M.Sc. and three Ph.D. students. He is a Board Member of the IEEE ComSoc Portugal chapter.

...

## Chapter 3

# Comparison between Semi-Empirical and Artificial Intelligence Propagation Models

Artificial Intelligence (AI) tries to simplify the resolution of problems whose current solutions are complex and sometimes associated with large resource needs. In line with Chapter 2 and in order to enable the use of a faster propagation model in the generation of results but maintaining the same performance, a model of propagation generated by AI is presented in the article inserted in this chapter. To compare the ACSPM model with this new model, two real scenarios and several metrics are also presented.

Some paper details:

- **Title:** Comparison of Artificial Intelligence and Semi-Empirical Methodologies for Estimation of Coverage in Mobile Networks;
- **Date of publication:** July 2020;
- **Journal:** IEEE Access;
- **Scimago/Scopus Journal Ranking:** Quartile 1;

- **Publisher:** IEEE.

Received July 9, 2020, accepted July 25, 2020, date of publication July 30, 2020, date of current version August 11, 2020.

Digital Object Identifier 10.1109/ACCESS.2020.3013036

# Comparison of Artificial Intelligence and Semi-Empirical Methodologies for Estimation of Coverage in Mobile Networks

DANIEL F. S. FERNANDES<sup>1,2</sup>, ANTÓNIO RAIMUNDO<sup>1,2</sup>, FRANCISCO CERCAS<sup>1,2</sup>, (Senior Member, IEEE), PEDRO J. A. SEBASTIÃO<sup>1,2</sup>, (Member, IEEE), RUI DINIS<sup>2,3</sup>, (Senior Member, IEEE), AND LÚCIO S. FERREIRA<sup>4,5,6</sup>, (Senior Member, IEEE)

<sup>1</sup>Instituto Universitário de Lisboa (ISCTE-IUL), 1649-026 Lisboa, Portugal<sup>2</sup>Instituto de Telecomunicações (IT), 1049-001 Lisboa, Portugal<sup>3</sup>FCT-Universidade Nova de Lisboa, 2829-516 Caparica, Portugal<sup>4</sup>ISTEC, 1750-142 Lisboa, Portugal<sup>5</sup>INESC-ID/COPELABS Lusófona University, Campo Grande, 1749-024 Lisboa, Portugal<sup>6</sup>Multivision-Consultoria, Rua Soeiro Pereira Gomes, 1600-196 Lisboa, Portugal

Corresponding author: Daniel F. S. Fernandes (dfsfs@iscte-iul.pt)

This work was supported in part by the OptiNET-5G Project, co-funded by Centro2020, Portugal2020, European Union under Project 023304, and in part by the Instituto de Telecomunicações, FCT/MCTES through national funds and when applicable co-funded EU funds under Project UIDB/50008/2020 and Project UIDB/04111/2020.

**ABSTRACT** To help telecommunication operators in their network planning, namely coverage estimation and optimisation tasks, this article presents a comparison between a semi-empirical propagation model and a propagation model generated using Artificial Intelligence (AI). These two types of propagation models are quite different in their design. The semi-empirical Automatically Calibrated Standard Propagation Model (ACSPM) is specific for an operating antenna, being calibrated every time a use case application is used and the Artificial Intelligence Propagation Model (AIPM) can be applied in different scenarios, once trained, allowing to estimate coverage for a new antenna location, using information from neighboring antennas. These models have quite different features and applicability. The ACSPM should be applied in network optimisation, when using data from the current state of the antennas. The AIPM can be used in the deployment of new antennas, as it uses data from a certain geographical area. For a better comparison of the models studied, extensive Drive Tests (DT) collection campaigns conducted by operators are used, since coverage estimations are more realistic when DTs are considered. Both models are generated using very different methodologies, but their resulting performance is very similar. The AIPM achieves a Mean Absolute Error (MAE) up to 6.1 dB with a standard deviation of 4 dB. When compared to the ACSPM we have an improvement of 0.5 dB, since this only achieves a MAE up to 6.6 dB. AIPM achieves better results and is characterised for being completely agnostic and definition-free, when compared with known propagation models.

**INDEX TERMS** Coverage estimation, network planning, drive tests, measurements, propagation model, artificial intelligence.

## I. INTRODUCTION

The advances of mobile networks technology have made possible to provide mobile devices with new features for its users. Of all generations of telecommunications, 4G was the most innovative one, since it provided multimedia streaming, which had several limitations on past generations. It is expected that by 2025, 90% of the world's population will

be covered by this technology, while 65% has already access to the newer 5G technology [1].

In large urban centers, one of the main concerns of telecommunication operators is the Quality of Service (QoS), which measures the overall performance of operators' services provided to their clients. These cellular networks are constituted by a deployment of antennas, each covering a service area around it, the so-called cell. The poor signal coverage within a cell can be an adverse effect in QoS, since it can reduce the customer service availability. To prevent these

The associate editor coordinating the review of this manuscript and approving it for publication was Chao Tong.

situations, a correct planning of a telecommunication network is one of the most important tasks for operators, since it has a high impact on the users' experience [2].

One of the methodologies that improves cellular planning is by collecting data in the field. This data is collected in a predefined route, and every point gathered is called a Drive Test (DT). On each DT, it is possible to measure the signal level received in certain georeferenced point for the signal from surrounding antenna, and thus to evaluate the network coverage status at that point. Telecommunications operators collect large quantities of DTs periodically. In most cases, operators only use DTs to identify local coverage or interference problems of a given cell. Therefore we felt the motivation to use DTs for signal estimation, namely for the study described in this article, using large amounts of data from multiple cells within a given region (e.g., a city), as these can be used to infer a more global and precise view of the network coverage.

In order to adjust the network coverage planning, DT data can be loaded into network planning tools such as Atoll [3] or into the Metric [4] platform, which is a network monitoring and management web platform developed by Multivision [5]. The current research is within the scope of OptiNet5G [6], a research project from Multivision, funded by the European Commission, to bring improvements to the Metric Software-as-a-Service (SaaS) platform. This software is currently used by several mobile operators worldwide, aggregating Configuration Management (CM) and Key Performance Indicators (KPIs) data, as well as DTs from their networks. A good coverage leads to an increase of the overall QoS of the network. In [7], an Automatically Calibrated Standard Propagation Model (ACSPM) is proposed. By using the Metric platform, it is possible to generate a coverage grid of a given operating cell with ACSPM, which combines DT, CM and KPI data to accurately portray reality. This task can be done automatically for all cells of the network, which reduces the operating and investment costs, being one of the goals for a Self-Organising Network (SON) [8], [9].

Pursuing the goal of SON to provide "plug & play" self-configured networks, the next step is to explore DTs of neighboring cells to estimate the coverage for a new antenna location. This would complement ACSPM, which is not capable of doing so. Once the data collected by the networks is substantial, its analysis can be seen as a Big Data approach. In fact, some researchers present a new approach to this data by using Artificial Intelligence (AI) algorithms to estimate path loss values based on that data [10]–[13]. The models generated by AI algorithms can be applied on different scenarios as long as the propagation conditions are similar (similar urban, suburban or rural environment and same frequency band), allowing the reuse of these AI-generated propagation models and decreasing the resource usage.

In the present work, an Artificial Intelligence Propagation Model (AIPM) is proposed, using DT data from neighboring cells to train and build a coverage estimation model capable

of estimating coverage for any new antenna location. Its performance is compared with the results achieved with ACSPM model for a given antenna, for different realistic scenarios, achieving similar results. The comparative study of these propagation models was only possible due to the availability of extensive DTs campaigns conducted by operators in their networks that were made available to us to be used with the Metric platform. This article also aims to analyse if the AIPM can achieve similar performance to the ACSPM. Since the AIPM does not rely on any of the known propagation models, their characteristics and definition formulas, it is considered to be completely agnostic and definition-free. Another objective of this article is to estimate the signal coverage for several antennas simultaneously. These two propagation models have quite different applicabilities. Although both use DT data, the ACSPM model is used to estimate the coverage of an operating antenna, while the AIPM, once trained with the DTs of a geographical area, complements ACSPM, allowing it to estimate coverage for antennas in new locations for which DT, KPI or CM data is still not available.

The remaining paper is structured as follows. Section II discusses some basic telecommunication concepts then presents the scenarios and the metrics that will allow a performance analysis of the propagation models used in this article. The propagation models that are compared in this article are presented in Section III. In Section IV the results achieved are presented, and Section V discusses all the work carried out.

## II. EXPLORATORY DATA ANALYSIS

Since signal coverage is one of the main concerns of operators, in this section some of the concepts related to wireless communications are detailed as well as scenarios and metrics that will allow to compare various models of coverage estimation.

### A. WIRELESS COMMUNICATIONS

Wireless communications emerged as a telecommunications revolution since it provides flexibility, mobility and ease of use. The correct establishment of wireless communications is influenced by several factors such as the received signal power, the noise power, transmission band and rate. All these factors are important, however, for this article it was only considered that communication could occur if the received signal power was higher than a minimum received power level,  $P_{rx_{min}}$ . The received power level for location vector  $\mathbf{p}$  (position with latitude, longitude and height) from antenna  $\mathbf{a}$  operating at frequency  $f$ , if considering the gain of the receiving antenna of 0 dB, can be expressed by [7]:

$$P_{rx[\text{dBm}]}(f, \mathbf{a}, \mathbf{p}) = P_{tx[\text{dBm}]}(\mathbf{a}) + G_{tx}(\varphi_p - \varphi_a, \theta_p - \theta_a)_{[\text{dB}]} - L(f, \mathbf{a}, \mathbf{p})_{[\text{dB}]}, \quad (1)$$

where,

- $P_{tx}$  [dBm]: Transmitted power;

- $G_{tx}$  [dB]: Transmitted antenna gain, considering the antenna's vertical and horizontal diagrams, for the vertical  $\theta$  and horizontal  $\varphi$  direction between antenna location vector  $\mathbf{a}$  (antenna latitude, longitude and height,  $h_a$ ), and position  $\mathbf{p}$ , using the deviation of the antenna azimuth  $\varphi_a$  and tilt  $\theta_a$ ;
- $L$  [dB]: Path loss attenuation between  $\mathbf{a}$  and  $\mathbf{p}$  ( $x, y, z$ ) positions, where  $x, y$  and  $z$ , correspond respectively to latitude, longitude and height of position  $\mathbf{p}$ .

One of the major concerns of telecommunications operators is precisely the signal level that reaches each of the points around an antenna. Thus it is defined as the coverage area of an antenna as all the points where the signal level is higher than the  $P_{rx,min}$ . The correct coverage area estimation for an antenna allows operators not only to offer their customers a good experience in the use of their services but also to achieve an optimisation in the management of the network planning. This management allows adding new antennas, change its parameters and control resource usage effectively increasing the operators' profits.

In order to help telecommunication operators in their network planning and optimisation tasks, propagation models can be used [14]. These models aim to reproduce as realistically as possible the behavior of electromagnetic waves under certain conditions. Depending on the information used in these models, they may have different classifications [15], [16]. Models that are built based on field measurements can be considered as Empirical if they do not use terrain information, or Semi-Empirical if terrain information is considered in the generation of the model. There are also models, known as Deterministic models, that follow the laws of electromagnetic propagation in their generation. These Deterministic models are quite accurate, however, they have a great need for computational processing.

As mentioned above, the Empirical and Semi-Empirical propagation models use measurement data collected in the field called DTs. These measurements are collected along a pre-defined route on a car equipped with devices capable of recording them. Apart from the use of DTs in the calibration of propagation models, data collected by the Mobile Terminal (MT) itself can also be used, substantially reducing the costs for operators to conduct DTs campaigns. The information collected by the MT is based on a standardisation called Minimisation of Drive Tests (MDT). The use of MDT can be activated at any time by operators and allows to increase in the number of measurement points, which implies a deeper knowledge of the covered areas as well as a faster detection of network problems. On the consumer side, if MDT is activated by the operators, it only has the disadvantage of consuming the battery of mobile devices more quickly [17]. In terms of privacy issues, the MDT gathering can lead to information leaks and exposed user data. The operators must ensure that MDT gathering does not include any user-related information, but only the power level received by the MT internal antenna on a specific georeferenced point.

DTs are often the real representations of field measurements at the time of its collection. However, their values can be affected by atmospheric conditions and they may have different values for the same georeferenced point on another DT gathering. The use of DTs not only makes it possible to understand the dynamics of the network but it also enables the cancellation of the fast fading effect that signals suffer when working with discrete areas [14].

### B. REFERENCE SCENARIOS

Based on a data set from a Nordic 4G operator using the Metric platform, different reference scenarios were built. The scenarios considered will allow to evaluate the estimation accuracy of the two models presented.

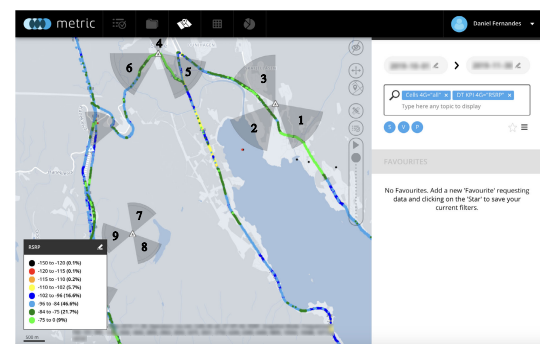


FIGURE 1. Scenario A depicted in Metric platform.

The first scenario has 9 transmitting antennas, numbered and identified in Fig. 1, and the second scenario has only 1 transmitting antenna. All the antennas have a transmission power,  $P_{tx}$ , of 46 dBm, they work at a downlink frequency of 796 MHz, and are located in an urban area. For each of the antennas, the respective horizontal and vertical radiation pattern was considered, and the gain of the receiver antenna (in downlink scenario the MT antennas) is 0 dB. More details of the antennas parameters are presented in Table 1.

TABLE 1. Synthesis of antennas parameters.

Scenario	Antenna	Height [m]	Mechanical Tilt [°]	Electrical Tilt [°]	Azimuth [°]
A	1	18.57	0	2	130
	2	18.57	0	2	220
	3	18.57	0	2	330
	4	15.5	0	6	0
	5	15.5	0	2	130
	6	15.5	0	2	240
	7	45	10	0	20
	8	45	10	0	140
	9	45	10	0	260
B	-	24	4	4	110

The selected DTs for both scenarios were collected by the operator within a time-window of 2 months, and then loaded into the Metric platform where they were dumped and processed in a transparent way. We required DTs with this time interval to ensure that the antenna parameters

were not changed in between, to ensure that the overall network configuration remained unchanged for this study. This interval is then divided into two sets in order to allow the calibration of the models and subsequently the assessment of the estimation accuracy. These two sets are divided temporally, being the first identified by period  $t$ , and the second,  $t + 1$ . The terminology  $t$  and  $t + 1$  is considered in order to allow the understanding of temporal continuity. This means the evaluation of the estimation (period  $t + 1$ ) is carried out sequentially after the considered calibration period (period  $t$ ).

The first scenario, scenario A, has 9 transmitting antennas, which presents a total of 2791 DTs in period  $t$  for the calibration of the ACSPM and 1126 DTs in period  $t + 1$  for evaluation of both models (ACSPM and AIPM). This scenario is depicted in Fig. 1.

In scenario B, presented in Fig. 2, the antenna is located approximately 22 km away from the antennas in scenario A, thus maintaining the same population density and buildings topology. This scenario is divided into 2 sub-scenarios in order to evaluate the impact on the ACSPM accuracy when the number of DTs used in its calibration changes. In sub-scenario B.1, 698 DTs are used in the calibration of the ACSPM and 1033 in the evaluation of both models (ACSPM and AIPM). In sub-scenario B.2 the number of DTs used to calibrate the ACSPM model increases to 1270. For evaluating the accuracy, 40 DTs were needed.

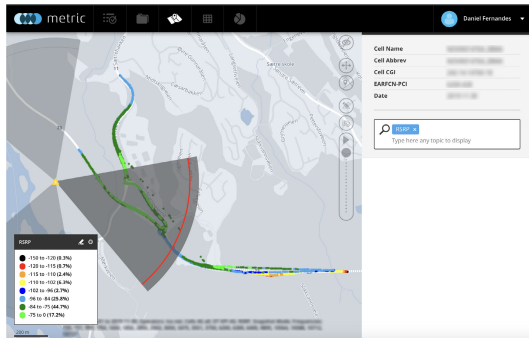


FIGURE 2. Scenario B depicted in the Metric platform.

A summary of the DTs number in each time interval for each scenario is detailed in Table 2.

TABLE 2. Specification of the number of DTs for each scenario, for the calibration ( $t$ ) and evaluation ( $t + 1$ ) time periods.

Scenario	$t$	$t + 1$
A	2791	1126
B.1	698	1033
B.2	1270	40

### C. PERFORMANCE EVALUATION METRICS

To compare the results achieved by different propagation models, some metrics of statistical analysis were chosen to analyse the results in several aspects.

These metrics will compare real values,  $P_{rx}$ , and the estimated values,  $\hat{P}_{rx}$ , for each model.  $N$  represents the number of samples considered in the comparison. Each of the metrics chosen is now detailed:

- **Mean Absolute Error (MAE):** The MAE measures the average absolute error between the real data and the estimated data. MAE is one of the most common metrics to evaluate the performance of regression models. The expression used in the MAE calculation is given by the following equation (2) [18].

$$MAE \text{ [dB]} = \frac{1}{N} \cdot \sum_{i=1}^N |P_{rx_i} - \hat{P}_{rx_i}|. \quad (2)$$

When MAE values are close to 0, the estimated data nearly matches the real data.

- **Standard Deviation ( $\sigma$ ):** The standard deviation measures the dispersion of values in relation to a mean value. When the estimated values are close to its mean values the standard deviation value tends to 0. The value of the standard deviation can be given by (3) [19].

$$\sigma \text{ [dB]} = \sqrt{\frac{\sum_{i=1}^N (P_{rx_i} - \bar{P}_{rx})^2}{N - 1}}, \quad (3)$$

where  $\bar{P}_{rx}$  denotes the average value of  $P_{rx}$ .

- **Pearson Correlation Coefficient ( $r$ ):** The correlation coefficient measures the degree of relationship between real and estimated measures. This coefficient can vary between -1 and 1 depending on whether it is a positive or negative correlation. This coefficient is calculated using equation (4) [20]–[22].

$$r = \frac{\sum_{i=1}^N (P_{rx_i} - \bar{P}_{rx}) \cdot \sum_{i=1}^N (\hat{P}_{rx_i} - \bar{\hat{P}}_{rx})}{\sqrt{\sum_{i=1}^N (P_{rx_i} - \bar{P}_{rx})^2} \cdot \sqrt{\sum_{i=1}^N (\hat{P}_{rx_i} - \bar{\hat{P}}_{rx})^2}}, \quad (4)$$

where  $\bar{P}_{rx}$  and  $\bar{\hat{P}}_{rx}$  denotes the average value of  $P_{rx}$  and  $\hat{P}_{rx}$  respectively.

Depending on the calculated absolute value of  $r$  the relationship between the measurements can be classified according to Table 3 [21].

TABLE 3. Correlation classification.

$ r $	Classification
0 – 0.19	very weak
0.2 – 0.39	weak
0.4 – 0.59	moderate
0.6 – 0.79	strong
0.8 – 1	very strong

According to [13], a propagation model is considered accurate when MAE is nearly 0, the  $\sigma$  is less than 9 dB and the coefficient of correlation,  $|r|$ , is more than 0.8.

### III. COVERAGE ESTIMATION METHODOLOGIES

Coverage in cellular networks is essential. Its estimation can be done following different methodologies. The ACSPM is

suited for operating cells with DT, KPI and CM data of their operation. On the other hand, AIPM is suited for estimating the received signal close to new antenna locations, using available DT information from neighboring operating cells. These two models are detailed next.

#### A. SEMI-EMPIRICAL PROPAGATION MODEL

The proposal for a new cloud-based framework of a semi-empirical propagation model is presented and detailed in [7]. This propagation model, called ACSMP has as main innovation the automatic model calibration and estimation of a received signal area using DTs reporting its signal within its service area, as well as CM and KPI data related to its operation. The cell coverage estimation model is represented in Fig. 3.

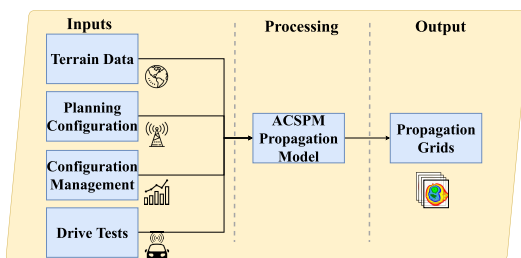


FIGURE 3. Cell coverage estimation model framework.

As indicated in Fig. 3 the inputs of the signal estimation framework are the data of terrain altimetry, the network configuration such as antenna location, or its operating parameters. The operator uses KPIs and DTs to make a fine-tuning and adjustment of the propagation model with the reality in order to portray a more realist approach of the network.

At the processing level, this semi-empiric model is based on two well-known propagation models, which are Walfish-Ikegami [23] and SPM [3]. The ACSMP combines these two models in order to build a new propagation model that can be used both in micro and macro cells.

The result of this propagation model is the creation of a grid with the signal received around an antenna that enables operators to perform various planning and network optimisation tasks.

As previously mentioned, one of ACSMP's innovations is the automatic calibration and generation of propagation grids. This propagation model, implemented using cloud services, was integrated into Metric platform. When new network information for a given antenna is available, such as DTs, KPI or configurations, the model is automatically calibrated and a new propagation grid is generated for that antenna allowing the operator to have a current status of the network. This automation follows the SON paradigm, as allows the implementation of this framework in SON systems since it allows the reduction of human actions in the network

because if there is a problem of network coverage it can be immediately detected through the automatically updated propagation grids, and then trigger the actions necessary to solve it. Since this processing is very intensive and uses a lot of computational resources, Metric transfers its computation to micro cloud services, namely the services provided by Amazon Web Services (AWS) [24].

#### B. MACHINE LEARNING PROPAGATION MODEL

Artificial Intelligence (AI) is a recurrent term nowadays and its main objective consists in solving specific problems by executing specific tasks. It is embedded in techniques and tools that execute those tasks. By being a difficult challenge for humans to perform and execute these tasks intuitively, for machines it is only a very challenging set of applied algorithms.

Artificial Neural Networks (ANNs) refers to artificial networks of neurons that were inspired (and they are very similar) to the natural functioning of a human brain [25]. Neurons, both natural and artificial ones, are the fundamental units responsible by the computation process. They are interconnected to form a network of data processing. Each individual neural has inputs and outputs and they are responsible to “consume” the data from the input in order to generate an output. These outputs, in the natural brain, can be, for example, responses to human reactions like emotions or sensations. The same outputs in an artificial neuron are expected to achieve a desired output. A common neural network is divided in three layers: the input layer, the hidden layers and the output layer. These layers are responsible for the input data (input layer), the intermediary layers that process the data, and the output layer that generates a result. Fig. 4 depicts an example of an ANN's architecture design.

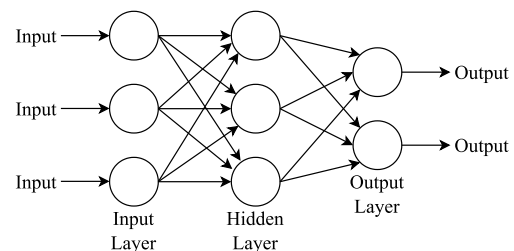


FIGURE 4. Configuration example of an ANN with three neurons in the input layer, one hidden layer and two output neurons.

The ANNs are much less complex that the natural ones, but both share a common principle: There is a “learning” process that is achieved when neurons reconnect each other. They can learn by “looking” at the input data - input dataset - and with that, they recognise patterns or structures within that data (learning or training process). A training dataset is composed by a set of input data and a set of output data, in which the ANN will try to estimate the output by learning the data characteristics and properties in

order to achieve the desired output given by the output data (supervised learning). This knowledge is then applied on other datasets in order to estimate, classify or predict the same (or a similar) results on unknown data (generalisation or validation process). However, there is always a difference between the estimated value given by the ANN and the real outputs values. This difference is called “error” or “loss” and is the value responsible to evaluate the ANN model’s performance [26], [27].

AI-based algorithms are known to be capable to process great amounts of data. When AI is applied to the telecommunications area, there are some tasks that require great amounts of data too. In this article, an AI-generated model will be used to predict path loss. [28] and [29] also used AI algorithms to estimate path loss regression for a given area.

In order to develop and implement the AI algorithm for this investigation, a custom ANN must be designed. The chosen ANN architecture is formed by 3 neurons in the input layer, 2 hidden layers with 5 and 3 neurons, respectively, and 1 neuron in the output.

As identified in Fig. 5, the input dataset contains, for each point, geographical information (latitude, longitude, and height), the distance from that location to the BS, the antenna gain at that same location and, finally, the losses that occur between transmission and reception. The output is the path loss value to reach that position. After testing several architectures that implement the ANN algorithm, the architecture depicted in Fig. 5 was the one presenting the best results, therefore it was chosen for further calibration and training.

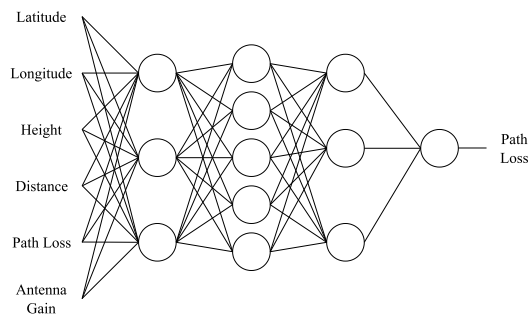


FIGURE 5. Custom architecture design of the implemented ANN algorithm.

### C. PROPAGATION MODELS TUNING/CALIBRATION

To apply the propagation models to the different scenarios presented, it is necessary to fine-tune them. For the ACSPM, its calibration occurs in each antenna, and is not applicable to others. According to [7], in DT locations there is no error between ACSPM and the DT measures (since the model uses the DT values whenever possible); for neighboring pixels, the values are calculated by weighting neighboring DTs, using all inputs as depicted in Fig. 3. In terms of accuracy, this model can achieve a MAE of about 5 dB.

The AIPM is a different model. Once calibrated/generated with available DT measurements from multiple antennas, the AIPM can generate coverage grids for any antenna location in the scenario area.

To better characterise the Reference Scenarios presented in Section II-B, the AIPM was generated with 13740 DTs as input data, collected from 31 antennas located in an urban environment, in the same geographical area in time period  $t$ . These 31 antennas include the antennas of scenarios A and B. The DTs of the input data present a mean value of  $-83.6$  dBm and a standard deviation of  $13.1$  dBm. The histogram with the distribution of the DT values is depicted in Fig. 6 and it is possible to see that the achieved mode for the received power level,  $P_{rx}$ , of each DT lies between  $-70$  dBm and  $-98$  dBm.

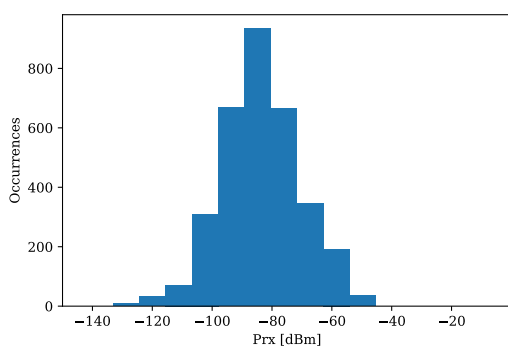


FIGURE 6. DT occurrences distributed by their  $P_{rx}$  value.

For the AIPM configuration, it was considered a dataset of DTs from period  $t$ , being 80% used for the training process and 20% for the validation process. To achieve the best possible performance, the chosen network configuration was trained along 1000 iterations, and by using callbacks, only the model that reached the lowest MAE value was stored. Since training is a random process, the chosen network configuration was trained 20 times and only the training with the lowest MAE value was considered.

The training that reached the best MAE values, which was 8.6 dB, took 16 seconds to train. In Fig. 7, the evolution of training and validation curves is depicted. Once the model has been trained, it can be applied to any scenario by simply predicting the data inputs provided. For scenario A, the prediction was done in 15 seconds, when using the AIPM model. For the case of ACSPM, the model had to be calibrated for each scenario, which resulted in about 173 seconds, for combining the results for scenario A and the estimation for each of the 9 antennas.

By analysing Fig. 7, it is possible to conclude that the training process converged smoothly and the loss values were very stable during the whole process, reaching its optimal values very quickly. It is also possible to conclude that the model achieved an acceptable performance. In order to

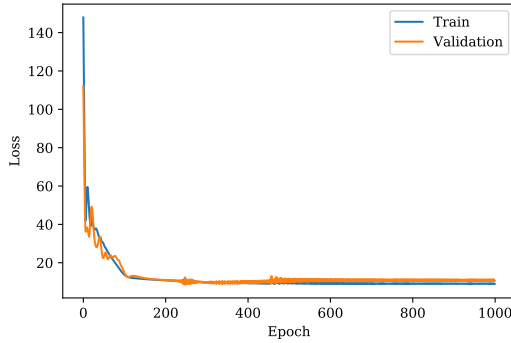


FIGURE 7. Loss values of Training and Validation sets.

develop the AI-generated model, a frontend framework called *Keras* [30] was used, which uses *TensorFlow* [31] as backend.

#### IV. RESULTS COMPARISON

In this section, the results for the metrics presented in Section II-C are discussed for each of the scenarios presented in Section II-B when the AIPM and ACSPM models presented in Section III are applied.

##### A. SCENARIO A

This scenario has 2791 DTs in time period  $t$  which are used to calibrate the ACSPM model. In period  $t + 1$ , 1126 DTs are used for performance evaluation purposes. For each of those models, a received signal power grid was obtained. In Fig. 8 the grid for the AIPM is shown and in Fig. 9 the result estimated with the ACSPM model. The ACSPM model initially estimates the coverage area for each of the antennas in the scenario and then all the areas are overlapped in a single area.

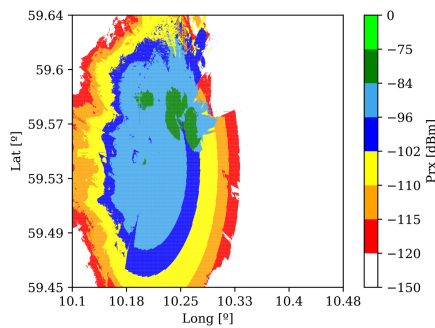


FIGURE 8. Estimated received power level using the AIPM model for the entire service area and considering all the antennas for scenario A.

By analysing the shapes, which are similar in each generated model, it is noticeable that ACSPM is a more optimistic model, since the green area (where  $P_{rx}$  lies

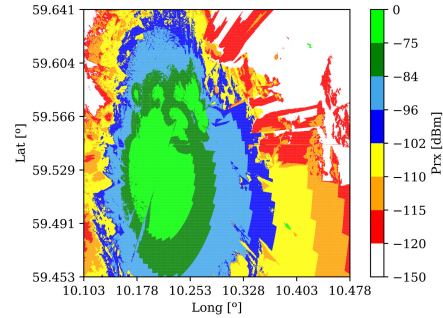


FIGURE 9. Estimated received power level using the ACSPM model for the entire service area and considering all the antennas for scenario A.

between 0 dBm and  $-75$  dBm) is greater. The results estimated by these models were compared with the real values. The AIPM obtained a MAE of 7.1 dB, which is 0.1 dB lower than the ACSPM. When comparing the  $\sigma$  of the AIPM with that of ACSPM, the AIPM obtains values which are 2.4 dB lower.  $r$  is 0.73 for the AIPM and 0.58 for the ACSPM.

For this scenario, according to the considered metrics, AIPM achieves better performance results when compared with ACSPM.

It can be concluded that, for the estimation of coverage within a scenario of several cells, AIPM achieves good and useful results. It is not needed to build individual grids of realistic coverage estimations for each antenna and to combine them.

##### B. SCENARIO B.1

In this single antenna scenario, depicted in Fig. 10, unlike the multi-antenna scenario, the ACSPM is the model that presents an area where the signal coverage between 0 dBm and  $-96$  dBm is lower. For the same propagation area, the AIPM shape, depicted in Fig. 11, is much more extended when compared to the shape estimated by the ACSPM.

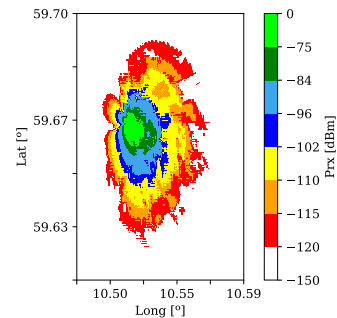


FIGURE 10. Estimated received power level using the ACSPM model for scenario B.1.

In this analysis with the chosen metrics, the ACSPM presents a MAE of 7.3 dB while the AIPM presents 7.2 dB.

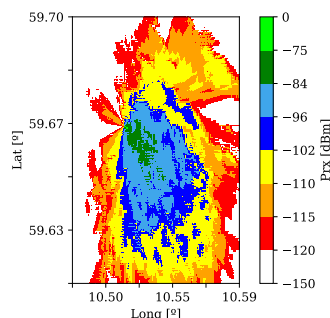


FIGURE 11. Estimated received power level using the AIPM model for scenario B.1.

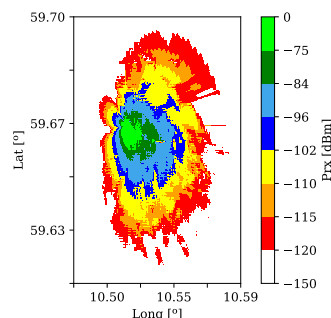


FIGURE 12. Estimated received power level using the ACSPM model for scenario B.2.

For the case of  $\sigma$ , the AIPM is 3 dB better. However, the ACSPM presents a value of 0.73 for  $r$ , which is higher than that obtained with AIPM, which is 0.69. Therefore, in terms of  $r$ , the ACSPM model is slightly better, since it presents a greater correlation between estimated and real data. This is due to the fact that here we are using a single antenna, which requires a more realistic estimation of coverage based on standard propagation aspects, and AIPM does not take it into account.

### C. SCENARIO B.2

For scenario B.2, the received signal grid estimated by ACSPM is presented in Fig. 12. For the AIPM the estimation is the same as in B.1 scenario, as shown in Fig. 11.

As noticed in scenario B.1, the AIPM presented better results. To try to improve the results of the ACSPM for the same scenario, the number of DTs used in the calibration of the ACSPM was increased. This increase improved all metrics. The ACSPM presents a MAE of 6.6 dB with a variation of 4.1 dB. In this scenario, the correlation between the measurements can be classified as “very strong” since the value of  $r$  obtained is 0.82. For the AIPM the MAE decreased to 6.0 dB with a variation of 4.0 dB. The correlation has a value of 0.80.

### D. SUMMARY

The fact that B scenarios addresses the estimation of coverage of a single antenna, while A scenario addresses the best signal level for a set of antennas, naturally affects the results. Nevertheless, each of the approaches is needed and has useful applications in the study and evaluation of a network.

Scenarios A and B show that the estimated grids for the signal level received have similar shapes for each of the models, the values of MAE differ, at most 0.5 dB from each other, which indicates that the models have similar performance.

Table 4 presents a summary with the values achieved for each metric and for each scenario.

TABLE 4. Synthesis of results for each of the scenarios under study.

Scenario	Model	MAE [dB]	$\sigma$ [dB]	$r$
A	ACSPM	7.2 (+1.4%)	7.0	0.58
	AIPM	7.1 (0%)	4.6	0.73
B.1	ACSPM	7.3 (1.4%)	8.1	0.73
	AIPM	7.2 (0%)	5.0	0.69
B.2	ACSPM	6.6 (+8.2%)	4.1	0.82
	AIPM	6.1 (0%)	4.0	0.80

By analysing Table 4, we observe that both models achieved similar MAE values. It is also verified that, as the number of DTs used in the model performance evaluation decreases, the value of the MAE also decreases, as presented in scenario B.2. The ACSPM model presents the highest variation between the samples tested, indicating a higher error associated with the signal level estimation. In scenarios B.1 and B.2, both models present a similar relationship between estimated and real measures. This situation changes in scenario A where the AIPM has a higher relationship of 0.15 when compared to the ACSPM.

Following the conditions presented at the end of Section II-C, both ACSPM and the AIPM can be considered as an accurate propagation model for B.2 scenario, for estimation of coverage of a single antenna, since in the remaining scenarios all models have a value of  $r$  less than 0.80. In fact, it is understandable that AIPM needs large data sets to provide realistic results, as a semi-empirical propagation model integrates physical aspects that are realistic (e.g., power decay with distance).

These results also indicate that, by increasing the number of DTs used in the ACSPM calibration, the signal estimation for that antenna improves. If we increase the number of DTs for the AIPM training, the model becomes more robust for estimating coverage of new antennas, as we should expect.

### V. CONCLUSION

Cellular network operators collect large amounts of DTs, measuring the signal strength received by antennas geolocated along a given path. These can be very useful to estimate

coverage for operating cells using the ACSPM model and for new cells, using the AIPM. Since AI can solve several problems in a simple, fast, and effective way and its solutions can be quite optimised, this study focused on comparing the performance of ACSPM, a semi-empirical propagation model with realistic results, with that of a model generated by AI.

The results achieved demonstrate that the ACSPM, which was designed for only one antenna at a time, obtains quite homogeneous results for that scenario or even when the estimation of each of the antennas is combined in a multi-antenna scenario to estimate the overall coverage of the network. It reaches an average MAE of 7.0 dB decreasing when the number of DT used in the calibration of the model is increased.

The AIPM presents similar results to the ACSPM, however, it can still overcome the results of this model by 0.5 dB. The use of these models is quite interesting because it does not require any previous knowledge of the propagation models.

As demonstrated the number of DTs used in the calibration of ACSPM or in the training of AIPM has a powerful impact on results, so, the greater the number of DTs the better the results achieved. By using a wide range of DTs for the training of the AIPM model, we can also use it in regions that are geographically similar.

The research and results undertaken with these models made it possible to foresee new applications for them. Since both exhibit quite similar performances, the ACSPM can be applied to estimate the coverage of existing cells using DTs, while the AIPM, once trained, useful for the deployment of new cells, in the same geographical area, based on the first estimation.

In terms of computational efficiency, AIPM is a model that presents results very quickly, while ACSPM requires more time, as it presents a greater computational complexity, and it can output much more detailed results.

As we have verified, the performance results achieved can be greatly improved by increasing the number of DTs. This increase in the number of DTs, which can be achieved by using MDTs, allows a much more efficient and precise training/calibration of the models, allowing to accurately portraying a region for a more accurate network planning and coverage.

The research results presented in this article are based on a Single Input Single Output (SISO) communication system. However with the evolution to 5G technology where, Multiple Input Multiple Output (MIMO) systems are used, it can be interesting to know the effective impact on the propagation of the signals by applying these models to a MIMO system.

## REFERENCES

- [1] *Ericsson Mobility Report 2019*, Ericsson, Stockholm, Sweden, Nov. 2019.
- [2] W. C. Hardy, *QoS—Measurement and Evaluation of Telecommunications Quality of Service*. Hoboken, NJ, USA: Wiley, Jul. 2001.
- [3] *Atoll 3.3.0 Technical Reference Guide for Radio Networks*, Forsk, 2015.
- [4] *Metric*. Accessed: Apr. 1, 2020. [Online]. Available: <https://metric.pt>
- [5] *Multivision*. Accessed: Apr. 1, 2020. [Online]. Available: <https://multivision.pt>
- [6] *OptiNET-5G—Planning and Optimization Framework of 5G Heterogeneous Networks in a Cloud Environment*, Multivision, Eur. Union, Funded Centro, Portugal, 2020.
- [7] D. Fernandes, D. Clemente, G. Soares, P. Sebastiao, F. Cercas, R. Dinis, and L. S. Ferreira, "Cloud-based implementation of an automatic coverage estimation methodology for self-organising network," *IEEE Access*, vol. 8, pp. 66456–66474, 2020.
- [8] M. Frankel, N. Shacham, and J. E. Mathis, "Self-organizing networks," *Future Gener. Comput. Syst.*, vol. 4, no. 2, pp. 95–115, Sep. 1988.
- [9] K. Zheng, Z. Yang, K. Zhang, P. Chatzimisios, K. Yang, and W. Xiang, "Big data-driven optimization for mobile networks toward 5G," *IEEE Netw.*, vol. 30, no. 1, pp. 44–51, Jan. 2016.
- [10] I. Popescu, I. Naformita, G. Gavrioloia, P. Constantinou, and C. Gordan, "Field strength prediction in indoor environment with a neural model," in *Proc. 5th Int. Conf. Telecommun. Mod. Satell., Cable Broadcast. Service*, 2001, pp. 640–643.
- [11] E. Ostlin, H. Zepernick, and H. Suzuki, "Macrocell path-loss prediction using artificial neural networks," *IEEE Trans. Veh. Technol.*, vol. 59, no. 6, pp. 2735–2747, Jul. 2010.
- [12] J. M. Mom, C. O. Mgbe, and G. A. Igwe, "Application of artificial neural network for path loss prediction in urban macrocellular environment," *Amer. J. Eng. Res.*, vol. 3, no. 2, pp. 270–275, 2014.
- [13] M. Ayadi, A. B. Zineb, and S. Tabbane, "A UHF path loss model using learning machine for heterogeneous networks," *IEEE Trans. Antennas Propag.*, vol. 65, no. 7, pp. 3675–3683, Jul. 2017.
- [14] A. F. Molish, *Wireless Communications*, 2nd ed. Hoboken, NJ, USA: Wiley, 2010.
- [15] M. F. Iskander and Z. Yun, "Propagation prediction models for wireless communication systems," *IEEE Trans. Microw. Theory Techn.*, vol. 50, no. 3, pp. 662–673, Mar. 2002.
- [16] F. Letourneux, S. Guivarch, and Y. Lostanlen, "Propagation models for heterogeneous networks," in *Proc. 7th Eur. Conf. Antennas Propag. (EuCAP)*, 2013, pp. 3993–3997.
- [17] W. A. Hapsari, A. Umesh, M. Iwamura, M. Tomala, B. Gyula, and B. Sebire, "Minimization of drive tests solution in 3GPP," *IEEE Commun. Mag.*, vol. 50, no. 6, pp. 28–36, Jun. 2012.
- [18] C. Willmott and K. Matsuura, "Advantages of the mean absolute error (MAE) over the root mean square error (RMSE) in assessing average model performance," *Climate Res.*, vol. 30, no. 1, pp. 79–82, 2005.
- [19] P. Barde and M. Barde, "What to use to express the variability of data: Standard deviation or standard error of mean?" *Perspect. Clin. Res.*, vol. 3, no. 3, pp. 113–116, 2012.
- [20] E. Östlin, H. Suzuki, and H.-J. Zepernick, "Evaluation of the propagation model recommendation ITU-R P.1546 for mobile services in Rural Australia," *IEEE Trans. Veh. Technol.*, vol. 57, no. 1, pp. 38–51, Jan. 2008.
- [21] M. J. Campbell and T. D. V. Swinscow, *Statistics at Square One*, 11th ed. Hoboken, NJ, USA: Wiley, 2011.
- [22] H. Wang, W. Du, and X. Chen, "Evaluation of radio over sea propagation based ITU-R recommendation P.1546-5," *J. Commun.*, vol. 10, no. 4, pp. 231–237, 2015.
- [23] A. R. Mishra, Ed., *Advanced Cellular Network Planning and Optimisation*. Chichester, U.K.: Wiley, Oct. 2006.
- [24] *AWS*. Accessed: Apr. 1, 2020. [Online]. Available: <https://aws.amazon.com>
- [25] L. Wang, O. Kisi, M. Zounemat-Kermani, G. A. Salazar, Z. Zhu, and W. Gong, "Solar radiation prediction using different techniques: Model evaluation and comparison," *Renew. Sustain. Energy Rev.*, vol. 61, pp. 384–397, Aug. 2016.
- [26] *A.I. Wiki*. Accessed: Apr. 15, 2020. [Online]. Available: <https://pathmind.com/wiki/neural-network>
- [27] P. M. Buscema, G. Massini, M. Breda, W. A. Lodwick, F. Newman, and M. Asadi-Zeydabadi, "Artificial neural networks," *Stud. Syst., Decis. Control*, vol. 131, pp. 11–35, 2018.
- [28] S. I. Popoola, E. Adetiba, A. A. Atayero, N. Faruk, and C. T. Calafate, "Optimal model for path loss predictions using feed-forward neural networks," *Cogent Eng.*, vol. 5, no. 1, 2018, Art. no. 1444345.
- [29] Y. Zhang, J. Wen, G. Yang, Z. He, and J. Wang, "Path loss prediction based on machine learning: Principle, method, and data expansion," *Appl. Sci.*, vol. 9, no. 9, p. 1908, May 2019.
- [30] *Keras*. Accessed: Apr. 15, 2020. [Online]. Available: <https://keras.io/>
- [31] *TensorFlow*. Accessed: Apr. 15, 2020. [Online]. Available: <https://www.tensorflow.org/>



**DANIEL F. S. FERNANDES** received the B.S. degree in telecommunications and computer engineering and the M.S. degree in telecommunications and computer engineering from ISCTE-IUL, Lisbon, Portugal, in 2012 and 2017, respectively, where he is currently pursuing the Ph.D. degree in information science and technology. As a Researcher, he is currently working at Multivision, Consultoria Informática. His research interests include telecommunications and 5G networks.

He has six scientific publications as the author in journals or at international conferences and nine scientific publications as a coauthor.



**ANTÓNIO RAIMUNDO** received the B.Sc. degree in computer science and the M.Sc. degree in computer science from the ISCTE-Lisbon University Institute, Lisbon, Portugal, in 2014 and 2016, respectively, where he is currently pursuing the Ph.D. degree in information science and technology. Since 2016, he has been a Junior Researcher with the Instituto de Telecomunicações, ISCTE-IUL branch, Lisbon. His research interest includes the development of applications

for Unmanned Aerial Vehicles (UAVs), using machine learning techniques. His Ph.D. research topics explore computer vision methods to perform automated classification by using UAVs on industrial applications.



**FRANCISCO CERCAS** (Senior Member, IEEE) received the Ph.D. degree from Lisbon University, Portugal, in 1996. He was a Researcher with INESC, from 1984 to 1985, CAPS, from 1986 to 1993, and the Instituto de Telecomunicações, in 1994. He was also a Visiting Researcher with the University of Plymouth, U.K., from 1987 to 1992. He is currently a Full Professor with more than 36 years of professional experience including

Research and Development at the industry and 35 years of university teaching at the Instituto Superior Técnico, Lisbon University, and ISCTE–University Institute of Lisbon, in 1999. He has participated in more than a dozen European Projects in the telecommunications area, namely as the Portuguese Delegate in four COST actions (European Cooperation in Science and Technology). He is the author and/or coauthor of a new class of codes, Tomlinson, Cercas, Hughes (TCH), one patent, and about 200 publications including book chapters, journal articles, and conference papers. He also supervised many Ph.D.'s and M.Sc.'s. His research interests include satellite and mobile communications, coding theory, spread spectrum communications, and related topics.



**PEDRO J. A. SEBASTIÃO** (Member, IEEE) received the Ph.D. degree in electrical and computer engineering from IST. He is currently a Professor with the ISCTE–IUL's Information Science and Technology Department. He is the Board Director of the AUDAX-ISCTE-Entrepreneurship and Innovation Center, ISCTE, responsible for the LABS LISBOA incubator and a Researcher at the Institute of Telecommunications. He has oriented several master's dissertations and Ph.D. theses.

He is the author or coauthor of more than two hundred scientific articles and he has been responsible for several national and international Research and Development projects. He has been an Expert and Evaluator of more than one hundred national and international Civil and Defense Research and Development projects. It has several scientific, engineering, and pedagogical awards. Also, he has organized or co-organized more than fifty national and international scientific conferences. He planned and developed several postgraduate courses in technologies and management, entrepreneurship and innovation, and transfer of technology and innovation. He has supported several projects involving technology transfer and creation of start-ups and spin offs of value to society and market. He has developed his professional activity in the National Defense Industries, initially in the Office of Studies and later as the Board Director of the Quality Department of the Production of New Products and Technologies. He was also responsible for systems of communications technology in the Nokia-Siemens business area. His main research interests include monitoring, control and communications of drones, unnamed vehicles, planning tools, stochastic process (modeling and efficient simulations), the Internet of Things, and efficient communication systems.



**RUI DINIS** (Senior Member, IEEE) received the Ph.D. degree from the Instituto Superior Técnico (IST), Technical University of Lisbon, Portugal, in 2001, and the Habilitation degree in telecommunications from the Faculdade de Ciências e Tecnologia (FCT), Universidade Nova de Lisboa (UNL), in 2010. From 2001 to 2008, he was a Professor with IST. He is currently an Associated Professor with FCT-UNL. In 2003, he was an Invited Professor with Carleton University, Ottawa, Canada. He was a Researcher with the Centro de Análise e

Processamento de Sinal (CAPS), IST, from 1992 to 2005, and a Researcher with the Instituto de Sistemas e Robótica (ISR), from 2005 to 2008. Since 2009, he has been a Researcher with the Instituto de Telecomunicações (IT). He has been actively involved in several national and international research projects in the broadband wireless communications area. His research interests include transmission, estimation, and detection techniques. He is a VTS Distinguished Lecturer and is or was Editor at the IEEE TRANSACTIONS ON WIRELESS COMMUNICATIONS, the IEEE TRANSACTIONS ON COMMUNICATIONS, the IEEE TRANSACTIONS ON VEHICULAR TECHNOLOGY, the IEEE OPEN JOURNAL ON COMMUNICATIONS, and *Physical Communication* (Elsevier). He was also a Guest Editor for *Physical Communication* (Elsevier), special issue on broadband single-carrier transmission techniques.



**LÚCIO S. FERREIRA** (Senior Member, IEEE) received the Licenciado (five years) and Ph.D. degrees in electrical and computer engineering from the IST, Technical University of Lisbon, Portugal. As a Researcher, he worked Deutsche Telekom Innovation Laboratories in 1998, Instituto de Telecomunicações, from 1999 to 2012, INOV-INESC, from 2012 to 2015. He has been a Researcher with INESC-ID, since 2016. As an Assistant Professor, he has worked with the Universidade da Beira Interior, the Universidade Lusíada de Lisboa, and ISTE, in the areas of computer science and telecommunications. He is currently also a Project Manager with the Multivision, Consultoria Informática.

He participated, as a Project Manager and a Researcher, in 17 Research and Development projects funded by the European Commission. At national level, he has worked as a Consultant for mobile providers and ANACOM national regulator. He has more than 50 scientific publications in books, journal articles, and international conferences. He is the Editor and a co-author of 63 technical reports for the European Commission. He reviewed 29 journal articles and conference papers, and participated in eight organizational committees and 15 technical committees of international conferences. He has supervised 12 M.Sc. and three Ph.D. students. He is a Board Member of the IEEE ComSoc Portugal Chapter.

...

# Chapter 4

## Extension of SISO propagation models to MIMO systems

As mentioned earlier, the real measures obtained in MIMO systems are sparse when compared to existing measures for SISO systems. Since these measures have a high financial cost associated with their collection, it would be interesting if the use of these measures was also possible in MIMO systems. In this context, this chapter presents a study of the impact on the coverage area with the switching of a SISO system to a MIMO system, allowing the use of SISO measures for the estimation of coverage in MIMO systems.

For this Chapter and also for Chapter 5 the simulations presented were obtained through Monte Carlo simulation using the MatLab software environment. In order to improve the accuracy of Monte Carlo simulations the simulations were conducted with data blocks of  $N = 256$  Quaternary Phase Shift Keying (QPSK) symbols per block and every channel has 100 slots, symbol-spaced, equal-power multipath components. It is assumed perfect synchronism between the transmitted blocks associated to the different users and perfect channel estimation.

Some paper details:

- **Title:** Estimating the Performance of MIMO SC-FDE Systems Using SISO Measurements;
- **Date of publication:** October 2020;
- **Journal:** *Applied Sciences*;
- **Scimago/Scopus Journal Ranking:** Quartile 1;
- **Publisher:** MDPI.

Article

## Estimating the Performance of MIMO SC-FDE Systems Using SISO Measurements

Daniel Fernandes <sup>1,2,\*</sup> , Francisco Cercas <sup>1,2</sup> , Rui Dinis <sup>2,3</sup>  and Pedro Sebastião <sup>1,2</sup> 

<sup>1</sup> Iscte—Instituto Universitário de Lisboa, Av. das Forças Armadas, 1649-026 Lisboa, Portugal; francisco.cercas@iscte-iul.pt (F.C.); pedro.sebastiao@iscte-iul.pt (P.S.)

<sup>2</sup> IT—Instituto de Telecomunicações, Av. Rovisco Pais, 1, Torre Norte, Piso 10, 1049-001 Lisboa, Portugal; rdinis@fct.unl.pt

<sup>3</sup> Faculty of Sciences and Technology, FCT—Universidade Nova de Lisboa, Monte da Caparica, 2829-516 Caparica, Portugal

\* Correspondence: dfsfs@iscte-iul.pt

Received: 30 August 2020; Accepted: 21 October 2020; Published: 25 October 2020



**Abstract:** The demand for ubiquitous telecommunications services forces operators to have a special concern about signal quality and the coverage area they offer to their customers. This was usually checked by using suitable propagation models for Single Input Single Output (SISO) systems, which are no longer the case for new and future mobile generations, such as 5G and beyond. To guarantee good signal quality coverage, operators started to replace these models with Multiple Input Multiple Output (MIMO) ones. To achieve the best results, these models are usually calibrated with Drive Test (DT) measures; however, the DTs available for MIMO propagation models are sparse, in contrast to SISO ones. The main contribution presented in this paper is a methodology to extend the propagation models of SISO systems so they can be applied in MIMO systems with Single-Carrier and Frequency-Domain Equalization (SC-FDE), while still using DTs acquired for SISO systems. This paper presents the impact on Bit Error Rate (BER) performance and its coverage area resulting from the application of our proposed method. We consider a MIMO SC-FDE system with an Iterative Block Decision Feedback Equalization (IB-DFE) receiver and we present the improvement expressions for the BER that we illustrate with some simulations.

**Keywords:** propagation model; SISO; MIMO; IB-DFE; BER performance

---

### 1. Introduction

The evolution of telecommunications has enabled operators to offer services increasingly adapted to users' needs, such as the possibility of voice and video communications, with a major concern regarding the Quality of Service (QoS) they provide to customers [1]. Despite the constant evolution of technologies towards the Fifth Generation (5G) of telecommunications, the Fourth Generation (4G) is only expected to reach its peak in 2022, being subsequently replaced by 5G [2].

To ensure QoS, operators initially plan their networks and analyse the signal coverage for a given geographical area, which can be validated by carrying out Drive Tests (DTs). One of the major drawbacks of DTs is the expensive way in which DT campaigns are carried out, since they are time-consuming, costly, and, after all, they only depict the network status at the time they were performed. Despite these disadvantages, the information collected by DTs is very valuable as it allows for detecting regions where the signal received power level is lower than expected, therefore allowing us to optimise network planning [3].

There are many tools to assist operators in network planning; however, the starting point is always the signal coverage, which can be estimated using appropriate propagation models and tools.

For example, a propagation model that uses terrain morphology data, network Key Performance Indicators (KPIs), and other data, has been implemented using AWS [4] services, which can be found in a network management tool called METRIC [5], developed by Multivision [6]. The referred model, named Automatically Calibrated Standard Propagation Model (ACSPM) is technology agnostic and can be used in any existing technology, such as third generation or 4G. The description of all details involved in the estimation of the ACSPM signal, as well as its implementation, are discussed in [7], where it is also possible to find validation metrics for the model. The implementation of this model was a base for new cellular planning algorithms, such as the estimation of neighbouring cells [8], which allows not only frequency planning [9], but also Scrambling Code (SC) planning for Universal Mobile Telecommunications System networks (UMTS) networks [10].

This ACSPM model was initially designed and implemented for Single Input Single Output (SISO) communication systems, which are now changing to Multiple Input Multiple Output (MIMO) systems due to the increase in required user's data rate and QoS [11]. The concept of MIMO in this research is related to spacial diversity, as multiple antennas are used in order to improve the quality of the transmission link and thus offer a better QoS to the user [12,13]. If this system changeover is key to improve the QoS it is therefore essential to know the impact on signal propagation when moving to the MIMO system and how it can be appropriately foreseen by the propagation model used.

Operator's DT campaigns using MIMO systems are still very limited and they only depict specific scenarios (e.g., two transmitting antennas and two receiving antennas), while DT campaigns for SISO systems are more widely available. The motivation for this study lies in the possibility of using these SISO DT campaigns, so as they can be used with propagation models for MIMO systems, which immediately brings a great cost advantage. The use of this methodology enables a simple estimation of coverage for a MIMO system, allowing for the application of algorithms for network planning and optimisation. In Figure 1, the motivation for this study is depicted.

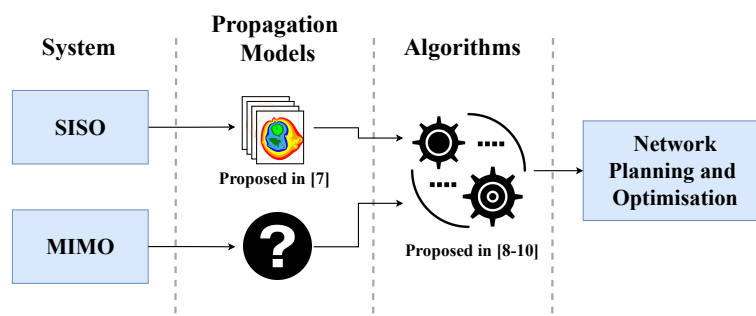


Figure 1. Motivation for this study.

In this paper, the authors present a theoretical methodology, with some simulation results, that allows us to verify the impact of the Bit Error Rate (BER) performance when changing from a SISO system to a MIMO system, which can also be used to estimate the received power level with the MIMO system in a given area.

This paper considers the use of MIMO systems with Single-Carrier and Frequency-Domain Equalization (SC-FDE) in order to allow, not only an efficient power amplification at the Mobile Terminal (MT), but also a reduction in envelope fluctuations when compared with Orthogonal Frequency Division Multiplexing (OFDM) [14–17]. In addition, when using SC-FDE, there is also a performance improvement when we use iterative Frequency-Domain Equalization (FDE), such as Iterative Block Decision Feedback Equalization (IB-DFE), instead of linear FDE, as is done in this research work [18].

The characterisation of the system considered in this study is presented in Section 2 and the BER performance of the SISO systems is theoretically calculated in Section 3. Section 4 presents the results

obtained through the BER performance simulation for both SISO and MIMO systems, allowing us to evaluate the impact when switching from SISO to MIMO scenarios. The model is then used with a real SISO scenario, described in Section 5 to evaluate how it would behave in a MIMO scenario. This paper ends with Section 6 where the main conclusions are drawn.

The following denotation is employed in this paper: In general, the upper-case letters denote frequency-domain variables, while lower case letters denote time-domain variable. Bold upper letters represent matrices or vectors and the Hermitian matrix of  $\mathbf{X}$  is denoted by  $\mathbf{X}^H$ . The expectation of  $x$  is represented by  $\mathbb{E}[x]$  and  $\tilde{x}$ ,  $\bar{x}$ ,  $\hat{x}$ , denotes samples—respectively, “soft decision” and “hard decision” estimation of  $x$ .

## 2. System Characterisation

The scenario considered in this paper is a point-to-point connection in a SISO system with a highly frequency selective channel.

The system is modelled assuming a data block, of size  $N$ , transmitted in the frequency-domain and expresses as  $\{X_k; n = 0, 1, \dots, N - 1\}$ , which is the Discrete Fourier Transform (DFT) of the time-domain as a data block  $\{x_n; n = 0, 1, \dots, N - 1\}$ , where data symbols  $x_n$  are selected according to the Quadrature Phase-Shift keying (QPSK) rule with Gray mapping. The received signal in the frequency-domain is denoted as  $\{Y_k; n = 0, 1, \dots, N - 1\}$  whose Inverse Discrete Fourier Transform (IDFT) corresponds to  $\{y_n; n = 0, 1, \dots, N - 1\}$  samples in the time-domain. The received signal can also be expressed by Equation (1):

$$Y_k = H_k X_k + N_k, \quad (1)$$

where the frequency-domain block of the transmitted block  $x_n$  is represented by  $X_k$ , the  $N_k$  and  $H_k$  represent the channel noise and the channel for the  $k^{\text{th}}$  subcarrier, respectively.

The iterative FDE receiver considered is the Iterative Block Decision Feedback Equalization (IB-DFE) [19] presented in Figure 2. This IB-DFE receiver has two filters the feedforward filter,  $F_k$ , which equalises the channel, and the feedback filter,  $B_k$ , which is responsible for removing the Inter-Symbol Interference (ISI), using the previous iteration values.

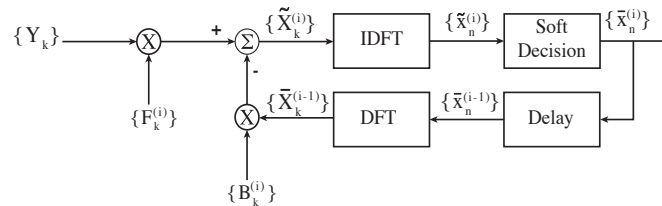


Figure 2. IB-DFE receiver structure.

For the  $i^{\text{th}}$  iteration and  $k^{\text{th}}$  subcarrier, the estimated signal,  $\tilde{X}_k^{(i)}$ , is given by:

$$\tilde{X}_k^{(i)} = F_k Y_k - B_k^{(i)} \tilde{X}_k^{(i-1)}, \quad (2)$$

which, for the first iteration, can be simplified to

$$\tilde{X}_k^{(1)} = F_k Y_k. \quad (3)$$

The “soft decision” of the previous iteration is expressed by  $\tilde{X}_k^{(i-1)}$ , which is the DFT of the time-domain block  $\tilde{x}_k^{(i-1)}$ , whose average value, according to [20], is given by:

$$\bar{x}_n = \tanh\left(\frac{L_n^{\text{Re}}}{2}\right) + j \tanh\left(\frac{L_n^{\text{Im}}}{2}\right), \quad (4)$$

where

$$L_n^{Re} = \frac{2}{\sigma_n^2} \text{Re}\{\tilde{x}_n\}, \quad (5)$$

$$L_n^{Im} = \frac{2}{\sigma_n^2} \text{Im}\{\tilde{x}_n\}, \quad (6)$$

and

$$\sigma_n^2 = \frac{1}{2N} \sum_{n'=0}^{N-1} |\tilde{x}_n - x_{n'}|^2 \simeq \frac{1}{2N} \sum_{n'=0}^{N-1} |\tilde{x}_{n'} - \hat{x}_{n'}|^2. \quad (7)$$

Coefficients  $F_k$  and  $B_k$  are chosen so as to minimise the Mean Square Error (MSE) and, consequently, to minimise the BER. They can be given by [21,22]:

$$F_k^{(i)} = \frac{H_k^*}{\frac{\sigma_n^2}{\sigma_s^2} + (1 - (\rho^{(i-1)})^2)|H_k|^2}, \quad (8)$$

$$B_k^{(i)} = \rho^{(i-1)}(F_k^{(i)} H_k - 1), \quad (9)$$

where  $\rho$  represents the correlation coefficient and is defined by:

$$\rho^{(i)} = \frac{\mathbb{E}[\hat{x}_k^{(i)} x_k^*]}{\mathbb{E}[|x_k|^2]}. \quad (10)$$

Considering QPSK modulation,  $\rho$  can be approximately given by:

$$\rho_p \approx \frac{1}{2N} \sum_{n=0}^{N-1} \left( |\rho_n^{Re}| + |\rho_n^{Im}| \right), \quad (11)$$

where

$$\rho_n^{Re(i)} = \tanh \left( \frac{|L_n^{Re(i)}|}{2} \right), \quad (12)$$

and

$$\rho_n^{Im(i)} = \tanh \left( \frac{|L_n^{Im(i)}|}{2} \right). \quad (13)$$

### 3. Theoretical BER Performance

As previously mentioned, coefficients  $F_k$  and  $B_k$  are chosen so as to minimise the MSE and BER. For a SISO system, these coefficients can be expressed by Equations (8) and (9), respectively.

The BER performance for a QPSK constellation is given by:

$$BER_p \simeq Q \left( \sqrt{\frac{1}{\theta}} \right), \quad (14)$$

where  $Q(x)$  denotes the Gaussian error function and

$$\theta = \frac{1}{N^2} \sum_{k=0}^{N-1} \Theta_k. \quad (15)$$

From Equation (15),  $\Theta_k$  depicts the MSE which can be calculated by Equation (16):

$$\Theta_k = \mathbb{E} \left[ |\tilde{X}_k - X_k|^2 \right] = \mathbb{E} \left[ |F_k Y_k - B_k \tilde{X}_k - X_k|^2 \right] \quad (16)$$

As  $\bar{X}_k$  can be given by:

$$\bar{X}_k = \rho \hat{X}_k, \quad (17)$$

where  $\hat{X}_k$  denotes “hard decision” and is expressed by:

$$\hat{X}_k = \rho X_k + \Delta_k. \quad (18)$$

Therefore, Equation (17) can be written as:

$$\bar{X}_k = \rho^2 X_k + \rho \Delta_k. \quad (19)$$

Knowing the expression for  $\bar{X}_k$ , Equation (16) can be expanded as:

$$\Theta_k = \mathbb{E} \left[ \left| F_k Y_k - B_k \rho^2 X_k + \rho \Delta_k - X_k \right|^2 \right] \quad (20)$$

Since  $\mathbb{E}[\Delta_k] = 0$ , after some mathematical manipulation, Equation (20) can be rewritten as:

$$\begin{aligned} \Theta_k = & F_k^* \mathbb{E} [Y_k^* Y_k] F_k - F_k^* \mathbb{E} [Y_k^* X_k] \rho^2 B_k^* - F_k^* \mathbb{E} [Y_k^* X_k] - B_k^* \rho^2 \mathbb{E} [X_k^* Y_k] F_k + \\ & B_k^* B_k \rho^4 \mathbb{E} [X_k^* X_k] + B_k^* \rho^2 \mathbb{E} [X_k^* X_k] - F_k \mathbb{E} [X_k^* Y_k] + B_k \rho^2 \mathbb{E} [X_k^* X_k] + \mathbb{E} [X_k^* X_k] \end{aligned} \quad (21)$$

Knowing that:

$$\mathbb{E} [Y_k^* Y_k] = R_Y; \quad (22)$$

$$\mathbb{E} [Y_k^* X_k] = R_{Y^* X} \quad (23)$$

and

$$\mathbb{E} [X_p X_p^*] = R_X. \quad (24)$$

Equation (21) can be simplified to:

$$\Theta_k = F_k^* R_Y F_k - 2Re \left\{ F_k^* \rho^2 R_{Y^* X} B_k \right\} - 2Re \left\{ F_k^* R_{Y^* X} \right\} + B_k^* B_k \rho^4 R_X - 2Re \left\{ B_k^* \rho^2 R_X \right\} + R_X. \quad (25)$$

By using Equations (14) and (25) it is then possible to evaluate the BER performance of a SISO system. When considering a MIMO system, Equation (25) should be replaced by Equation (26). Equation (26) is fully derived and explained in [23], where the BER performance of receivers that can be used in MIMO systems are analysed and compared. Each element depends on both the user and the subcarrier and this increases the complexity, since, in MIMO systems, it is necessary to work with matrices. Therefore, in this expression, the elements  $\mathbf{F}$  and  $\mathbf{B}$  are matrices for each subcarrier. The matrix  $\mathbf{F}$  equalises the channel and the matrix  $\mathbf{B}$  is responsible for removing the ISI, using the previous iteration values, as explain in Section 2 for an SISO system. Just for simplicity, user and subcarrier dependency have been dropped out, with the exception for the  $X_p$  factor.

$$\Theta = \mathbf{F}^H \mathbf{R}_Y \mathbf{F} + \mathbf{B}^H \mathbf{R}_{\bar{X}\bar{X}} \mathbf{B} - 2Re \left\{ \mathbf{F}^H \mathbf{R}_{Y, X_p} \right\} + 2Re \left\{ \mathbf{B}^H \mathbf{R}_{\bar{X}, X_p} \right\} - 2Re \left\{ \mathbf{B}^H \mathbf{R}_{\bar{X}, Y} \mathbf{F} \right\} + \mathbf{R}_X. \quad (26)$$

#### 4. Simulation Results

To obtain theoretical values of BER performance as a function of  $E_b/N_0$  achieved by SISO and MIMO systems, simulation was used. The simulation parameters considered were 100 blocks with 256 transmitted data symbols ( $N = 256$ ), and a duration of 4 microseconds. As usual,  $E_b/N_0$  is the relation between the average bit energy for the receiving antenna,  $E_b$ , and the unilateral power spectral density of the Additive White Gaussian Noise (AWGN) channel noise,  $N_0$ . In both SISO and MIMO scenarios, the number of active users was always 1. The number of receiving antennas in that user varied from the SISO scenario to the MIMO scenario.

In terms of simulation parameters, it is considered a MIMO scenario where the different pairs of antennas are uncorrelated and there is Rayleigh fading in the different multipath components. It is also important to point out that the average power is uncorrelated. We consider linear amplification and a perfect channel synchronisation and estimation.

The theoretical values for the BER performance achieved by this procedure clearly show us the advantage of using previous DTs in a SISO system to infer the performance of a MIMO system. The obtained results (depicted in Figure 3, and only the first iteration of IB-DFE was considered) show that the greater the ratio between transmitting antennas ( $P$ ) and receiving antennas ( $R$ ) the higher the BER performance achieved, as it is supposed in a MIMO system.

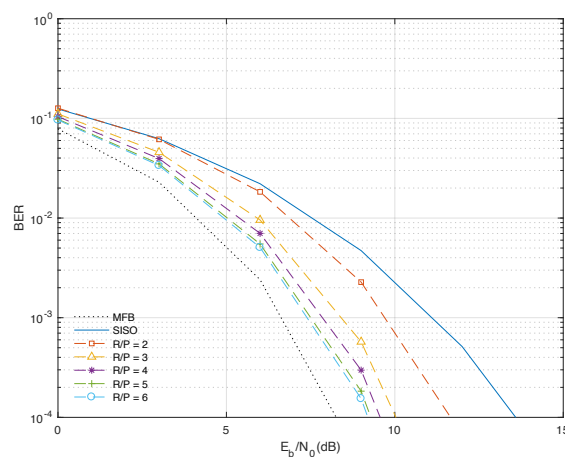


**Figure 3.** Theoretical BER performance for the first iteration when using IB-DFE for different  $R/P$  values.

By using the iterative process of the receiver, the performance improves significantly, approaching the Matched Filter Bound (MFB), which represents the best performance that the receiver can ever achieve [24]. In this study, we have verified that the performance for the third iteration of IB-DFE already presents results very satisfactory and close to the MFB. It must be emphasised that this performance close to the MFB is only possible due to the use of IB-DFE. If we were only using linear FDE, as it is the case for the first iteration shown in Figure 3, the MIMO coverage would be worse and that is the main difference when we compare the results of Figures 3 and 4. Accordingly, it is also possible to verify that, for a given BER value, the  $E_b/N_0$  values of the different  $R/P$  ratios are closer, when compared with the first iteration.

For each  $R/P$  ratio studied, the BER values considered for obtaining the performance were  $10^{-2}$ ,  $10^{-3}$  and  $10^{-4}$ , for which the corresponding  $E_b/N_0$  values were obtained. By obtaining these  $E_b/N_0$  values, it was then possible to calculate the difference between the performance of SISO and MIMO systems, which is represented by  $G\Delta$ . This difference, for the first iteration of IB-DFE, is shown in Figure 5, where the fitted lines for each case are also depicted.

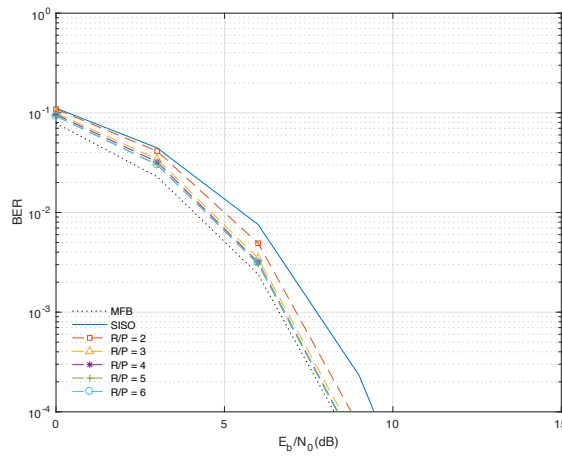


**Figure 4.** Theoretical BER performance for the third iteration when using IB-DFE for different  $R/P$  values.

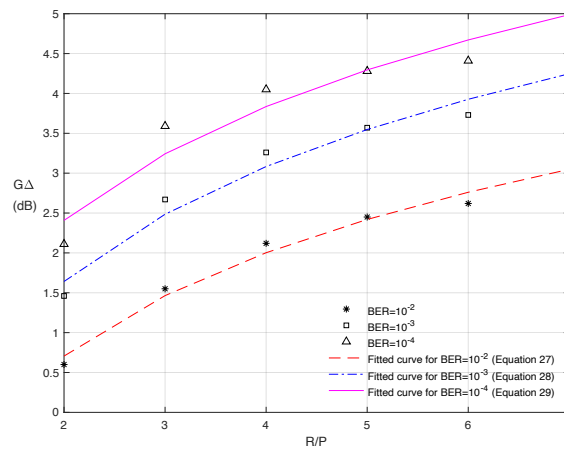


**Figure 5.** Difference between theoretical BER performance for SISO and MIMO systems for the first iteration when using IB-DFE.

As depicted in Figure 6, the difference between the SISO and MIMO systems decreases for the third iteration of the IB-DFE.

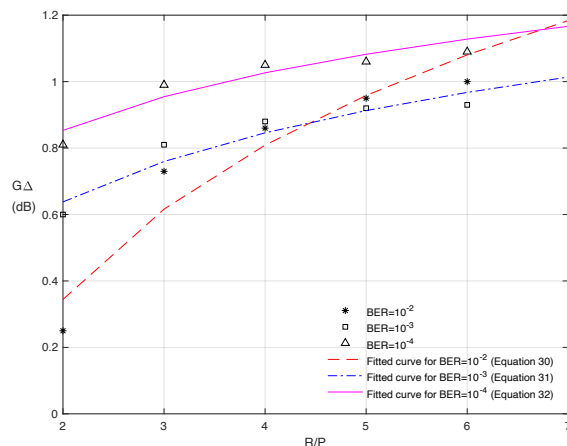


**Figure 6.** Difference between theoretical BER performance for SISO and MIMO systems for the third iteration when using IB-DFE.

Through the fitted curves, shown in Figure 6, it is possible to predict the  $G\Delta$  (the difference between SISO and MIMO systems for a given BER performance), considering the variation in the  $R/P$  ratio. For the first iteration and considering a BER performance of  $10^{-2}$  the fitted curve is given by Equation (27). Equation (28) corresponds to a BER of  $10^{-3}$  and Equation (29) denotes the fitted curve for a BER of  $10^{-4}$ .

$$G\Delta_{BER=10^{-2}} = 1.87 \times \ln(R/P) - 0.59; \quad (27)$$

$$G\Delta_{BER=10^{-3}} = 2.08 \times \ln(R/P) + 0.20; \quad (28)$$

$$G\Delta_{BER=10^{-4}} = 2.06 \times \ln(R/P) + 0.98. \quad (29)$$

In the third iteration, Equations (30)–(32) represent the fitted curves for the BER values of  $10^{-2}$ ,  $10^{-3}$  and  $10^{-4}$ , respectively.

$$G\Delta_{BER=10^{-2}} = 0.67 \times \ln(R/P) - 0.12; \quad (30)$$

$$G\Delta_{BER=10^{-3}} = 0.30 \times \ln(R/P) + 0.43; \quad (31)$$

$$G\Delta_{BER=10^{-4}} = 0.25 \times \ln(R/P) + 0.68. \quad (32)$$

Using the previous equations, it is now possible, for a given BER performance, to know the impact on the  $E_b/N_0$  ratio of changing from a SISO system to a MIMO system. Note that this relationship is a function of the  $R/P$  ratio, so the higher this ratio the greater the impact. As an example, and according to Equation (27), for a BER of  $10^{-2}$  and the first iteration of IB-DFE, the value of  $E_b/N_0$ , improves by approximately 2.4 dB ( $G\Delta = 2.4$  dB), when moving from a SISO system to a MIMO system with 2 transmitting antennas and 10 receiving antennas ( $R/P = 5$ ).

When changing from a SISO system to a MIMO system, the associated complexity will also be increased, as the number of transmitting and receiving antennas will increase. For the specific case of IB-DFE, this complexity is associated with the need to invert matrices, in order to calculate the  $\mathbf{F}$  factor, whose dimensions will always be at least  $R \times P$ . The complexity of this receiver is therefore greater than for the linear case, since one more IDFT/DFT pair exists per iteration [25,26].

## 5. Performance Results

The Signal-to-Noise Ratio (SNR) is the ratio between signal and noise power. Therefore, if we assume that the noise power remains constant, we can derive the signal power as a function of the SNR. The SNR ratio can be expressed in decibels (dB), as denoted in Equation (33):

$$SNR_{[dB]} = P_{S[dBm]} - P_{N[dB]}, \quad (33)$$

where  $P_S$ , and  $P_N$  denote signal and noise power, respectively.

The  $E_b/N_0$  expression, in linear terms, can be written as:

$$\left(\frac{E_b}{N_0}\right) = \frac{P_S \times B}{P_N \times R_b} \iff \left(\frac{E_b}{N_0}\right) = SNR_{linear} \times \frac{B}{R_b}, \quad (34)$$

where  $B$ , and  $R_b$  denote signal bandwidth and bit rate, respectively. In our analyses,  $B/R_b$  is negligible since it is the same for both SISO and MIMO. Thus, the Equation (33) can be rewritten as:

$$E_b/N_{0[dB]} = P_{S[dBm]} - P_{N[dB]}. \quad (35)$$

After some mathematical manipulation, it is possible to arrive at the relationship between the signal power in a SISO and in a MIMO system, indicated by Equation (36):

$$P_{SMIMO[dBm]} = P_{SSISO[dBm]} - G\Delta_{[dB]} \quad (36)$$

If we now assume that both the noise and the BER performance value remain constant, it is possible to estimate the coverage area of a MIMO system based on the coverage of a SISO system, considering a downlink scenario.

In order to test this possibility of extending the coverage area of a SISO system to a MIMO system, a 4G antenna from a northern European country manufacturer was considered, working on a downlink frequency of 796 MHz and a transmission power of 46 dBm. This scenario, illustrated in Figure 7, was taken from the METRIC platform [5], which is a network monitoring and management web platform developed by the MULTIVISION company [6]. This platform is currently used by several mobile operators worldwide, aggregating Configuration Management (CM) and Key Performance Indicators (KPI) data, as well as DTs from their networks.

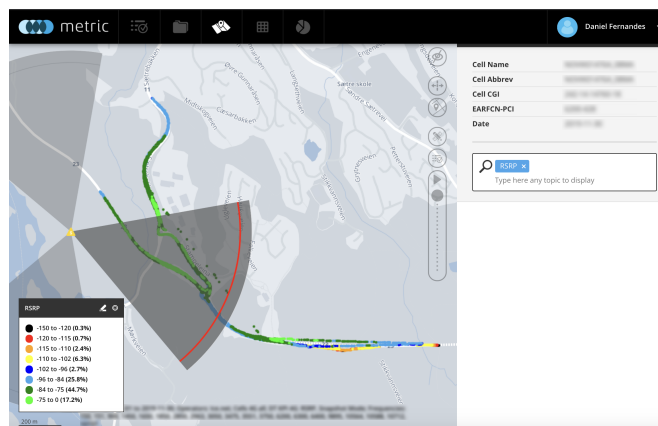


Figure 7. Considered scenario to validate our model.

If the radiation pattern of the transmitting antenna was considered, with the gain in the receiving antenna of 0 dB, and the DT campaign measures taken, it is possible to apply the ACSPM model and to estimate the coverage area for this scenario as in [27], depicted in Figure 8.

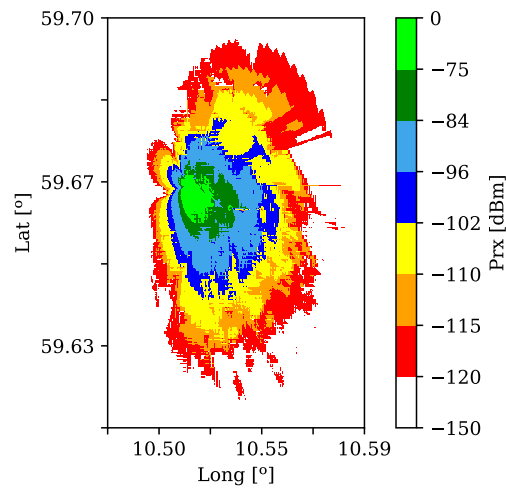


Figure 8. Coverage area of the considered scenario.

As mentioned above,  $E_b/N_0$  values improve by 2.4 dB ( $G\Delta = 2.4$  dB) when changing from a SISO system to a MIMO system with an  $R/P = 5$  and a BER of  $10^{-2}$ . For example, if the power received at a given point in the SISO system that was estimated as  $-100$  dBm, the value corresponding to the MIMO system in this same scenario will now be estimated as  $-102.4$  dBm for the scenario presented. Accordingly, the coverage scenario presented in Figure 8 would then be changed to that depicted in Figure 9.

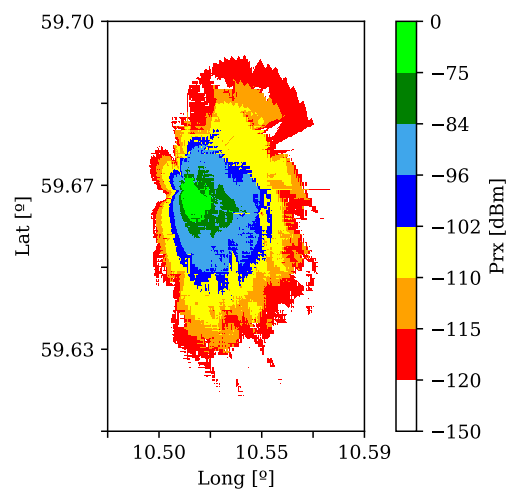
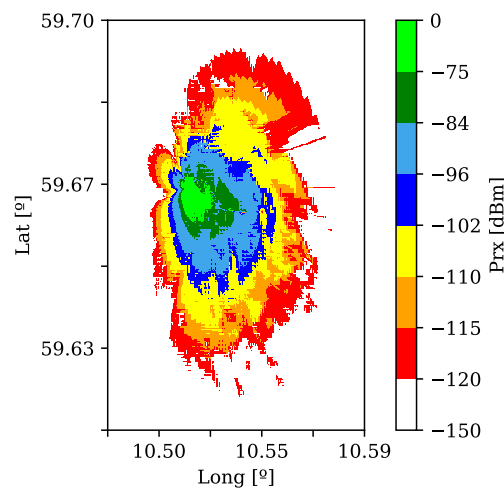


Figure 9. Coverage area extrapolated for a MIMO system with a BER of  $10^{-2}$  and for the first iteration of IB-DFE.

If we consider a minimum sensitivity of  $-120$  dBm required for the correct establishment of communications between the base station and a mobile receiving terminal, and by comparing the coverage results depicted in Figures 8 and 9, it can be concluded that the useful area for communications has been reduced about 6%.

If we now consider the third iteration of IB-DFE on the mobile receivers, the value of  $E_b/N_0$  reduces by approximately 1.3 dB ( $G\Delta = 1.3$  dB), when extrapolating coverage from a SISO system to a MIMO system with 20 transmitting antennas and 2 receiving antennas; that is, an  $R/P$  ratio of 10, and a BER of  $10^{-4}$ . The resulting coverage area for this system is depicted in Figure 10. In this case, we conclude that if we have MIMO coverage instead of SISO, the coverage area is reduced by about 3.5%.



**Figure 10.** Estimated coverage area of the considered scenario for a MIMO system with a BER of  $10^{-4}$  when using the third iteration of IB-DFE receivers, based on coverage estimation with DTs for a SISO system.

As we can verify from these results, the overall coverage area of a MIMO system is reduced, once the directivity of multiple antennas concentrates radiation in some more specific and desired areas. However, we must be aware that MIMO systems have simultaneous data streams covering the different antenna sectors from each Base Station, as opposed to SISO systems. Therefore, and although there is a slightly smaller global coverage area for MIMO systems, the increase in the number of data streams allows for an increase in the data rate, which improves the QoS for users and the overall capacity, when compared to a SISO system. Despite the results achieved, it should be noted that with the change from a SISO system to a MIMO system the complexity associated with the receiver also increases. The methodology presented is independent of the geographical area where it is applied as this factor only influences the signal estimation through the propagation models. If a propagation model is influenced by terrain morphology, the values obtained for MIMO systems will also take this fact into account, if we use this methodology.

## 6. Conclusions

The main objective of the work carried out and described in this paper was to estimate the signal coverage of a MIMO system based on the coverage of a SISO system, already optimised with DTs taken for it, in an efficient and practical way.

To meet these objectives, the theoretical BER performance achieved by the SISO systems was initially evaluated and then compared with the BER performance of equivalent MIMO systems. From this theoretical analysis it was then possible to estimate the BER performance improvement that occurs, for a given BER and  $R/P$  ratio, when switching from SISO systems to MIMO systems. The expressions obtained in this study allows for the propagation models created and tested for SISO systems to be easily extended to MIMO systems, enabling the use of well-known propagation models in MIMO systems.

The scenario and simulation data chosen to validate this concept has shown that, for a given BER performance, MIMO systems using IB-DFE receivers can in fact improve the system, as we should expect. It was shown that, although the signal coverage area can be reduced by 3.5%, the existence of more independent and simultaneous data streams in MIMO systems improves the user experience and increases the overall capacity of the system.

As future work, it would be interesting to experimentally validate the methodology presented and confirm that the coverage for an actual MIMO system corresponds to the predictions.

**Author Contributions:** Conceptualization and Investigation, D.F., F.C., R.D. and P.S.; Software, D.F.; Supervision and Validation, F.C., R.D. and P.S.; Visualization, D.F.; Writing—original draft, D.F., F.C., R.D. and P.S.; Writing—review and editing, F.C., R.D. and P.S. All authors have read and agreed to the published version of the manuscript.

**Funding:** This work is part of the OptiNET-5G project, co-funded by Centro2020, Portugal2020, European Union (project 023304). This work is also supported by Instituto de Telecomunicações, FCT/MCTES through national funds and when applicable co-funded EU funds under the project UIDB/50008/2020.

**Conflicts of Interest:** The authors declare no conflict of interest.

## References

1. Hardy, W.C. *QoS—Measurement and Evaluation of Telecommunications Quality of Service*; Wiley: Hoboken, NJ, USA, 2001. [CrossRef]
2. Ericsson. *Ericsson Mobility Report 2019*; Ericsson: Stockholm, Sweden, 2019.
3. Hapsari, W.A.; Umesh, A.; Iwamura, M.; Tomala, M.; Gyula, B.; Sebire, B. Minimization of drive tests solution in 3GPP. *IEEE Commun. Mag.* **2012**, *50*, 28–36. [CrossRef]
4. AWS. Available online: <https://aws.amazon.com> (accessed on 1 June 2020).
5. Metric. Available online: <https://metric.pt> (accessed on 1 June 2020).
6. Multivision. Available online: <https://multivision.pt> (accessed on 1 June 2020).
7. Fernandes, D.; Clemente, D.; Soares, G.; Sebastiao, P.; Cercas, F.; Dinis, R.; Ferreira, L.S. Cloud-Based Implementation of an Automatic Coverage Estimation Methodology for Self-Organising Network. *IEEE Access* **2020**, *8*, 66456–66474. [CrossRef]
8. Pina, P.M.; Godinho, A.F.; Fernandes, D.F.S.; Clemente, D.J.A.; Sebastiao, P.; Soares, G.E.; Ferreira, L.S. Automatic Coverage Based Neighbour Estimation System: A Cloud-Based Implementation. *IEEE Access* **2020**, *8*, 69671–69682. [CrossRef]
9. Godinho, A.; Fernandes, D.; Soares, G.; Pina, P.; Sebastião, P.; Correia, A.; Ferreira, L.S. A Novel Way to Automatically Plan Cellular Networks Supported by Linear Programming and Cloud Computing. *Appl. Sci.* **2020**, *10*, 3072. [CrossRef]
10. Cortesao, R.; Fernandes, D.; Clemente, D.; Soares, G.; Sebastiao, P.; Ferreira, L.S. Cloud-based Implementation of a SON Automatic Planning System: A proof-of-concept for UMTS. In Proceedings of the 2019 22nd International Symposium on Wireless Personal Multimedia Communications (WPMC), Lisbon, Portugal, 24–27 November 2019; pp. 6–11. [CrossRef]
11. F. Molish, A. *Wireless Communications*, 2nd ed.; Wiley-IEEE Press: Hoboken, NJ, USA, 2010.
12. Alamouti, S. A simple transmit diversity technique for wireless communications. *IEEE J. Sel. Areas Commun.* **1998**, *16*, 1451–1458. [CrossRef]
13. Bergaoui, H.; Mlayah, Y.; Tlili, F.; Rouissi, F. Switching Between Diversity and Spatial Multiplexing in Massive MIMO Systems. In *Lecture Notes in Computer Science (Including subseries Lecture Notes in Artificial Intelligence*

- and *Lecture Notes in Bioinformatics*); Springer International Publishing: Berlin/Heidelberg, Germany, 2018; Volume 11277, pp. 49–57.5. [[CrossRef](#)]
14. Chang, R.W. Synthesis of Band-Limited Orthogonal Signals for Multichannel Data Transmission. *Bell Syst. Tech. J.* **1966**, *45*, 1775–1796. [[CrossRef](#)]
  15. Sari, H.; Karam, G.; Jeanclaude, I. An analysis of orthogonal frequency-division multiplexing for mobile radio applications. In Proceedings of the IEEE Vehicular Technology Conference (VTC), Stockholm, Sweden, 8–10 June 1994; pp. 1635–1639. [[CrossRef](#)]
  16. Falconer, D.; Ariyavisitakul, S.; Benyamin-Seeyar, A.; Eidson, B. Frequency domain equalization for single-carrier broadband wireless systems. *IEEE Commun. Mag.* **2002**, *40*, 58–66. [[CrossRef](#)]
  17. Benvenuto, N.; Dinis, R.; Falconer, D.; Tomasin, S. Single Carrier Modulation With Nonlinear Frequency Domain Equalization: An Idea Whose Time Has Come—Again. *Proc. IEEE* **2010**, *98*, 69–96. [[CrossRef](#)]
  18. Rajaram, A.; Dinis, R.; Jayakody, D.N.K.; Kumar, N. Receiver Design to Employ Simultaneous Wireless Information and Power Transmission with Joint CFO and Channel Estimation. *IEEE Access* **2019**, *7*, 9678–9687. [[CrossRef](#)]
  19. Benvenuto, N.; Tomasin, S. Block iterative DFE for single carrier modulation. *Electron. Lett.* **2002**, *38*, 1144–1145.20020767. [[CrossRef](#)]
  20. Gusmao, A.; Torres, P.; Dinis, R.; Esteves, N. A Turbo FDE Technique for Reduced-CP SC-Based Block Transmission Systems. *IEEE Trans. Commun.* **2007**, *55*, 16–20. [[CrossRef](#)]
  21. Silva, F.; Dinis, R.; Montezuma, P. Estimation of the Feedback Reliability for IB-DFE Receivers. *ISRN Commun. Netw.* **2011**, *2011*, 1–7. [[CrossRef](#)]
  22. Casal Ribeiro, F.; Dinis, R.; Cercas, F.; Silva, A. Analytical BER Performance Evaluation in SISO and MIMO Environments with SC-FDE Modulations and IB-DFE Receivers. *Wirel. Pers. Commun.* **2017**, *96*, 3831–3850. [[CrossRef](#)]
  23. Fernandes, D.; Cercas, F.; Dinis, R. Analytical Performance Evaluation of Massive MIMO Techniques for SC-FDE Modulations. *Electronics* **2020**, *9*, 533. [[CrossRef](#)]
  24. Silva, F.; Dinis, R.; Souto, N.; Montezuma, P. Approaching the matched filter bound with block transmission techniques. *Trans. Emerg. Telecommun. Technol.* **2012**, *23*, 76–85. [[CrossRef](#)]
  25. Ribeiro, F.C.; Guerreiro, J.; Dinis, R.; Cercas, F.; Silva, A. Reduced complexity detection in MIMO systems with SC-FDE modulations and iterative DFE receivers. *J. Sens. Actuator Netw.* **2018**, *7*, 17. [[CrossRef](#)]
  26. Pereira, A.; Bento, P.; Gomes, M.; Dinis, R.; Silva, V. Complexity analysis of FDE receivers for massive MIMO block transmission systems. *IET Commun.* **2019**, *13*, 1762–1768. [[CrossRef](#)]
  27. Fernandes, D.; Raimundo, A.; Cercas, F.; Sebastiao, P.; Dinis, R.; Ferreira, L.S. Comparison of Artificial Intelligence and Semi-Empirical Methodologies for Estimation of Coverage in Mobile Networks. *IEEE Access* **2020**, *8*, 139803–139812. [[CrossRef](#)]

**Publisher’s Note:** MDPI stays neutral with regard to jurisdictional claims in published maps and institutional affiliations.



© 2020 by the authors. Licensee MDPI, Basel, Switzerland. This article is an open access article distributed under the terms and conditions of the Creative Commons Attribution (CC BY) license (<http://creativecommons.org/licenses/by/4.0/>).



# Chapter 5

## Analysis of BER performance achieved in MIMO systems

With the results achieved in Chapter 4, it is noticeable that the coverage area of a SISO system is reduced when these systems are replaced by a MIMO system. Despite this reduction, the better the performance of the receiver used, the smaller this reduction. So this chapter presents and compares, for an uplink scenario, the BER performance of these receivers used in MIMO and mMIMO systems.

Some paper details:

- **Title:** Analytical Performance Evaluation of Massive MIMO Techniques for SC-FDE Modulations;
- **Date of publication:** March 2020;
- **Journal:** *Electronics*;
- **Scimago/Scopus Journal Ranking:** Quartile 2;
- **Publisher:** MDPI.



Article

## Analytical Performance Evaluation of Massive MIMO Techniques for SC-FDE Modulations

Daniel Fernandes <sup>1,2,\*</sup> , Francisco Cercas <sup>1,2</sup> and Rui Dinis <sup>2,3</sup>

<sup>1</sup> Instituto Universitário de Lisboa (ISCTE – IUL), Av. das Forças Armadas, 1649-026 Lisboa, Portugal; francisco.cercas@iscte-iul.pt

<sup>2</sup> IT—Instituto de Telecomunicações, Av. Rovisco Pais, 1, Torre Norte, Piso 10, 1049-001 Lisboa, Portugal; rdinis@fct.unl.pt

<sup>3</sup> FCT—Universidade Nova de Lisboa, Monte da Caparica, 2829-516 Caparica, Portugal

\* Correspondence: dfsfs@iscte.pt

Received: 29 February 2020; Accepted: 20 March 2020; Published: 24 March 2020



**Abstract:** In the Fifth Generation of telecommunications networks (5G), it is possible to use massive Multiple Input Multiple Output (MIMO) systems, which require efficient receivers capable of reaching good performance values. MIMO systems can also be extended to massive MIMO (mMIMO) systems, while maintaining their, sometimes exceptional, performance. However, we must be aware that this implies an increase in the receiver complexity. Therefore, the use of mMIMO in 5G and future generations of mobile receivers will only be feasible if they use very efficient algorithms, so as to maintain their excellent performance, while coping with increasing and critical user demands. Having this in mind, this paper presents and compares three types of receivers used in MIMO systems, for further use with mMIMO systems, which use Single-Carrier with Frequency-Domain Equalization (SC-FDE), Iterative Block Decision Feedback Equalization (IB-DFE) and Maximum Ratio Combining (MRC) techniques. This paper presents and compares the theoretical and simulated performance values for these receivers in terms of their Bit Error Rate (BER) and correlation factor. While one of the receivers studied in this paper achieves a BER performance nearly matching the Matched Filter Bound (MFB), the other receivers (IB-DFE and MRC) are more than 1 dB away from MFB. The results obtained in this paper can help the development of ongoing research involving hybrid analog/digital receivers for 5G and future generations of mobile communications.

**Keywords:** MIMO; mMIMO; SC-FDE; IB-DFE; MRC

---

### 1. Introduction

With the constant increase in users' needs, in particular, the interconnection of all their communication devices, and its access to the Internet everywhere, the Fourth Generation (4G) of telecommunications has to be rethought. The Fifth Generation (5G) of telecommunications networks arises as a response to existing technology limitations. The 5G network is predicted to have an increase of 10 times in spectral efficiency and 1000 times of system capacity when compared to 4G. It is also expected that this technology is energy efficient [1].

According to the report published by [2], at the end of 2019, about 13 million subscribers to the 5G technology were already expected. In October 2019, right before the official launch of this technology, more than 10 million users have already been registered. Despite the 5G launch ramp, 4G will still be dominant and will reach its peak in 2022, and then it will become superseded by 5G technology. It is also expected that by 2025, 4G will cover around 90% of the world's population, and 5G will cover only 65% of the population but at half of the data traffic. Also, according to the same report, the providers

of this technology are working on a second generation that intends to reduce power consumption, increase frequencies and implement more integrated designs.

The migration to 5G implies new developments in the system design, changes in components and system architecture. One way to achieve these changes is to use massive Multiple Input Multiple Output (mMIMO) [3]. This architecture consists of the existence of multiple antennas in the receiver and transmitter. This implementation allows these systems to have a substantial increase in the data rate and an improvement, not only in energy efficiency, but also in reliability of the connections [1,4].

Channel estimation is one of the limiting factors in this type of system. Another problem is related to the assignment of sequences of finite orthogonal pilots. When the sequences of pilots is reused, it increases the contamination of pilots and coherent interference [3].

With the mMIMO system, the Single-Carrier with Frequency-Domain Equalization (SC-FDE) can be used since this technique allows a lower envelope fluctuation, when compared with Orthogonal Frequency Division Multiplexing (OFDM) [5–7]. SC-FDE allows an efficient power amplification at the Mobile Terminal (MT). In the uplink transmission, the linear Frequency-Domain Equalization (FDE) can be replaced with an iterative FDE on the receiver, such as the Iterative Block Decision Feedback Equalization (IB-DFE) [8]. This replacement leads to an increase in the receiver performance [9].

In the mMIMO system, the number of antennas in the receiver and transmitter increases to tens or hundreds of antennas. This implies the use of large matrices, which is a serious problem in receivers based on the IB-DFE concept [10,11], since this type of receiver requires matrix inversions for each subcarrier and each iteration implies intensive computational processing. Some iterative receivers that achieve similar performance do not require matrix inversions. These receivers can implement, e.g., Maximum Ratio Combining (MRC), which requires the calculation of the hermitian of the channel matrix, or the Equal Gain Combining (EGC) that only needs phase rotations [12,13]. The main problems associated with these low complexity receivers are related to the high interference between different transmitted streams and the Inter-Symbol Interference (ISI).

There are several studies regarding the different receivers that can be used with mMIMO systems [14–17], where the performance achieved is compared with the Matched Filter Bound (MFB). Authors from in [18] propose a hybrid receiver that combines IB-DFE with MRC, achieving performance values similar to MFB in its second iteration.

In this paper, the performance achieved by IB-DFE, MRC, the hybrid receiver and the correlation factor is presented and compared with the theoretical values for the same receiver. The work presented in this paper can be extended to hybrid analog/digital equalization scenarios for massive MIMO systems as presented in [19,20].

In Section 2 the comparison of receivers that can be used in mMIMO systems is presented. In Section 3 the proposed system is described and in Section 4 the IB-DFE, MRC and hybrid receivers are presented, followed by Section 5 where the Bit Error Rate (BER) performance and the correlation factors are calculated for the same receivers. In Section 6, the results are presented and discussed. Lastly, in Section 7, the conclusions achieved are drawn.

The following denotation is employed in this paper: In general, the lower case letters denote time-domain variables, while upper case letters denote frequency-domain variables. Bold upper letters represent matrices or vector;  $I_N$  is the identity matrix  $N \times N$ ; the complex conjugate, transpose and Hermitian of  $\mathbf{x}$  is denoted by  $\mathbf{x}^*$ ,  $\mathbf{x}^T$  and  $\mathbf{x}^H$  respectively. The expectation of  $x$  is represented by  $\mathbb{E}[x]$  and  $\tilde{x}$ ,  $\hat{x}$ ,  $\bar{x}$ , denotes respectively sample, "hard decision" and "soft decision" estimation of  $x$ .

## 2. Receivers

In the literature [14–17] we can find the description of very efficient and appropriate receivers for use in MIMO systems, able to be extended for mMIMO. This section summarizes their main properties.

- ZF: Zero Forcing (ZF) [21] is a simple receiver technique that applies the inverse of the channel frequency response to the received signal to equalize the communications channel. It allows for a perfect separation of the different users as well as the removal of the ISI, however, it cannot be

used in most practical applications as when the received signal is very weak, that is when the Signal-to-Noise ratio (SNR) is very low, it compensates by amplifying the received signal and completely deteriorates the overall SNR when trying to invert values close to zero. In terms of complexity it is not very efficient as well, since it requires the inversion of matrices;

- IB-DFE: The IB-DFE receiver is an iterative receiver where each stream is detected one at a time and the interference is canceled with the help of the streams already detected. When the number of iteration increases, the interference cancellation is improved, improving the overall performance. As with the ZF, this receiver also has the disadvantage of using matrix inversions;
- MRC: The MRC receiver combines the different received branch signals in order to maximize the received SNR ratio. The main advantage is that there are no matrices inversions;
- EGC: The EGC receiver only involves phase rotations, combining all received signals with unitary weights to achieve a high SNR. Like MRC, the EGC does not need matrices inversions.

Table 1 presents a summary of the BER performance achieved by the previous receivers, as well as the number of required iterations to achieve it, where applicable, based on the work presented in [15].

**Table 1.**  $E_b/N_0$  [dB] for the Bit Error Rate (BER) performance of the scenarios presented in [15].

BER	Iteration	MFB	ZF	IB-DFE	MRC	EGC
$10^{-2}$	1	4.2	4.8	4.8	9.1	10.9
$10^{-4}$	4	8.4	—	8.5	—	—

As we can observe, the referred ZF and IB-DFE receivers have the same BER performance as the MFB, for very similar values of  $E_b/N_0$ , remarkably for the IB-DFE. In this table, only the non-iterative versions of MRC and EGC receivers were considered.

### 3. System Characterization

This paper explores a scenario that implements massive MIMO communications in a highly frequency selective channel and a Single Carrier modulation in the uplink transmission. In this scenario, the communication is established between a MT equipped with  $P$  single transmitting antennas and a Base Station (BS) equipped with  $R$  receiving antennas, with  $R \gg P$  and a perfect synchronization.

In order to remove the ISI, a cyclic prefix, which is larger than the maximum system delay, is added to each transmitted block and removed in the reception side. The MT  $p^{th}$  transmits a block of  $N$  data symbols  $\{x_{n,p}; n = 0, 1, \dots, N - 1\}$  which is received in the  $r^{th}$  BS antenna as  $\{y_n^{(r)}; n = 0, 1, \dots, N - 1\}$  corresponding to a frequency-domain block  $\{Y_k^{(r)}; n = 0, 1, \dots, N - 1\}$ . The  $\{Y_k^{(r)}\}$  block can also be represented in the matrix format  $\mathbf{Y}_k^{(r)} = [Y_k^{(1)}, \dots, Y_k^{(R)}]^T$ , being given by Equation (1):

$$\mathbf{Y}_k = \mathbf{H}_k \mathbf{X}_k + \mathbf{N}_k, \tag{1}$$

where the channel matrix  $R \times P$  for the  $k^{th}$  subcarrier is represented by  $H_k$ , the frequency-domain block of the transmitted block  $x_n$  is represented by  $X_k$  and  $N_k$  represents the channel noise. In Figure 1 the considered scenario is depicted.

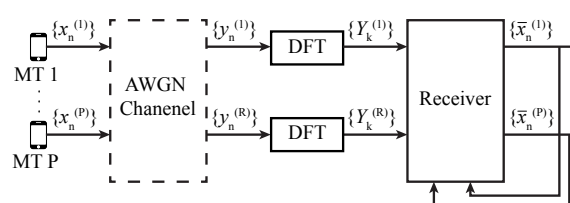


**Figure 1.** System scenario.

#### 4. Receivers Design

Since massive MIMO systems are expected to operate with a great number of antennas in the transmitter and the receiver, it is important that the receivers used in these systems have as few matrix inversions as possible. The necessary resources used in matrix inversion increase significantly with the number of entries in that matrix. The greater the number of  $R$  and  $T$ , the higher the associated complexity.

Throughout this section, different iterative receivers based on FDE are presented. In this type of receiver, the estimated signal at the  $i$ th iteration for the  $k$ th subcarrier  $\tilde{\mathbf{X}}_{k,p}^{(i)}$  is given by:

$$\tilde{\mathbf{X}}_{k,p}^{(i)} = \mathbf{F}_{k,p}^T \mathbf{Y}_k - \mathbf{B}_{k,p}^{(i)T} \tilde{\mathbf{X}}_{k,p}^{(i-1)}, \quad (2)$$

with  $\mathbf{F}_{k,p}^T = [F_{k,p}^{(1)}, \dots, F_{k,p}^{(R)}]^T$  denoting the feedforward coefficients and  $\mathbf{B}_{k,p}^T = [B_{k,p}^{(1)}, \dots, B_{k,p}^{(P)}]^T$  denoting the feedback coefficients, responsible to reduce the residual ISI after the first iteration.  $\tilde{\mathbf{X}}_{k,p}^{(i-1)}$  represents the estimated signal for the previous iteration which is the Discrete Fourier Transform (DFT) of  $\bar{x}_{n,p}$ .  $\bar{x}_{n,p}$  is selected according to a mapping rule, in this case, a Quadrature Phase-Shift Keying (QPSK) with Gray mapping, (i.e.,  $x_{n,p} = \pm 1 \pm j$ ). The average values for  $\bar{x}_{n,p}$ , according to [22], are given by:

$$\bar{x}_{n,p} = \tanh\left(\frac{L_{n,p}^{Re}}{2}\right) + j \tanh\left(\frac{L_{n,p}^{Im}}{2}\right), \quad (3)$$

where

$$L_{n,p}^{Re} = \frac{2}{\sigma_{n,p}^2} \text{Re}\{\tilde{s}_{n,p}\}, \quad (4)$$

$$L_{n,p}^{Im} = \frac{2}{\sigma_{n,p}^2} \text{Im}\{\tilde{s}_{n,p}\}, \quad (5)$$

and

$$\sigma_{n,p}^2 = \frac{1}{2N} \sum_{n'=0}^{N-1} |\tilde{s}_{n',p} - s_{n',p}|^2 \simeq \frac{1}{2N} \sum_{n'=0}^{N-1} |\tilde{s}_{n',p} - \hat{s}_{n',p}|^2. \quad (6)$$

For the first iteration, and since there are no previous iterations, Equation (2) can be simplified to:

$$\tilde{\mathbf{X}}_{k,p}^{(i)} = \mathbf{F}_{k,p}^T \mathbf{Y}_k. \quad (7)$$

Each FDE receiver has different equations for the  $\mathbf{F}_{k,p}$  and  $\mathbf{B}_{k,p}$  coefficients. Sections 4.1, 4.2 and 4.3 present the equations for three distinct receivers.

##### 4.1. IB-DFE

The IB-DFE receiver has already been extensively tested and validated, as mentioned in Section 1. In order to minimize error probability, authors from [11,14,16] define expressions for  $\mathbf{F}_{k,p}$  and  $\mathbf{B}_{k,p}$  coefficients, which are given by:

$$\mathbf{F}_{k,p}^T = \kappa \mathbf{\Lambda}_{k,p} \mathbf{H}_{k,p}^H \mathbf{I}, \quad (8)$$

and

$$\mathbf{B}_{k,p}^T = \mathbf{F}_{k,p}^T \mathbf{H}_{k,p}^H - \mathbf{I}, \quad (9)$$

where  $\kappa$  is a normalization parameter ensuring that the overall frequency-response of the "channel plus receiver" for each MT has an average value of 1, i.e.,

$$\frac{1}{N} \sum_{k=0}^{N-1} \sum_{r=1}^R F_{k,p}^{(r)} H_{k,p}^{(r)} = 1. \quad (10)$$

The  $\Lambda$  is given by:

$$\Lambda_{k,p} = \left( \mathbf{H}_{k,p}^H (\mathbf{I}_P - \mathbf{P}^2) \mathbf{H}_{k,p} + \frac{\sigma_N^2}{\sigma_S^2} \mathbf{I}_R \right)^{-1}, \quad (11)$$

where  $\mathbf{P}$  is a diagonal matrix containing the correlation factor between transmitted and detected symbols.  $\sigma_N^2$  and  $\sigma_S^2$  represents the variance of the real and imaginary parts of the channel noise and data samples, respectively.

#### 4.2. MRC

As shown in Section 4.1, the IB-DFE receiver requires the inversion of the channel matrix in the estimation of the received signal. This situation requires too much complexity when moving to an mMIMO system, where there are multiple receiving and transmitting antennas.

As explained in [14,15,17], the MRC receiver combines the different received branch signals in order to maximize the received SNR ratio. In fact, the phases of the received signals are fixed and the conjugate of the channel matrix is used to weight them. The small correlation between the different transmitting and receiving antennas allows us to make the following approach:

$$\mathbf{H}_{k,p}^H \mathbf{H}_{k,p} \approx \mathbf{R} \mathbf{I}. \quad (12)$$

When considering moderate  $R/P$  values, the residual interference cannot be neglected. In order to improve the performance of this receiver, an iterative version should be implemented, such as the IB-DFE receiver. Equation (2) is also considered by this receiver by only changing the feedforward and feedback coefficient equations. Therefore, feedback coefficients are given by Equation (9) and the feedforward coefficients are given by:

$$\mathbf{F}_{k,p}^T = \kappa \mathbf{H}_{k,p}^H, \quad (13)$$

where  $\kappa$  is a diagonal matrix and the element  $(t, t)^{th}$  is given by  $\left( \sum_{k=0}^{N-1} \sum_{r=1}^R |H_{k,p}^{(r,t)}|^2 \right)^{-1}$ .

#### 4.3. IB-DFE Receiver Combined with MRC

A receiver for mMIMO scenarios was provided in [18] and it reduces the complexity of matrix inversion since it only occurs on the first iteration, achieving performance values very close to MFB at the end of the second iteration. This receiver, in the first iteration, behaves as an IB-DFE receiver and, in the remaining iterations, as the MRC receiver.

The feedforward coefficients are given by Equations (8) and (11), which can be simplified to:

$$\Lambda_{k,p} = \left( \mathbf{H}_{k,p}^H \mathbf{H}_{k,p} + \frac{\sigma_N^2}{\sigma_S^2} \mathbf{I}_R \right)^{-1}, \quad (14)$$

In the remaining iterations, the feedforward and feedback coefficients are given by Equations (9) and (13), respectively.

In Figure 2, the structure of this receiver is depicted.

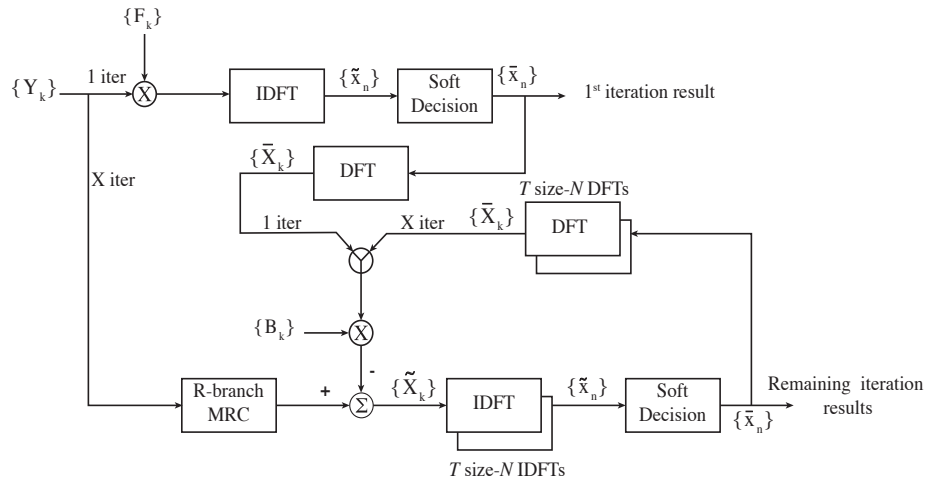


**Figure 2.** Iterative Block Decision Feedback Equalization (IB-DFE) receiver combined with the Maximum Ratio Combining (MRC) structure.

### 5. Theoretical BER Performance

Each of the receivers presented so far aims to minimize the Mean Squared Error (MSE) which, in turn, decreases BER performance. This minimization takes place through precise selection of feedforward and feedback coefficients. For a QPSK constellation with Gray mapping rule, as considered in this paper, the BER can be calculated by:

$$BER_p \approx Q\left(\sqrt{\frac{1}{\theta_p}}\right), \quad (15)$$

where  $Q(x)$  represents the Gaussian error function and  $\theta_p$  is given by:

$$\theta_p = \frac{1}{N^2} \sum_{k=0}^{N-1} \Theta_{k,p}. \quad (16)$$

The MSE, represented by  $\Theta_{k,p}$ , can be calculated using:

$$\Theta_{k,p} = \mathbb{E} \left[ \left| \hat{X}_{k,p} - X_{k,p} \right|^2 \right] = \mathbb{E} \left[ \left| \mathbf{F}_{k,p}^T \mathbf{Y}_k - \mathbf{B}_{k,p}^T \bar{X}_{k,p} - X_{k,p} \right|^2 \right] \quad (17)$$

As presented in [23] and [11],  $\bar{X}_{k,p} \approx \rho_p \hat{X}_{k,p}$  where  $\hat{X}_{k,p} \approx \rho_p X_{k,p} + \Delta_{k,p}$  allowing the redefinition of  $\bar{X}_{k,p}$  to  $\bar{X}_{k,p} \approx \rho_p^2 X_{k,p} + \rho_p \Delta_{k,p}$ . In matrix format,  $\bar{X}_{k,p}$  is given by:

$$\bar{X}_{k,p} \approx \mathbf{P}^2 \mathbf{S}_{k,p} + \mathbf{P} \Delta_{k,p}, \quad (18)$$

where  $\Delta_{k,p}$  is a mean zero error vector for  $p^{\text{th}}$  MT and  $\mathbf{P} = \text{diag}(\rho_1, \dots, \rho_p)$ , with  $\rho$  defined by:

$$\rho_p = \frac{\mathbb{E} \left[ \hat{x}_{n,p} x_{n,p}^* \right]}{\mathbb{E} \left[ |x_{n,p}|^2 \right]}, \quad (19)$$

which, in turn, defines the correlation factor that supplies a blockwise reliability measure of the estimates employed in the feedback loop and associated to the  $(i - 1)$ th iteration [22,24]. For a QPSK constellations,  $\rho_p = 1 - P_e$  and can be approximately given by:

$$\rho_p \approx \frac{1}{2N} \sum_{n=0}^{N-1} \left( |\rho_{n,p}^{Re}| + |\rho_{n,p}^{Im}| \right), \quad (20)$$

with

$$\rho_{n,p}^{Re(i)} = \tanh \left( \frac{|L_{n,p}^{Re(i)}|}{2} \right), \quad (21)$$

and

$$\rho_{n,p}^{Im(i)} = \tanh \left( \frac{|L_{n,p}^{Im(i)}|}{2} \right). \quad (22)$$

Once the data and noise components have zero mean and are uncorrelated, Equation (17) which represents the MSE can be extended, resulting in Equation (23):

$$\begin{aligned} \Theta = & \mathbf{F}^H \mathbb{E} [\mathbf{Y}^* \mathbf{Y}^T] \mathbf{F} - \mathbf{F}^H \mathbb{E} [\mathbf{Y}^* \bar{\mathbf{X}}^T] \mathbf{B} - \mathbf{F}^H \mathbb{E} [\mathbf{Y}^* X_p] \mathbf{B} - \mathbf{B}^H \mathbb{E} [\bar{\mathbf{X}}^* \mathbf{Y}^T] \mathbf{F} + \\ & \mathbf{B}^H \mathbb{E} [\bar{\mathbf{X}}^* \bar{\mathbf{X}}^T] \mathbf{B} + \mathbf{B}^H \mathbb{E} [\bar{\mathbf{X}}^* X_p] - \mathbf{F}^T \mathbb{E} [\mathbf{Y} X_p^*] + \mathbf{B}^T \mathbb{E} [\bar{\mathbf{X}} X_p^*] + \mathbb{E} [X_p^* X_p], \end{aligned} \quad (23)$$

For simplicity, in Equation (23), the user and subcarrier dependency has been dropped, with the exception for the  $S_p$  factor. We assume:

$$\mathbb{E} [\mathbf{Y}^* \mathbf{Y}^T] = \mathbf{R}_Y; \quad (24)$$

$$\mathbb{E} [\bar{\mathbf{X}}^* \bar{\mathbf{X}}^T] = \mathbf{R}_{\bar{\mathbf{X}}, \bar{\mathbf{X}}}; \quad (25)$$

$$\mathbb{E} [\mathbf{Y}^* X_p] = \mathbf{R}_{Y, X_p}; \quad (26)$$

$$\mathbb{E} [\bar{\mathbf{X}}^* X_p] = \mathbf{R}_{\bar{\mathbf{X}}, X_p}; \quad (27)$$

$$\mathbb{E} [\bar{\mathbf{X}}^* \mathbf{Y}] = \mathbf{R}_{\bar{\mathbf{X}}, Y} \quad (28)$$

and

$$\mathbb{E} [X_p X_p^*] = \mathbf{R}_X. \quad (29)$$

Equation (23), after some manipulation, can be written as:

$$\Theta = \mathbf{F}^H \mathbf{R}_Y \mathbf{F} + \mathbf{B}^H \mathbf{R}_{\bar{\mathbf{X}}, \bar{\mathbf{X}}} \mathbf{B} - 2Re \left\{ \mathbf{F}^H \mathbf{R}_{Y, X_p} \right\} + 2Re \left\{ \mathbf{B}^H \mathbf{R}_{\bar{\mathbf{X}}, X_p} \right\} - 2Re \left\{ \mathbf{B}^H \mathbf{R}_{\bar{\mathbf{X}}, Y} \mathbf{F} \right\} + \mathbf{R}_X. \quad (30)$$

With Equation (30), it is possible to obtain the BER performance through Equation (15) for any of the receivers previously presented.

## 6. Performance Results

In this section, performance results for the three mentioned receivers are presented. For these results, there are different scenarios where the number of transmitting and receiving antennas are changed. Initially, a MIMO scenario with 3 iterations, 4 transmitting antennas and 8 receiving antennas is presented. Then, this scenario is extended to a massive MIMO scenario and the number of antennas was increased 8 times, while keeping the same  $R/P$  ratio and number of iterations.

For simulation purposes, it is considered that in each MT,  $P$ , a SC-FDE modulation is applied transmitting 100 blocks with 256 data symbols ( $N = 256$ ), selected from a QPSK constellation under Gray mapping. Perfect synchronization and channel estimation are also assumed.

Performance values are presented as BER values, which in turn is in function of  $E_b/N_0$ , where  $E_b$  is the average bit energy associated with the receiving antennas and  $N_0$  represents the unilateral power spectral density of the Additive White Gaussian Noise (AWGN) channel noise. The lowest bound for the BER performance that a receiver can reach is fixed in the MFB performance which is also presented.

### 6.1. MIMO Scenario

In this scenario, a set of 3 iterations with  $P = 4$  and  $R = 8$  antennas is considered.

In Figure 3, the theoretical/simulated BER performance for both receivers (IB-DFE and MRC) is depicted in Figure 3a, as well as the correlation factor, shown in Figure 3b.

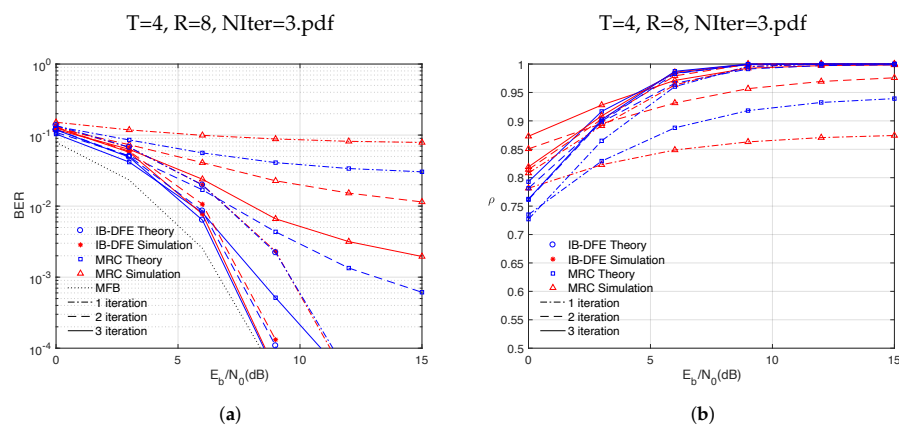


**Figure 3.** Theoretical/simulated BER performance and correlation factor for IB-DFE and MRC receivers in a Multiple Input Multiple Output (MIMO) system with 3 iterations. (a) BER performance. (b) Correlation factor ( $\rho$ ).

According to Figure 3a, it is possible to verify that the IB-DFE receiver has a BER performance closer to the MFB. In its third iteration, for a BER of  $10^{-4}$ , this receiver presents a difference of less than 1 dB to the MFB. For the same BER, MRC receivers present a worse performance. When comparing the simulated and theoretical values of BER performance, it should be pointed out that the theoretical curves achieve better performance, with the exception of the first IB-DFE iteration where the two curves are identical. In Figure 3b, both receivers, for the first iteration, present values for the correlation factor that never reach the optimum value 1, which implies a worse BER performance, as depicted in Figure 3a. From the second iteration onward, the correlation factor values are close to 1, allowing the achievement of BER performance values close to the MFB.

The performance results of a receiver that combines IB-DFE in the first iteration with MRC in the remaining iterations are depicted in Figure 4. According to Figure 4a, the BER performance of the receiver, in its first iteration is about 3 dB away from MFB and in the remaining iterations, the result approaches the MFB. The theoretical and simulated BER performance values are also very similar. The poor values of BER performance are accompanied by the correlation factor values. As represented in Figure 4b in its first iteration, these values are quite far from the optimal value 1. In the remaining iterations, the value of the correlation factor converges faster to 1.

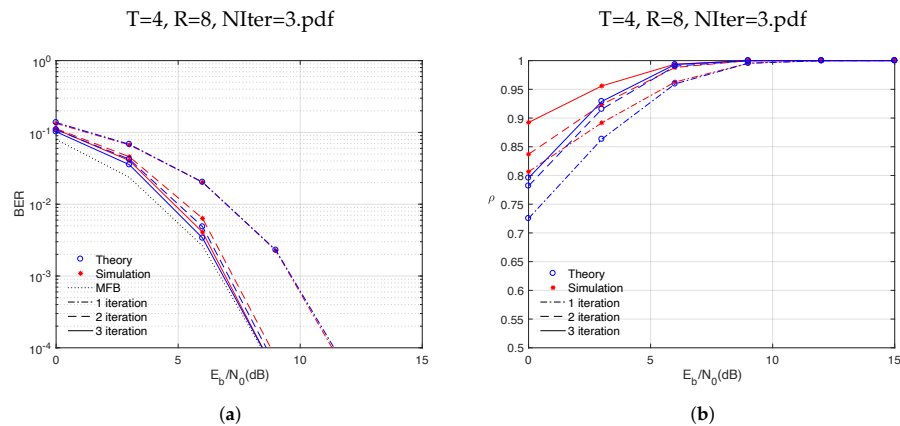


**Figure 4.** Theoretical/simulated BER performance and correlation factor for a receiver that combines IB-DFE and MRC in a MIMO system with 3 iterations. (a) BER performance. (b) Correlation factor ( $\rho$ ).

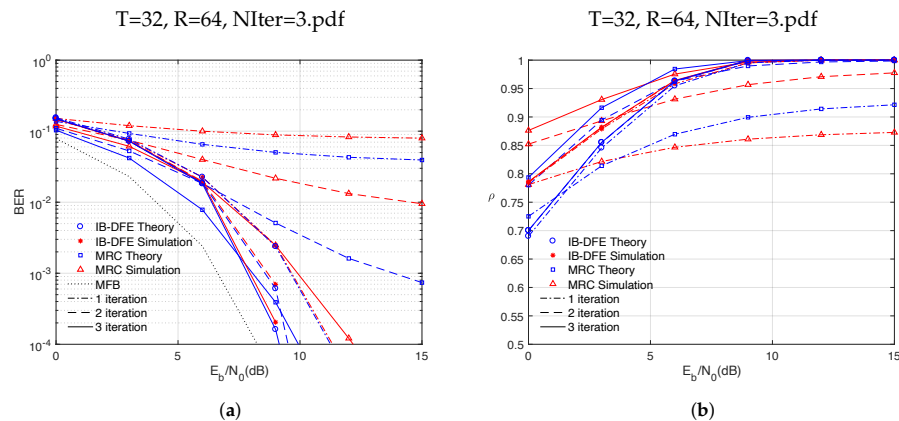
In fact, in the third iteration, this receiver has a difference of 0.5 dB when compared with the MFB, for a BER of  $10^{-2}$  while for a BER of  $10^{-4}$  this difference is reduced to approximately 0.1 dB.

#### 6.2. Massive MIMO Scenario

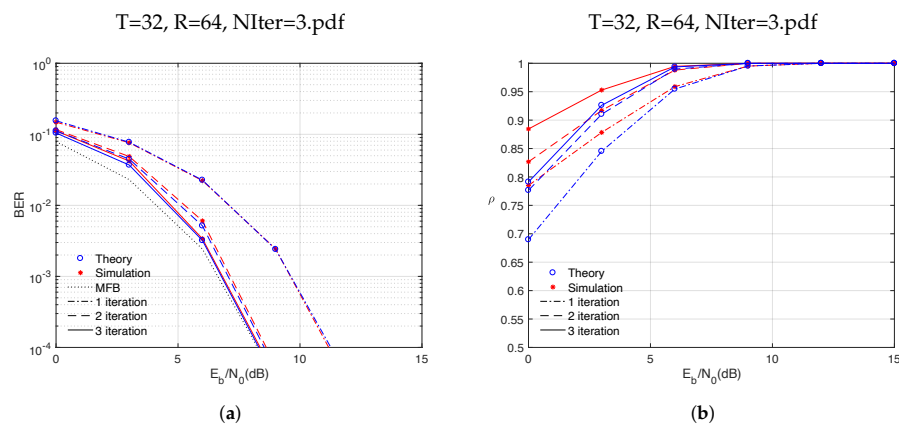
By increasing the number of transmitting and receiving antennas  $P = 32$  and  $R = 64$ , the system can be considered as a massive MIMO system.

Figure 5 shows the performance results for IB-DFE and MRC receivers. As for the MIMO system, the first iteration of the MRC presents weak values as shown in Figure 5a. For a BER of  $2 \times 10^{-4}$ , the simulated value for IB-DFE is 1.2 dB higher than MFB. In the case of MRC, when compared to MFB, the theoretical value is increased by 1.7 dB and the simulated value also increases by 3.8 dB. In Figure 5b the correlation factor is very similar to the one presented in Figure 3b. This is due to the fact that the  $R/P$  ratio is the same.

When analyzing the results for the receiver that combines the IB-DFE with the MRC (Figure 6), the results obtained via simulation practically match with the theoretical values for the BER performance, as shown in Figure 6a. At the end of the second iteration, for a BER of  $10^{-4}$ , the receiver is approximately 0.4 dB away from MFB and in its third iteration, the difference for the MFB is only 0.1 dB. The correlation factor, depicted in Figure 6b in the second iteration of the receiver, for an  $E_b/N_0$  of 5 dB, is practically 1.



**Figure 5.** Theoretical/simulated BER performance and correlation factor for IB-DFE and MRC receivers in an mMIMO system with 3 iterations. (a) BER performance. (b) Correlation factor ( $\rho$ ).



**Figure 6.** Theoretical/simulated BER performance and correlation factor for a receiver that combines IB-DFE and MRC in an mMIMO system with 3 iterations. (a) BER performance. (b) Correlation factor ( $\rho$ ).

## 7. Conclusions

This paper presents the study of FDE-type receivers that can be used in massive MIMO systems. The structures of three receivers, where the complexity depends on the estimation of the received signal, are discussed.

The BER performance of these receivers is simulated and compared with theoretical values. The impact of the correlation factor on BER performance is also studied.

One of the receivers proposed in this paper is a receiver that combines, in its first iteration, the IB-DFE receiver and in the remaining iterations the MRC receiver. The BER performance achieved by this receiver, in massive MIMO scenarios, is only 0.1 dB away from the MFB, in its third iteration, and the simulated/theoretical values match very closely.

**Author Contributions:** Conceptualization, D.F., F.C. and R.D.; investigation, D.F., F.C. and R.D.; software, D.F.; supervision, F.C. and R.D.; validation, F.C. and R.D.; visualization, D.F.; writing—original draft, D.F., F.C. and R.D.; writing—review and editing, F.C. and R.D. All authors have read and agreed to the published version of the manuscript.

**Funding:** This work was supported by projects CoSHARE (LISBOA-01-0145-FEDER-0307095-PTDC/EEL-TEL/30709/2017), MASSIVE5G (SAICT-45-2017-02) and Instituto de Telecomunicações (UIDB/EEA/

50008/2020), and funded by Fundo Europeu de Desenvolvimento Regional (FEDER), through Programa Operacional Regional LISBOA (LISBOA2020), and by national funds, through Fundação para a Ciência e Tecnologia (FCT).

**Conflicts of Interest:** The authors declare no conflict of interest.

## References

1. Wang, C.X.; Haider, F.; Gao, X.; You, X.H.; Yang, Y.; Yuan, D.; Aggoune, H.M.; Haas, H.; Fletcher, S.; Hepsaydir, E. Cellular architecture and key technologies for 5G wireless communication networks. *IEEE Commun. Mag.* **2014**, *52*, 122–130. [\[CrossRef\]](#)
2. Ericsson. *Ericsson Mobility Report—November 2019*; Technical report; Ericsson: Stockholm, Sweden, 2019.
3. Boccardi, F.; Heath, R.; Lozano, A.; Marzetta, T.; Popovski, P. Five disruptive technology directions for 5G. *IEEE Commun. Mag.* **2014**, *52*, 74–80. [\[CrossRef\]](#)
4. Larsson, E.G.; Edfors, O.; Tufvesson, F.; Marzetta, T.L. Massive MIMO for next generation wireless systems. *IEEE Commun. Mag.* **2014**, *52*, 186–195. [\[CrossRef\]](#)
5. Chang, R.W. Synthesis of Band-Limited Orthogonal Signals for Multichannel Data Transmission. *Bell Syst. Tech. J.* **1966**, *45*, 1775–1796. [\[CrossRef\]](#)
6. Sari, H.; Karam, G.; Jeanclaude, I. An analysis of orthogonal frequency-division multiplexing for mobile radio applications. In Proceedings of IEEE Vehicular Technology Conference (VTC), Stockholm, Sweden, 8 June 1994; pp. 1635–1639. [\[CrossRef\]](#)
7. Falconer, D.; Ariyavisitakul, S.; Benyamin-Seeyar, A.; Eidson, B. Frequency domain equalization for single-carrier broadband wireless systems. *IEEE Commun. Mag.* **2002**, *40*, 58–66. [\[CrossRef\]](#)
8. Benvenuto, N.; Tomasin, S. Block iterative DFE for single carrier modulation. *Electron. Lett.* **2002**, *38*, 1144–1145. [\[CrossRef\]](#)
9. Benvenuto, N.; Dinis, R.; Falconer, D.; Tomasin, S. Single Carrier Modulation With Nonlinear Frequency Domain Equalization: An Idea Whose Time Has Come—Again. *Proc. IEEE* **2010**, *98*, 69–96. [\[CrossRef\]](#)
10. Dinis, R.; Kalbasi, R.; Falconer, D.; Banihashemi, A. Iterative Layered Space-Time Receivers for Single-Carrier Transmission Over Severe Time-Dispersive Channels. *IEEE Commun. Lett.* **2004**, *8*, 579–581. [\[CrossRef\]](#)
11. Ribeiro, F.; Dinis, R.; Cercas, F.; Silva, A. Receiver design for the uplink of base station cooperation systems employing SC-FDE modulations. *EURASIP J. Wirel. Commun. Netw.* **2015**, *2015*, 7. [\[CrossRef\]](#)
12. Dinis, R.; Carvalho, P.; Borges, D. Low Complexity MRC and EGC Based Receivers for SC-FDE Modulations With Massive MIMO Schemes. *IEEE Glob. Conf. Signal Inf. Process. Glob. SIP* **2016**, *1*, 1–4.
13. Montezuma, P.; Dinis, R. Iterative receiver based on the EGC for massive MIMO schemes using SC-FDE modulations. *Electron. Lett.* **2016**, *52*, 972–974. [\[CrossRef\]](#)
14. Bento, P.; Pereira, A.; Dinis, R.; Gomes, M.; Silva, V. Frequency-Domain Detection without Matrix Inversions for mmWave Communications with Correlated Massive MIMO Channels. *IEEE Veh. Technol. Conf.* **2017**, *2017*, [\[CrossRef\]](#)
15. Cabral, L.; Fernandes, D.; Cercas, F.; Dinis, R. Efficient frequency-domain detection for massive MIMO systems. In Proceedings of the 2017 South Eastern European Design Automation, Computer Engineering, Computer Networks and Social Media Conference (SEEDA-CECNSM), Kastoria, Greece, 23 September 2017; pp. 1–5. [\[CrossRef\]](#)
16. Ribeiro, F.C.; Guerreiro, J.; Dinis, R.; Cercas, F.; Silva, A. Reduced complexity detection in MIMO systems with SC-FDE modulations and iterative DFE receivers. *J. Sens. Actuator Netw.* **2018**, *7*. [\[CrossRef\]](#)
17. Pereira, A.; Bento, P.; Gomes, M.; Dinis, R.; Silva, V. Iterative MRC and EGC Receivers for MIMO-OFDM Systems. *IEEE Veh. Technol. Conf.* **2018**, *2018*, 1–4. [\[CrossRef\]](#)
18. Fernandes, D.; Cercas, F.; Dinis, R. Iterative Receiver Combining IB-DFE with MRC for Massive MIMO Schemes. *Procedia Comput. Sci.* **2017**, *109*, 305–310. [\[CrossRef\]](#)
19. Magueta, R.; Enes, R.; Teodoro, S.; Silva, A.; Castanheira, D.; Dinis, R.; Gameiro, A. Hybrid Nonlinear Multiuser Equalizer for mmWave Massive MIMO CE-OFDM Systems. *IEEE Int. Symp. Pers. Indoor Mob. Radio Commun. PIMRC* **2019**, *2019*. [\[CrossRef\]](#)
20. Magueta, R.; Castanheira, D.; Pedrosa, P.; Dinis, R. Wideband Millimeter Wave Massive MIMO Systems. *Sensors* **2020**, *20*, 575. [\[CrossRef\]](#) [\[PubMed\]](#)
21. Goldsmith, A. *Wireless Communications*; Cambridge University Press: Cambridge, UK, 2005. [\[CrossRef\]](#)

22. Gusmão, A.; Torres, P.; Dinis, R.; Esteves, N. A turbo FDE technique for reduced-CP SC-based block transmission systems. *IEEE Trans. Commun.* **2007**, *55*, 16–20. [[CrossRef](#)]
23. Casal Ribeiro, F.; Dinis, R.; Cercas, F.; Silva, A. On the performance of SC-FDE receivers for Base Station cooperation systems with rate-limited backhaul links. In Proceedings of 2013 9th International ITG Conference on Systems, Communication and Coding, SCC 2013. Munich, Germany, 1 June 2013; p. 9.
24. Silva, F.; Dinis, R.; Montezuma, P. Estimation of the Feedback Reliability for IB-DFE Receivers. *ISRN Commun. Netw.* **2011**, *2011*, 1–7. [[CrossRef](#)]



© 2020 by the authors. Licensee MDPI, Basel, Switzerland. This article is an open access article distributed under the terms and conditions of the Creative Commons Attribution (CC BY) license (<http://creativecommons.org/licenses/by/4.0/>).



# Chapter 6

## Conclusions

One of the main objectives of this research is to develop an automated and agnostic solution that performs signal estimation. This solution includes data from real networks in order to increase the accuracy of the estimation. The automatism associated with this solution allows the implementation of the SON concept in the networks. The creation of a new estimation model, named ACSPM, its study and analysis was detailed throughout Chapter 2.

One of the advantages of the ACSPM, besides the use of real data in the calibration, is in its implementation, since cloud resources were used. This use allows easy integration with other tools and has the advantages of a cloud service, such as scalability, easier access, and easier distribution of the solution.

The need for real measures to accurately estimate the coverage of an antenna, which is an advantage of the proposed model, can also be seen as a serious issue to be overcome when planning new antennas since this data does not exist at an early stage. In order to solve this problem, Chapter 3 presented a propagation model generated from real measures, using AI models, named AIPM. Besides the fact that the whole design associated with the model is different from the ACSPM, this model presents not only better results when compared with ACSPM, but also different applicability in the planning of a new antenna in the area where the calibration occurs.

The accuracy of each model, through real scenarios, was also studied in Chapter 3. The MAE associated with the AIPM is 6.1 dB, with a standard deviation of 4 dB, while the MAE of the ACSPM is 6.6 dB, with a standard deviation of 4.1 dB. The similar performance of the models allows each one to be used under certain conditions. For example, in terms of speed in generating results, the model generated by AI is faster, so for applications where speed is more important than accuracy, the model to be used is the AIPM.

With the implementation and study of the presented propagation models, most of the objectives proposed in this thesis would be achieved. However, the abundance of real network data, that allowed part of this work in coverage estimation, brought new considerations, which were presented and discussed in Chapter 4. These new considerations intended to use the data from real networks, that were SISO in the estimation of the coverage of MIMO systems.

A methodology that easily allows the use of SISO measures in the estimation of MIMO coverage was presented and detailed. This methodology uses the analysis and comparison of the BER performance of the SISO and MIMO systems and presents a set of equations that quantify the impact on the transition of these systems. The results presented are for an IB-DFE receiver and for a specific scenario and they show that when we move from a SISO to a MIMO system the coverage area is reduced by 3.5%.

Another conclusion that was reached in Chapter 4 is that the closer the MFB was to the receiver performance, the smaller the difference between the coverage area of the SISO and MIMO systems. This improvement in the performance of the receiver, in this case, the IB-DFE, is achieved due to the iterative process, which results in an increase in the complexity associated with signal estimation.

When working with MIMO or mMIMO systems, one of the major problems is associated with the computational complexity, which, as previously mentioned, increases with the number of iterations. This complexity derives from the necessity of the inversion of matrices. Chapter 5 presented some receivers that can be used in mMIMO systems. One of the receivers presented showed a performance similar to

IB-DFE but with a significant reduction in the associated complexity since it only presents the need for matrix inversions in its first iteration. This receiver presents theoretical results very close to the simulated ones and in its third iteration is only 0.1 dB away from the value reached by the MFB.

In conclusion, the work carried out aimed to solve and simplify the daily tasks of telecommunications operators on planning and optimising their networks. Automatic propagation models were designed using real network signal estimation measurements. In fact, the design of two propagation models whose applicability is different, have been presented. One of these propagation models can be used for network optimisation and another one can be used for new antennas planning. The existence of several real measures, served as motivation to extend the applicability of the propagation models presented for MIMO or mMIMO systems, calculating the impact on coverage areas through the BER performance analysis.

## 6.1 Future Work

The utility of the research presented in this thesis can be applied in new mechanisms for resource optimisation in telecommunications networks. This is an important issue to be addressed as future work.

Another task that can be studied is the applicability of the models presented in scenarios with different user characteristics, such as countries with different living conditions. It may be interesting to use Minimisation of Drive Tests standardisation in order to increase the number of DT available and therefore improving the performance of the presented models

Similar to what was done with SISO measures, it would also be interesting to collect and analyse measures from MIMO systems in order to create propagation models from that data, and check if the extension methodology results presented correspond to reality.

Other point that can be addressed in future work is the analysis of receiver performance in MIMO/mMIMO systems with modulations other than QPSK and when the signal estimation is not perfect.

# Bibliography

- [1] ANACOM, “COVID-19 - Electronic communications traffic increases by about 50%,” ANACOM, Tech. Rep., 2020, [Online]. Available: <https://anacom.pt/render.jsp?contentId=1522133>. [Accessed July 01, 2020].
- [2] European Commission and BEREC, “Joint Statement from the Commission and the Body of European Regulators for Electronic Communications (BEREC) on coping with the increased demand for network connectivity due to the Covid-19 pandemic.” European Commission and BEREC, Tech. Rep., 2020, [Online]. Available: [https://berec.europa.eu/eng/document\\_register/subject\\_matter/berec/others/9236-joint-statement-from-the-commission-and-the-body-of-european-regulators-for-electronic-communications-berec-on-coping-with-the-increased-demand-for-network-connectivity-due-to-](https://berec.europa.eu/eng/document_register/subject_matter/berec/others/9236-joint-statement-from-the-commission-and-the-body-of-european-regulators-for-electronic-communications-berec-on-coping-with-the-increased-demand-for-network-connectivity-due-to-). [Accessed July 01, 2020].
- [3] C. X. Wang, F. Haider, X. Gao, X. H. You, Y. Yang, D. Yuan, H. M. Aggoune, H. Haas, S. Fletcher, and E. Hepsaydir, “Cellular architecture and key technologies for 5G wireless communication networks,” *IEEE Communications Magazine*, vol. 52, no. 2, pp. 122–130, Feb. 2014.
- [4] Ericsson, “Ericsson Mobility Report 2019,” Ericsson, Tech. Rep. Nov., 2019.
- [5] “Multivision,” [Online]. Available: <https://multivision.pt>. [Accessed Apr. 01, 2020].
- [6] Multivision, “OptiNET-5G - Planning and Optimization Framework of 5G Heterogeneous Networks in a Cloud Environment,” *Project 023304, Funded by Centro2020, Portugal2020 and European Union*, 2017.

- [7] “Metric,” [Online]. Available: <https://metric.pt>. [Accessed Apr. 01, 2020].
- [8] M. Frankel, N. Shacham, and J. E. Mathis, “Self-Organizing Networks,” *Future Generation Computer Systems*, vol. 4, no. 2, pp. 95–115, Sept. 1988.
- [9] NGMN, “NGMN Use Cases related to Self Organising Network, Overall Description,” NGMN, Tech. Rep., Oct. 2007.
- [10] P. V. Klaine, M. A. Imran, O. Onireti, and R. D. Souza, “A Survey of Machine Learning Techniques Applied to Self-Organizing Cellular Networks,” *IEEE Communications Surveys & Tutorials*, vol. 19, no. 4, pp. 2392–2431, July 2017.
- [11] A. De Mauro, M. Greco, and M. Grimaldi, “What is big data? A consensual definition and a review of key research topics,” in *AIP Conference Proceedings*, vol. 1644, Feb. 2015, pp. 97–104.
- [12] Forsk, “Atoll 3.3.0 Technical Reference Guide for Radio Networks,” Forsk, France, Tech. Rep., 2015.
- [13] “AWS,” [Online]. Available: <https://aws.amazon.com>. [Accessed Apr. 01, 2020].
- [14] W. C. Hardy, *QoS - Measurement and Evaluation of Telecommunications Quality of Service*. Hoboken, NJ, USA: Wiley, July 2001.
- [15] F. Boccardi, R. Heath, A. Lozano, T. Marzetta, and P. Popovski, “Five disruptive technology directions for 5G,” *IEEE Communications Magazine*, vol. 52, no. 2, pp. 74–80, Feb. 2014.
- [16] E. G. Larsson, O. Edfors, F. Tufvesson, and T. L. Marzetta, “Massive MIMO for next generation wireless systems,” *IEEE Communications Magazine*, vol. 52, no. 2, pp. 186–195, Feb. 2014.
- [17] D. Fernandes, F. Cercas, and R. Dinis, “Analytical Performance Evaluation of Massive MIMO Techniques for SC-FDE Modulations,” *Electronics*, vol. 9, no. 3, p. 533, Mar. 2020.

- [18] D. Fernandes, D. Clemente, G. Soares, P. Sebastiao, F. Cercas, R. Dinis, and L. S. Ferreira, "Cloud-Based Implementation of an Automatic Coverage Estimation Methodology for Self-Organising Network," *IEEE Access*, vol. 8, pp. 66 456–66 474, Apr. 2020.
- [19] P. M. Pina, A. F. Godinho, D. F. S. Fernandes, D. J. A. Clemente, P. Sebastiao, G. E. Soares, and L. S. Ferreira, "Automatic Coverage Based Neighbour Estimation System: A Cloud-Based Implementation," *IEEE Access*, vol. 8, pp. 69 671–69 682, Apr. 2020.
- [20] A. Godinho, D. Fernandes, G. Soares, P. Pina, P. Sebastião, A. Correia, and L. S. Ferreira, "A Novel Way to Automatically Plan Cellular Networks Supported by Linear Programming and Cloud Computing," *Applied Sciences*, vol. 10, no. 9, p. 3072, Apr. 2020.
- [21] D. Fernandes, A. Raimundo, F. Cercas, P. Sebastiao, R. Dinis, and L. S. Ferreira, "Comparison of Artificial Intelligence and Semi-Empirical Methodologies for Estimation of Coverage in Mobile Networks," *IEEE Access*, vol. 8, pp. 139 803 – 139 812, July 2020.
- [22] D. Fernandes, F. Cercas, R. Dinis, and P. Sebastião, "Estimating the Performance of MIMO SC-FDE Systems Using SISO Measurements," *Applied Sciences (Switzerland)*, vol. 10, no. 21, pp. 1–13, 2020.
- [23] R. Cortesao, D. Fernandes, G. Soares, D. Clemente, P. Sebastiao, and L. S. Ferreira, "Cloud-based Implementation of a SON Radio Resources Planning System for Mobile Networks and Integration in SaaS Metric," *Submitted, under peer review in IEEE Access*, 2020.
- [24] D. Fernandes, F. Cercas, and R. Dinis, "Iterative Receiver Combining IB-DFE with MRC for Massive MIMO Schemes," in *Procedia Computer Science*, vol. 109, June 2017, pp. 305–310.
- [25] L. Cabral, D. Fernandes, F. Cercas, and R. Dinis, "Efficient frequency-domain detection for massive mimo systems," in *2017 South Eastern European Design*

- Automation, Computer Engineering, Computer Networks and Social Media Conference (SEEDA-CECNSM)*, Kastoria, Sept. 2017, pp. 1–5.
- [26] D. Fernandes, L. S. Ferreira, M. Nozari, P. Sebastiao, F. Cercas, and R. Dinis, “Combining Drive Tests and Automatically Tuned Propagation Models in the Construction of Path Loss Grids,” in *2018 IEEE 29<sup>th</sup> Annual International Symposium on Personal, Indoor and Mobile Radio Communications (PIMRC)*, Bologna, Sept. 2018, pp. 1–2.
- [27] D. Fernandes, G. Soares, D. Clemente, R. Cortesão, P. Sebastião, F. Cercas, R. Dinis, and L. S. Ferreira, “Combining Measurements and Propagation Models for Estimation of Coverage in Wireless Networks,” in *2019 IEEE 90<sup>th</sup> Vehicular Technology Conference: VTC2019-Fall*, Honolulu, Hawaii, Sept. 2019, pp. 1–5.
- [28] D. Clemente, G. Soares, D. Fernandes, R. Cortesao, P. Sebastiao, and L. S. Ferreira, “Traffic forecast in mobile networks: Classification system using machine learning,” in *2019 IEEE 90<sup>th</sup> Vehicular Technology Conference: VTC2019-Fall*, vol. 2019, Honolulu, Hawaii, Sept. 2019.
- [29] D. Fernandes, G. Soares, D. J. Alves Clemente, R. Cortesão, P. Sebastião, F. Cercas, R. Dinis, and L. S. Ferreira, “Integration of a Cloud-Based Realistic and Automatic Coverage Estimation Methodology in Metric SaaS,” in *2019 22<sup>nd</sup> International Symposium on Wireless Personal Multimedia Communications (WPMC) (WPMC’19)*, Lisbon, Portugal, Nov. 2019, pp. 1–4.
- [30] P. V. Pina, A. F. Godinho, D. Fernandes, D. J. Alves Clemente, G. Soares, P. Sebastião, and L. S. Ferreira, “Cloud-based Implementation of an Automatic Pixel-based Neighbour Identification System for Cellular Networks,” in *2019 22<sup>nd</sup> International Symposium on Wireless Personal Multimedia Communications (WPMC) (WPMC’19)*, Lisbon, Portugal, Nov. 2019, pp. 1–6.
- [31] A. Godinho, D. Fernandes, D. Clemente, G. Soares, P. Sebastiao, P. Pina, and L. S. Ferreira, “Cloud-based Cellular Network Planning System: Proof-of-Concept Implementation for GSM in AWS,” in *2019 22<sup>nd</sup> International*

- Symposium on Wireless Personal Multimedia Communications (WPMC) (WPMC'19)*, vol. 2019, Nov. 2019, pp. 1–5.
- [32] R. Cortesao, D. Fernandes, D. Clemente, G. Soares, P. Sebastiao, and L. S. Ferreira, “Cloud-based Implementation of a SON Automatic Planning System: A proof-of-concept for UMTS,” in *2019 22<sup>nd</sup> International Symposium on Wireless Personal Multimedia Communications (WPMC) (WPMC'19)*, vol. 2019, Nov. 2019, pp. 1–6.
- [33] D. Clemente, D. Fernandes, R. Cortesao, G. Soares, P. Sebastiao, and L. S. Ferreira, “Assessment of Traffic Prediction Models for Mobile Communication Networks,” in *2019 22<sup>nd</sup> International Symposium on Wireless Personal Multimedia Communications (WPMC) (WPMC'19)*, vol. 2019, Nov. 2019, pp. 1–4.
- [34] D. Fernandes, F. Cercas, and R. Dinis, “Enhanced MIMO Techniques for 5G,” in *Poster presentation at Instituto de Telecomunicações, Aveiro, Portugal*, Nov. 2018.
- [35] Multivision, “Technical, Economical and Environmental Optimisation Modules,” in *Deliverable Report D4.1, OptiNet-5G Project*, Lisbon, Feb. 2019, (translated from Portuguese).
- [36] —, “Operation of the Technical Optimisation Modules,” in *Deliverable Report D4.2, OptiNet-5G Project*, Lisbon, Feb. 2019, (translated from Portuguese).
- [37] —, “Testing and Evaluation of Modules,” in *Deliverable Report D6.1, OptiNet-5G Project*, Lisbon, Apr. 2019, (translated from Portuguese).
- [38] —, “Tests and intermediate Evaluation of Module Integration,” in *Deliverable Report D6.2, OptiNet-5G Project*, Lisbon, Apr. 2019, (translated from Portuguese).

- [39] —, “Tests and Final Evaluation and Acceptance of the Prototype Produced,” in *Deliverable Report D6.3, OptiNet-5G Project*, Lisbon, Aug. 2019, (translated from Portuguese).
- [40] D. Fernandes, D. Clemente, G. Soares, P. Sebastiao, F. Cercas, R. Dinis, and L. S. Ferreira, “Automatically Calibrated Standard Propagation Model,” in *OptiNet-5G Project*, Lisbon, Portugal, Dec. 2019.
- [41] A. R. Mishra, *Advanced Cellular Network Planning and Optimisation*, A. R. Mishra, Ed. Chichester, UK: John Wiley & Sons, Ltd, Oct. 2006.